The Role of Fluctuations in Network Performance Evaluation

Submitted to
Graduate School of Information Science and Technology
Osaka University

January 2014

Kohei WATABE

List of Publications

Journal Papers

1. Kohei Watabe, Yudai Honma, and Masaki Aida, "Probe Interval Designs that Improve Accuracy of CoMPACT Monitor," *Simulation Modelling Practice and Theory*, vol.19, no.1, pp.56–68, January 2011.

2. Kohei Watabe and Masaki Aida, "Modeling Fluctuations in the Quasi-static Approach Describing the Temporal Evolution of Retry Traffic," *WSAES Transactions on Communications*, vol.12, no.9, pp.488–498, September 2013.

3. Kohei Watabe and Masaki Aida, "On Optimal Magnitude of Fluctuations in Probe Packet Arrival Intervals," *IEICE Transactions on Communications*, vol.E96-B, no.12, pp.3028-3040, December 2013.

Refereed Conference Papers

1. Kohei Watabe, Yudai Honma, and Masaki Aida, "Verification of Accuracy Improvement for CoMPACT Monitor Due to Suboptimal Inter-Probe Time," in *Proceedings of the 9th Annual International Symposium on Applications and the Internet (SAINT 2009)*, pp.133–136, Seattle, WA, USA, July 2009.

2. Kohei Watabe, Yudai Honma, and Masaki Aida, "Accuracy Improvement of CoMPACT Monitor by Using New Probing Method," in *Proceedings of the 12th Asia-Pacific Network Operations and Management Symposium (APNOMS 2009)*, pp.31–40, Jeju, Korea, September 2009.

3. Kohei Watabe, Yudai Honma, and Masaki Aida, "Design of Probe Intervals to Improve Accuracy of CoMPACT Monitor," in *Proceedings of International Conference on Intelligent Networking and Collaborative Systems (INCoS 2009) Workshop*, pp.335–340, Barcelona, Spain, November 2009.

4. Yoshiyuki Ishii, Kohei Watabe, and Masaki Aida, "Quasi-Static Approach for Retry Traffic with Different Service Time," in *Proceedings of the 2nd International Symposium on Aware Computing (ISAC 2010)*, Tainan, Taiwan, November 2010.

5. Kohei Watabe and Masaki Aida, "Analysis on the Fluctuation Magnitude in Probe Interval for Active Measurement," in *Proceedings of the 30th IEEE International Conference on Computer Communication (INFOCOM 2011) Mini-Conference*, pp.161–165, Shanghai, China, April 2011.

6. Kohei Watabe and Masaki Aida, "On Modeling of Fluctuations in Quasi-Static Approach Describing the Temporal Evolution of Retry Traffic," in *Proceedings of the 23rd International Teletraffic Congress (ITC 2011) Student Poster*, pp.308–309, San Francisco, CA, USA, September 2011.

7. Kohei Watabe and Hiroyuki Ohsaki, "Effect of Locality of Node Mobility on Epidemic Broadcasting in DTNs," in *Proceedings of the 6th Joint IFIP Wireless and Mobile Networking Conference (WMNC 2013)*, Dubai, United Arab Emirates, April 2013.

8. Kosuke Matsuda, Kohei Watabe, and Hiroyuki Ohsaki, "An Epidemic Broadcasting Mechanism in Delay/Disruption-Tolerant Networks Utilizing Contact Duration Distribution," in *Proceedings of the 6th Joint IFIP Wireless and Mobile Networking Conference (WMNC 2013)*, Dubai, United Arab Emirates, April 2013.

Non-Refereed Technical Papers

1. Yoshiyuki Ishii, Kohei Watabe, Yudai Honma, Masaki Aida, "Quasi-Static Approach for Retrial Traffic with Different Service Time," in *Proceedings of IEICE General Conference 2009*, B-7-56, Ehime, Japan, March 2009 (*in japanese*).

2. Kohei Watabe, Yudai Honma, Masaki Aida, "Design of Probe Intervals to Improve Accuracy of CoMPACT Monitor," in *Proceedings of IEICE General Conference 2009*, B-7-12, Ehime, Japan, March 2009 (*in japanese*).

3. Kohei Watabe, Yudai Honma, Masaki Aida, "Verification of Accuracy Improvement for CoMPACT Monitor Due to Suboptimal Inter-probe Time," *Technical Report of IEICE*, IN2008-162, pp.179–184, March 2009 (*in japanese*).

4. Kohei Watabe, Yudai Honma, Masaki Aida, "A Study on the Probing Method and Accuracy for CoMPACT Monitor," *Technical Report of IEICE*, IN2009-30, pp.31–36, July 2009 (*in japanese*).

5. Yoshiyuki Ishii, Kohei Watabe, Yudai Honma, Masaki Aida, "Quasi-Static Approach for Retrial Traffic with Different Service Time," *Technical Report of IEICE*, NS2009-239, pp.433–438, March 2010 (*in japanese*).

6. Kohei Watabe, Masaki Aida, "Optimization of the Magnitude of Fluctuations for Timing of Active Probe Packets," em Technical Report of IEICE, IN2010-50, pp.37–42, July 2010 (*in japanese*).

7. Ryo Sasaki, Kohei Watabe, Masaki Aida, "A Study on Decomposition of Timescales in Layered Structure of Autonomous Decentralized Control," in *Proceedings of IEICE Society Conference 2010*, B-7-52, Osaka, Japan, September 2010 (*in japanese*).

8. Shotaro Motomura, Hirokazu Kariya, Kohei Watabe, Masaki Aida, "Search Range for Finding Hub Users in Social Networks," in *Proceedings of IEICE Society Conference 2010*, B-7-34, Osaka, Japan, September 2010 (*in japanese*).

9. Kohei Watabe, Masaki Aida, "Analysis of the Magnitude of Fluctuations in Probe Timing for Active Measurement," in *Proceedings of IEICE Society Conference 2010*, B-7-20, Osaka, Japan, September 2010 (*in japanese*).

10. Shotaro Motomura, Hirokazu Kariya, Kohei Watabe, Masaki Aida, "Range of Hub User Search in Social Networks," *Technical Report of IEICE*, IN2010-199, pp.331–336, March 2011 (*in japanese*).

11. Kohei Watabe, Makiko Tanabe, Masaki Aida, "On Modeling of Fluctuations on Quasi-Static Approach Analyzing the Behavior of the Retry Traffic," *Technical Report of IEICE*, IN2010-178, pp.205–210, March 2011 (*in japanese*).

12. Masaki Aida, Kohei Watabe, Hiroki Takayama, Chisa Takano, "A Scenario of Quasi-Static Approach Based on Renormalization Group for Composing Hierarchical Architecture by Time Scales of Network Operations," *Technical Report of IEICE*, IN2011-36, pp.43–48, June 2011 (*in japanese*).

13. Ranko Kusaka, Kohei Watabe, Masaki Aida, "Flow Aggregation Scheme Improving Scalability in Diffusion-Type Flow Control," in *Proceedings of IEICE Society Conference 2011*, B-7-49, Hokkaido, Japan, September 2011 (*in japanese*).

14. Kosuke Matsuda, Kohei Watabe, Hiroyuki Ohsaki, "A Proposal of an Epidemic Broadcast Mechanism in DTN Utilizing Contact Duration Distribution," in *Proceedings of IEICE Society Conference 2012*, B-7-16, Toyama, Japan, July 2012 (*in japanese*).

15. Kosuke Matsuda, Kohei Watabe, Hiroyuki Ohsaki, "An Epidemic Broadcast Mechanism in DTN utilizing Contact Duration Distribution," *Technical Report of IEICE*, CQ2012-54, pp.71–76, September 2012 (*in japanese*).

16. Minoru Harada, Yuki Koizumi, Kohei Watabe, Hiroyuki Ohsaki, Makoto Imase, "On Evaluating the Effect of Micro-Robot Functionality on Target Discovery in Survivor Discovery Systems in Disaster Areas," *Technical Report of IEICE*, CNR2012-22, pp.21–26, February 2013 (*in japanese*).

17. Ryuichi Hayashida, Kohei Watabe, Hiroyuki Ohsaki, "System Identification of Network Service Processing Time with Genetic Programming," *Technical Report of IEICE*, IN2013-21, pp.55–60, May 2013 (*in japanese*).

Preface

As importance of networked systems in infrastructure increases, precisely measuring and modeling them have been becoming important. With increase of dependency of our social activities on them, higher reliability is required to them. To design/manage highly reliable systems, precise evaluations of these systems are significant. To achieve precise evaluation, it requires an evaluator who does measuring and modeling to precisely know or infer current and future states of the system. A state is a set of numerous variables like delay on each link, the number of packets in each router, and traffic demand for each source-destination pair, and the variables are represented as deterministic processes. If an evaluator is able to precisely obtain knowledge of the states by measurement or modeling, the evaluation result is deterministic.

However, fluctuations of knowledge of states appear when we evaluate actual systems by measuring or modeling, and the evaluation result is not deterministic. In evaluations of actual systems, an evaluator uses incomplete knowledge of the states since he or she cannot precisely obtain every variable of the system all the time. Depending on how an evaluator measures or models variables of an actual system, his or her knowledge of the states is fluctuated, and the evaluation result is not deterministic.

It is critically important how we control these fluctuations in performance evaluations if we want to provide precise performance evaluations of networked systems. Some earlier researches provided guidelines to help us when we control these fluctuations. Works by Baccelli et al. provide us some insights regarding how to control fluctuations due to measurement timing. They investigated the relationship between precision of active measurement and an inter-probe time distribution, and proposed new probing policy, called Gamma-probing. We can grasp that the work tackled the control problem of fluctuations

due to measurement timing because controlling probing timing in active measurement corresponds to controlling the measurement timing. On the other hand, regarding fluctuations in modeling, to evaluate systems with retry traffic due to user impatience, the quasi-static approach is proposed. In the quasi-static approach, a temporal evolution of a system state is described by a deterministic process and stochastic fluctuations that are accumulation of small fluctuations at each time. The deterministic process means average process of system state.

We focus on fluctuations in network performance evaluation in this thesis, and we improve precision of performance evaluations by controlling fluctuation magnitude. In various frameworks, we provide method to obtain knowledge of states of a system through measurement or modeling to achieve precise performance evaluations. A precision improvement of evaluation in networked systems allows us to design/manage network systems with higher reliability.

First, in the framework of Change-of-Measure-based Passive/ACTive monitoring (CoMPACT monitor) that offers scalable per-flow QoS measurement, we apply Gamma-probing that Baccelli et al. have proposed as the active measurement component of it to improve precision of evaluation. We should carefully investigate the characteristics of CoMPACT monitor with Gamma-probing since there is the difference between the assumptions of CoMPACT monitor and those of the work of Baccelli et al. We verify the precision improvement of CoMPACT monitor by Gamma-probing and clarified the requirement that assures the achievement of precision improvement. As a result, we show that the Gamma-probing can be useful to be added to CoMPACT monitor.

Second, in the framework of active measurement, we analyze the optimal magnitude of fluctuations in inter-probe time by the description on which we separate the probing process into a deterministic process and stochastic fluctuations. Since it is not provided how to decide upon the optimal parameter of Gamma-probing, it has remained a unsolved problem. We understand that the important point in precise measurement is to shift the cycle of the probe packet timing by adding fluctuations and to determine the optimal magnitude of the fluctuations. Therefore, we introduce a probing policy in which we explicitly separate the probing process into a deterministic process and stochastic fluctuations with normal distribution, and we show how to determine the optimal fluctuation magnitude for

the target process.

Third, in the framework of the quasi-static approach, we model the fluctuations and determine its appropriate magnitude for precisely evaluating the probability of rare system outages on highly reliable systems. In the quasi-static approach, a target system behavior is described by separating the deterministic process and stochastic fluctuations just as we described the probing process of active measurement. We discuss how to model the fluctuations for precisely replicating the behavior of retry traffic caused by user impatience using the quasi-static approach, and show the modeling method to determine the appropriate magnitude of stochastic fluctuations. We demonstrate modeling of the fluctuations in M/M/1- and M/M/s-based systems with retry traffic, and compare the results of the quasi-static approach and those of the conventional Monte Carlo simulation of queuing systems.

Acknowledgements

First of all, I would like to express my sincere appreciation to my supervisor, Professor Toru Hasegawa, Graduate School of Information Science and Technology, Osaka University, for his proper guidance and valuable advice. He carefully reviewed my papers and gave me much advice for completing this thesis. His advice taught me not only how to write this thesis, but also how to live as a researcher.

I would like to express my heartfelt gratitude to the members of my thesis committee, Professor Masayuki Murata, Professor Takashi Watanabe, Professor Teruo Higashino, and Professor Morito Matsuoka, Graduate School of Information Science and Technology, Osaka University, for carefully reviewing this thesis and providing valuable comments. Especially, I would like to express my deepest appreciation to Professor Masayuki Murata for insightful suggestions in research meetings.

I am deeply grateful to Dr. Makoto Imase, Vice President of National Institute of Information and Communications Technology, Professor Masaki Aida, Graduate School of System Design, Tokyo Metropolitan University, and Professor Hiroyuki Ohsaki, Department of Informatics, School of Science and Technology, Kwansei Gakuin University, for irreplaceable guidance and support. In particular, I would like to express my deepest appreciation to Professor Masaki Aida. His enthusiasm in teaching and research and interesting researches motivated me to become a researcher.

I am cordially thankful to members of research meetings, Emeritus Professor Konosuke Kawashima, Tokyo University of Agriculture and Technology, Professor Naoki Wakamiya, Graduate School of Information Science and Technology, Osaka University, Associate Professor Harumasa Tada, Faculty of Education, Kyoto University of Education, Associate Professor Takano Chisa, Graduate School of Information Sciences, Hi-

roshima City University, Assistant Professor Yuki Koizumi, Graduate School of Information Science and Technology, Osaka University, Assistant Professor Yudai Honma, Waseda Institute for Advanced Study, Assistant Professor Yusuke Sakumoto, Graduate School of System Design, Osaka University, and Assistant Professor Sho Tsugawa, Faculty of Engineering, Information and Systems, University of Tsukuba, for comments to raise the quality of my research.

Special thanks to all members of the Information Sharing Platform Laboratory, Graduate School of Information Science and Technology, Osaka university, and Aida Laboratory, Graduate School of System Design, Tokyo Metropolitan University. I am thankful to Ms. Hiroko Hatagami, Ms. Yoshimi Fujita, Ms. Rie Shindo and Ms. Yoshiko Horiuchi, for their kind help. I thank Mr. Keiichiro Tsukamoto and Mr. Takamichi Nishijima for continuous discussions regarding my researches in the Information Sharing Platform Laboratory. I thank Mr. Yoshiyuki Isii, Mr. Hirokazu Kariya, Mr. Shotaro Motomura, and Ms. Makiko Tanabe, for their support and encouragement in Aida Laboratory.

Finally, I would like to express my greatly appreciation to Mr. and Mis. Watabe, my parents, and Dr. Shoji Watabe, my uncle, for their heartily help and financial support.

Contents

List of Figures

List of Tables

Chapter 1

Introduction

1.1 Background

As networked systems have been playing an important role in infrastructure, precisely measuring and modeling them have been becoming important. As our social activities depend on them, higher reliability is required to them. To design/manage highly reliable systems, precise evaluations of these systems are essential. Evaluating a system is clarifying how often the system enters an undesirable state like system outage and congestion or how long the system is in the state. To achieve precise evaluation, it requires an evaluator who does measuring and modeling to precisely know or infer current and future states of the system. A state is a set of numerous variables (e.g. delay on each link, the number of packets in each router, traffic demand for each source-destination pair, etc.), and a system transits one state from another over time. Each variable is changing in time, and does not take multiple values at the same time. Therefore, variables are represented as deterministic processes. If an evaluator is able to precisely obtain its every variable all the time, the evaluation result is unique and it is not stochastic but deterministic. There are two ways to obtain its every variable all the time. One is precisely measuring every variable all the time. The other is to model variables of a system by completely understanding the dynamics of the state transition. In this case, he or she can determine the next state transition from the current state, thereby obtaining the future states inductively.

However, when we evaluate actual systems by measuring or modeling, fluctuations of

knowledge of states appear, and the evaluation result is not deterministic. In evaluations of actual systems, an evaluator uses incomplete knowledge of the states since he or she cannot precisely obtain every variable of the system all the time. This is because, generally, it is difficult to precisely measure every variable of an actual system all the time or to model variables of an actual system by completely understanding the dynamics of the state transition. Depending on how an evaluator measures or models variables of an actual system, his or her knowledge of the states is fluctuated. Therefore, the evaluation result is not deterministic.

Fluctuations appear when an evaluator measure variables of an actual system. He or she obtains a value of variable at a certain time and obtain the knowledge of the states as values of variables by one or more measurements. He or she may be able to measure only a part of the variables, and they are not measured all the time. Hence, the knowledge of the states that he or she can obtain is fluctuated depending on measured variables and measurement timing. The fluctuations due to measured variables and measurement timing cause nondeterministic evaluation result. A typical example in which the fluctuations due to measured variables appear is that in large-scale network measurement wherein it is difficult to measure traffic on every link. In large-scale network measurement, variables correspond to traffic volume on links. Therefore, measured variables are only a part of the variables since an evaluator cannot measure traffic at all links in the network. As a result, an evaluation result is not deterministic since the knowledge of the states can be fluctuated depending what sets of links are measured. Moreover, in each measurement, fluctuations due to measurement precision provided by measuring equipment and fluctuations due to measurement indirection also appear. The former fluctuations mean a difference between measured value provided by a measuring equipment and true value of variable due to limit of a measuring equipment, and the knowledge of states can be fluctuated. The later fluctuation is caused by the fact that an evaluator often infers a variable that is difficult to measure from other variables that are related to it. We call this a indirect measurement of the variable. Error due to indirect measurement is contained in each measured value unless relation between the variable and the other variables is one-to-one correspondence, and the knowledge of states can be fluctuated.

Fluctuations appear when an evaluator models variables of an actual system as well.

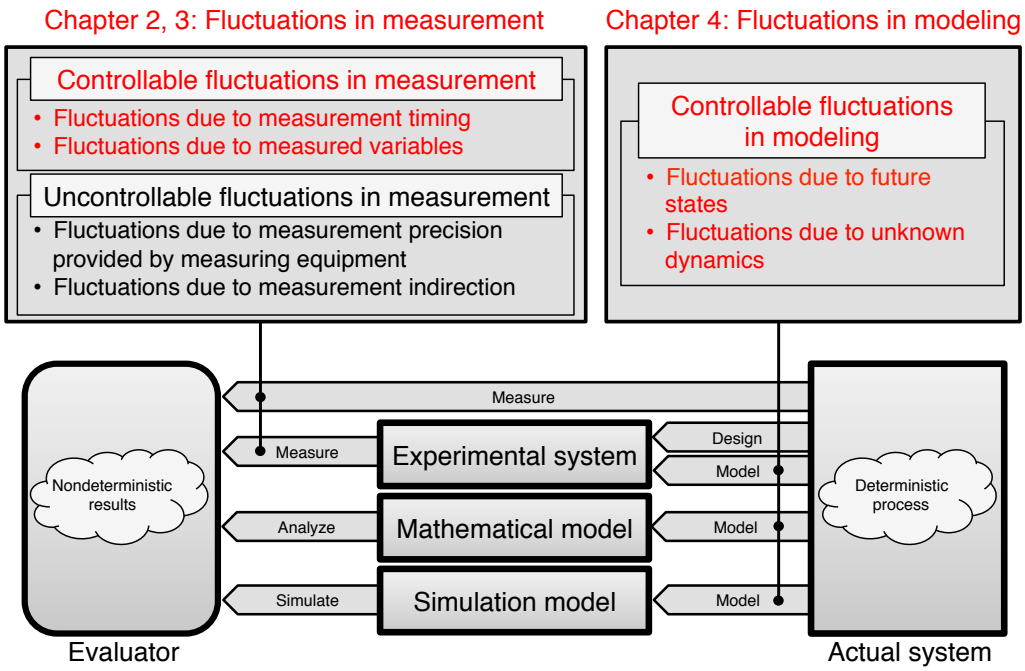

Figure 1.1: Controllable/uncontrollable part of fluctuations in performance evaluations

He or she cannot determine the state transition from the current state since he or she cannot completely understand dynamics of the state transition because the system usually includes a number of variables and does not know future states. Therefore, using model of variables of an actual system by incompletely understanding the dynamics of the state transition is unavoidable. The values of variables of a system depend on a model. Hence, knowledge of the states can be fluctuated depending on a model. The fluctuations due to unknown dynamics and fluctuations of future states in modeling cause the nondeterministic evaluation result. Due to the fluctuations, an evaluator is often forced to use stochastic models to describe the probability of various state transitions of an actual system, and the evaluation results are not deterministic.

To provide precise performance evaluations of networked systems, it is critically important how we control these fluctuations in performance evaluations.

1.2 Approaches for Controlling Fluctuations in Performance Evaluations

There are several approaches to evaluate actual systems, but fluctuations appear in performance evaluations even if an evaluator takes any approach (see Figure 1.1). Approaches for networked system evaluations are classified into the three approaches: evaluation based on actual systems in operation, mathematical analysis, simulation, and experiments with actual machines. When an evaluator takes the approach of an evaluation based on actual system in operation, an evaluation requires measurement like active or passive measurement. Hence, the fluctuations in measurement appear in performance evaluations. On the other hand, when an evaluator takes the approaches of evaluation based on mathematical analysis and simulation, fluctuations in modeling appear in performance evaluations, since an evaluator use models to perform analysis or simulation. In evaluations based on experimental system including benchmark test, both fluctuations in measurement and modeling appear, since an evaluator measures an experimental system and uses models partially.

Several fluctuations shown in Figure 1.1 are often controllable, and it is important to appropriately control these fluctuations. Usually, fluctuations due to measurement precision provided by measuring equipment and fluctuations due to measurement indirection are uncontrollable, and there has already been many prior works that yielded rich harvests in the field of statistics. The other factors are usually controllable though there are several limitations due to an implementation, analysis, and simulation. For example, in passive measurement in which an evaluator captures packets on wires, an evaluator controls positions of packet capturing cards on a target network thereby controlling the fluctuations due to measured variables. In performance evaluations by modeling, an evaluator can also decide how to model. In this thesis, we focus on these controllable fluctuations since there is probability that we can improve precision of performance evaluations by controlling the fluctuations.

Some earlier researches provided guidelines when we control these controllable fluctuations. In the following, we introduce two researches that provided guidelines to control these controllable fluctuations in performance evaluations.

In the framework of active measurement of networks, works by Baccelli et al. provide us some insights regarding how to control fluctuations due to measurement timing that is classified into fluctuations in measurement [1]. Active measurement is an end-to-end Quality of Service (QoS) measurement technique that derives QoS from information obtained by injecting probe packets into a target network path, and it can measure one-way delay, Round-Trip Time (RTT), loss rate, link capacity [2, 3], available bandwidth [4, 5], and so on. In active measurement, there is a dilemma that resembles the one underlying Heisenberg's uncertainty principle [6] on physics since the probe packets injection affects the path's performance. The dilemma is that a measurement perturbs the system, thereby reducing the precision of a measurement (Roughan showed the fundamental bounds on precision as the inequality whose form resembles Heisenberg's inequality on active measurement [7]). Therefore, it is important to be able to achieve highly precise measurements with a limited number of probe packets. In active measurement for delay and loss, we can consider that delay/loss that is experienced by probe packet is a sample of a target delay/loss process. How to obtain characteristics of processes by the limited number of samples has been discussed in the field of signal processing, ergodic theory, statistics etc. for a long time and rich harvests including the Shannon sampling theorem [8] have been yielded. By using the harvests and dividing the case where the effect of probe packets on the path performance is negligible and the other case, Baccelli et al. clarified conditions to achieve appropriate measurement for each case in active measurement [9]. Moreover, based on the results of [9], they investigated the relationship between precision of active measurement and an inter-probe time distribution, and proposed a new probing policy, called Gamma-probing [1]. To control an inter-probe time distribution is to control the fluctuations of sampling timing. Therefore, we can grasp that one of the method (i.e. Gamma-probing) to control fluctuations due to measurement timing on the framework of active measurement was proposed in the work.

In regards to fluctuations in modeling, to evaluate the probability of rare system outages on systems with retry traffic due to user impatience, Aida et al. provide the *quasi-static approach* in which a system behavior is described by deterministic process and fluctuations separately [10]. In the system model that is treated in the work, future traffic intensity including retry traffic depends on a system variable (the average of the number

of users in the system), and the system state fluctuates because the number of users in the system is averaged on a finite period. Therefore, the system state in the future is not determined. In the quasi-static approach, a temporal evolution of a system state is described by a deterministic process that means average process of system state and fluctuations that are accumulation of small fluctuations at each time. Therefore, if we can appropriately control these small fluctuations, future states of the system is exactly evaluated.

The fluctuations that we deal with in this thesis are fluctuations of probe packet timing in active measurement and fluctuations of the traffic intensity in the quasi-static approach. The former is categorized into the fluctuations due to measurement timing. Active measurement is a typical example in which the fluctuations due to measurement timing appear. In active measurement, the role of the fluctuations of probe packet timing is to cancel the effect of a specific pattern of measurement timing. If an evaluator measures a variable at measurement time with a specific pattern that corresponds to a pattern of a target variable, the value of variable by the measurement cannot represent the original variable. On the other hand, the latter is categorized into the fluctuations due to future states since future states are inferred by a stochastic model in the quasi-static approach. The role of the fluctuation in the quasi-static approach is to describe atypical transition of a system state. In high reliable systems, atypical transition of state arises when a system enters an undesirable state since it is rare that a system enters an undesirable state. In the quasi-static approach, temporal evolution of a value of a system variable (traffic intensity) is described by an average process and fluctuations. Typical transition of the variable is described by an average process. Atypical transition differs from typical transition that is described by an average process, and fluctuations that are represented by white Gaussian noise describe the difference.

In this thesis, we focus on fluctuations in network performance evaluation, and we improve precision of performance evaluations by controlling fluctuation magnitude. We show how to determine magnitude of fluctuations, to achieve precise performance evaluations. It is a key technology goal to perform precise evaluations in networked systems since they provide useful information for design/management of reliable networked systems. A precision improvement of evaluation in networked systems allows us to design/manage reliable system.

1.3 Outline of Thesis

The following challenges are tackled in this thesis.

Probe Interval Control that Improve Precision of CoMPACT Monitor [11–16]

In Chapter 2, in the framework of CoMPACT monitor that offers scalable per-flow QoS measurement, we apply Gamma-probing [1] that Baccelli et al. have proposed as the active measurement component of it to improve precision of evaluation. We discuss how to control fluctuations due to measurement timing for deterministic process. The significant issue in this application lies in the difference between the objects targeted for measurement. In reference [1], the process observed by probe packets is assumed to be stationary and ergodic stochastic process. This means that precision improvement is guaranteed only when the ensemble mean of a stationary stochastic process is measured. However, CoMPACT monitor measures the time average of the sample path that is deterministic process. Therefore, we should carefully investigate the characteristics of CoMPACT monitor with Gamma-probing.

We investigate the characteristics of CoMPACT monitor and Gamma-probing, and verify the improved precision of CoMPACT monitor. The requirement that assures the achievement of precision improvement was clarified. By using both theoretical investigation and simulation results complementarily, we show that the Gamma-probing proposed in [1] can be useful to be added to CoMPACT monitor for estimating the time average of sample paths. Moreover, through the investigation, we obtain the knowledge in sample path observation regarding the synchronization problem between probe packets timing and network congestions. The problem is referred to as the phase-lock phenomenon. If probe packets timing synchronizes network congestion, the estimator is not correspond to true value. We understand that the phase-lock phenomenon is possible only when the measurement period is finite, and the cause of the phase-lock phenomenon is accidental periodicity of sample path on finite measurement period.

On Optimal Magnitude of Fluctuations in Probe Packet Arrival Intervals [17–20]

In Chapter 3, in the framework of active measurement, we analyze the optimal magnitude of fluctuations in inter-probe time by the description on which we separate the probing process into a deterministic process and stochastic fluctuations. Gamma-probing provides multiple selections lying between traditional PASTA-based probing in which probe packets timing obeys Poisson arrivals and periodic-probing through parameter, and it is a great advance in network measurement techniques. However, since reference [1] did not indicate how to decide upon the optimal parameter, it has remained a unsolved problem.

Based on the knowledge obtained by the above-mentioned study regarding CoMPACT monitor, we understand that the important point in avoiding the phase-lock phenomenon caused by accidental periodicity is to shift the cycle of the probe packet injection by adding fluctuations. Therefore, we introduce a probing policy in which we explicitly separate the probing process into a deterministic process and stochastic fluctuations with normal distribution, and we determine the optimal fluctuation magnitude for the target process. Moreover, we introduce some evaluation examples to provide guidance on designing experiments to network researchers and practitioners. The examples yield insights on the relationships among measurement parameters, network parameters, and the optimal fluctuation magnitude.

As a result, we can understand how we should optimize fluctuations due to measurement timing corresponding to characteristics of a target system. The knowledge that is obtained by the above results (including the study with regard to CoMPACT monitor) can be applied to fluctuations due to measured variables.

Modeling Fluctuations in the Quasi-static Approach Describing the Temporal Evolution of Retry Traffic [21–23]

In Chapter 4, in the framework of the quasi-static approach, we model the fluctuations and determine appropriate magnitude of the fluctuations for precisely evaluating the probability of rare system outages on highly reliable systems. In the quasi-static approach, a target system state is described by separating the deterministic process and stochastic fluctuations just as we described the probing process in the above-mentioned study of active

measurement. It is easily expected that the exactness of fluctuations magnitude in the quasi-static approach greatly affect precision of models and evaluations. We discuss how to model the fluctuations for precisely replicating the state of retry traffic caused by user impatience using the quasi-static approach, and show the modeling method to determine the appropriate magnitude of stochastic fluctuations. We demonstrate modeling of the fluctuations in M/M/1- and M/M/s-based systems with retry traffic, and compare the results of the quasi-static approach and those of the conventional Monte Carlo simulation of queuing systems.

Finally, Chapter 5 concludes this thesis.

Chapter 2

Probe Interval Control that Improve Precision of CoMPACT Monitor

2.1 Introduction

With the rapid growth of the Internet over the last few years, it has come to play an important role as a key social infrastructure. Various applications provide new services including telephony and live video on the Internet, and the traffic they stream exhibits complex characteristics. These various applications require various QoS guarantees and so differ from traditional e-mail and web browsing applications. Given that even more unusual applications will arise in the future, the diversification of QoS requirements can only strengthen.

In order to meet such the varied network control requirements, we need a measurement technology that can produce detailed QoS information. Measuring the QoS for each flow (e.g., users, applications, or organizations) is important since it is a key parameter in service level agreements (SLAs) between the Internet service provider (ISP) and the user. One-way packet delay is one of the most important QoS metrics. This paper focuses on the measurement of one-way delay for each flow.

Many tools have been proposed to assess QoS including one-way delay [24, 25], and have also been evaluated in previous studies [26–28]. Conventional techniques of measuring network performance and QoS can be classified as either passive or active mea-

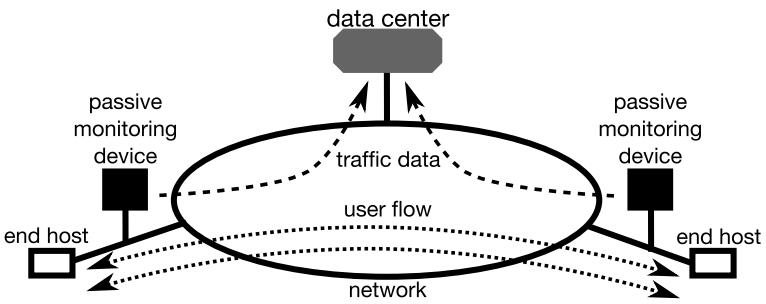

Figure 2.1: Two-point passive measurement

surements.

Passive measurement monitors the target user packet directly, by capturing the packets, including the target information (see Figure 2.1). Passive measurement is used to measure the volume of traffic, one-way delay, RTT, loss, etc. It can get any desired information about the traffic since it observes the actual traffic. Passive measurement can be categorized into two-point monitoring with data-matching processes (to measure one-way delay etc.) and one-point monitoring (to measure the volume of traffic etc.).

Passive measurement has the advantage of precision. However, if we perform passive measurements in a large-scale network, the number of monitored packets is enormous, and network resources are wasted by gathering the monitored data at the data center. Moreover, in order to measure delay, it is necessary to determine the difference in arrival time of a particular packet at different points in the network. This requires searching for the packet which was recorded in the data monitored at one point from the data monitored at other point. This packet matching process lacks scalability, so passive measurement lacks scalability.

Active measurement monitors QoS by injecting probe packets into a network path and monitoring them (see Figure 2.2 and [29–32]). Active measurement can be used to measure one-way delay, RTT, loss, available bandwidth [4], etc. It cannot obtain the per-flow QoS, but this is easy for the end user to perform. Unfortunately, the QoS data obtained by active measurement does not represent the QoS of the user packets, only QoS of the probe packets.

The authors previously described how the advantages of active and passive measure-

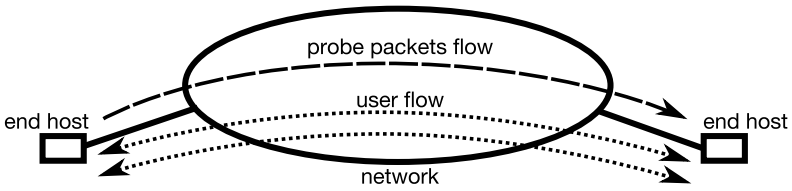

Figure 2.2: Active measurement

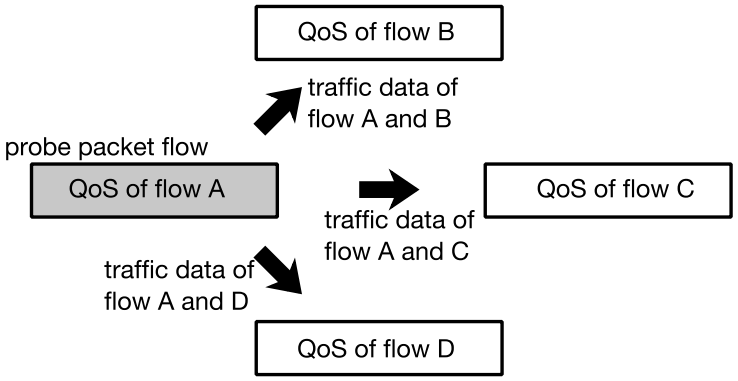

Figure 2.3: The transformation of QoS by CoMPACT monitor

ments could be joined in their scalable measurement proposal called CoMPACT monitor; it offers per-flow QoS measurement [33–35].

The idea of CoMPACT monitor is as follows. The direct measurement of QoS of the target flow by passive measurement is not really feasible due to the scalability problem. Instead, the QoS of the target flow is gained by transforming QoS data obtained by active measurement. The transformation reflects the passively monitored traffic data (volume of traffic) of the target flow (see Figure 2.3). We show the composition of CoMPACT monitor in Figure 2.4. The problem of scalability is well suppressed, because the volume of traffic can be measured by one-point passive measurement without requiring data-matching processes.

We original assumed that Poisson arrivals (intervals follow an exponential distribution) would be most appropriate for designing a policy of probe packet arrival since it

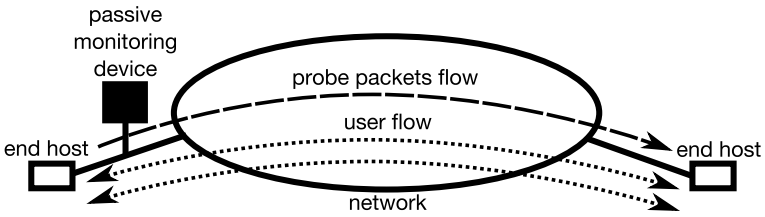

Figure 2.4: The composition of CoMPACT monitor

permits the application of Poisson Arrivals See Time Averages (PASTA) property [36]. In addition, we applied the exponential distribution, as an inter-probe time distribution, in verifying CoMPACT monitor.

However, recent work [9] indicates that there maybe many distributions that are more precise than an exponential distribution if a non-intrusive context (ignoring the existence of probe packets) can be assumed. Moreover, according to [1], we can find a distribution that is suboptimal in precision by setting the inter-probe time according to a parameterized Gamma distribution.

This paper confirms that applying Gamma-probing to CoMPACT monitor can improve its precision in measuring the one-way delay distribution of individual flows. The significant issue in this application lies in the difference between the objects targeted for measurement. In [1], the process observed by probe packets is assumed to be stationary and ergodic stochastic. This means that precision improvement is guaranteed only when the ensemble mean of a stationary stochastic process is estimated. However, CoMPACT monitor estimates the time average of the sampled path. Therefore, we should carefully investigate the characteristics of CoMPACT monitor with Gamma-probing.

Our investigation is based on both theoretical and simulation-based approaches. In the theoretical approach, we verify the relation between the stochastic process of probe packet arrivals and the precision of CoMPACT monitor, and clarify the requirement for improvement of the precision. In the simulation-based approach, we show the following three facts.

- The requirement for the precision improvement is applicable also to CoMPACT monitor.

- CoMPACT monitor with Gamma-probing can estimate the true value without bias.
- Gamma-probing can decrease the variance of the estimator which is measured by CoMPACT monitor (namely the precision can be improved).

By using both theoretical investigation and simulation results complementarily, we show the effectiveness of Gamma-probing for CoMPACT monitor.

The rest of the paper is organized as follows. We describe the concept and mathematical formulation of CoMPACT monitor in section 2.2. Next, we briefly summarize the theory of Gamma-probing for active measurement in section 2.3. Section 2.4 discusses the difference in objects targeted between Gamma-probing and CoMPACT monitor. To confirm that the precision of CoMPACT monitor can be improved by Gamma-probing, we execute some simulations in section 2.5 and section 2.7. We summarizes the paper in section 2.8.

2.2 Summary of CoMPACT Monitor

2.2.1 The Concept

CoMPACT monitor estimates an empirical QoS for the target flow by converting observed values of network performance at timing of probe packet arrivals into a measure of the target flow timing. Now, let $v(t)$ be a continuous-time stochastic process that represents the value of a certain QoS metric at time t (e.g. the virtual one-way delay of the network path at time t), and let $X_k = v(T)$ be a random variable which represents the value of the QoS metric at a certain time T. T is the time of the packet arrival from a certain user k. It is worth noting that X_k depends on user k. That is, different users experience different QoS, in general. X_k means the value of QoS metric which is experienced by user k. Our measurement objective is the distribution of a QoS metric (one-way delay) that is experienced by individual user. The probability of X_k exceeding c is

$$\begin{aligned}\Pr(X_k > c) &= \int 1_{\{x>c\}} \mathrm{d}F_k(x) \\ &= \mathrm{E}_{F_k}[1_{\{x>c\}}]\end{aligned}$$

where $F_k(x)$ and $1_{\{.\}}$ denote, respectively, the distribution function of X_k and the indicator function, and E_{F_k} denotes the expectation with respect to F_k.

If we can directly monitor X_k, its distribution can be estimated by

$$\frac{1}{m}\sum_{n=1}^{m} 1_{\{X_k(n)>c\}}, \qquad \text{for sufficiently large } m.$$

where $X_k(n)$ $(n = 1, 2, \ldots, m)$ denotes the nth observed value of X_k. Now, let us consider the situation that X_k cannot be directly monitored (actually, we cannot directly monitor X_k by using passive measurement in large-scale networks). Let Y denote a random variable which is observed $v(t)$ with a different timing (e.g. timing of probe packet arrivals), independent of X_k. This forces us to consider the relationship between X_k and Y.

Observed values of X_k and Y are different if their timing is different, even if they observe a common process $v(t)$ (see Figure 2.5). X_k and Y can be related by each distribution functions $F_k(x)$ and $G(y)$, and $\Pr(X_k > c)$ expressed by measure of X_k can be transformed into measure of Y as follows.

$$\begin{aligned}
\Pr(X_k > c) &= \int 1_{\{x>c\}} \mathrm{d}F_k(x) \\
&= \int 1_{\{y>c\}} \frac{\mathrm{d}F_k(y)}{\mathrm{d}G(y)} \mathrm{d}G(y) \\
&= \mathrm{E}_G\left[1_{\{Y>c\}} \frac{\mathrm{d}F_k(Y)}{\mathrm{d}G(Y)}\right]
\end{aligned}$$

where E_G denotes the expectation with respect to G.

Therefore, $\Pr(X_k > c)$ can be estimated by

$$\frac{1}{m}\sum_{n=1}^{m} 1_{\{Y(n)>c\}} \frac{\mathrm{d}F_k(Y(n))}{\mathrm{d}G(Y(n))}, \quad \text{for sufficiently large } m. \tag{2.1}$$

where $Y(n)$ $(n = 1, 2, \ldots, m)$ denotes the nth observed value of Y. Note that this estimator does not need to know $X_k(n)$, if we can get $\mathrm{d}F_k(Y(n))/\mathrm{d}G(Y(n))$. This means the QoS of a specific flow (as decided by k) can be estimated by just one probe packet flow which arrives with timing of Y.

2.2.2 Mathematical Formulation

This subsection briefly summarizes the mathematical formulation of the CoMPACT monitor with regard to one-way delay [35]. We assume the traffic in the target flow can be

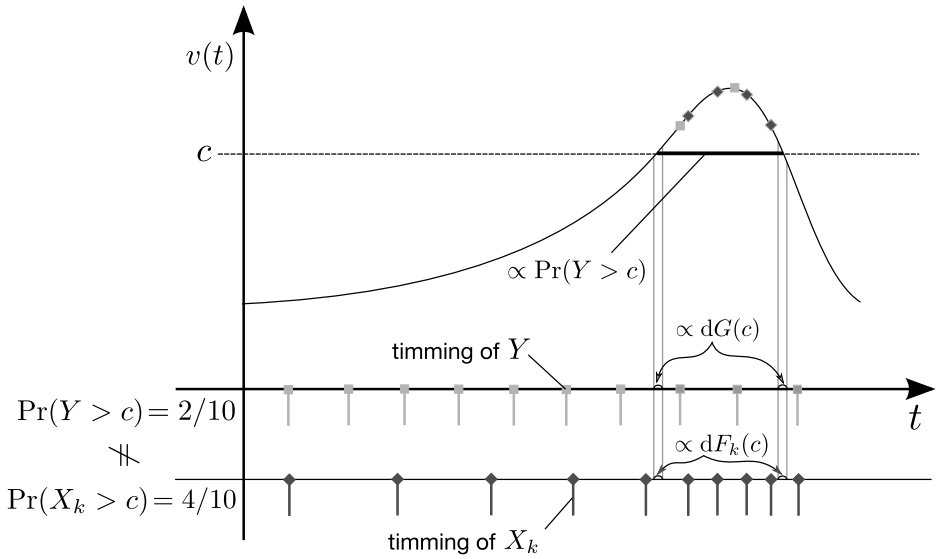

Figure 2.5: The relation between timing of arrivals and empirical QoS

treated as a fluid. In other words, we assume the target flow packets outnumber the active probe packets.

Let $a(t)$ and $v(t)$ denote, respectively, the traffic in the target flow at time t (≥ 0) and the virtual one-way delay on the path that we want to measure. $a(t)$ and $v(t)$ are nonnegative deterministic processes assumed to be right-continuous with left limits and bounded on $t \geq 0$. We can take $a(t)$ and $v(t)$ as sample paths of the corresponding stochastic processes.

Considering the measurement of the empirical one-way delay distribution $\pi(c)$, the value we want to measure is the ratio of traffic whose delay exceeds c to all traffic of the target flow, which is given by

$$\pi(c) = \lim_{t\to\infty} \frac{\int_0^t 1_{\{v(s)>c\}} a(s)\mathrm{d}s}{\int_0^t a(s)\mathrm{d}s}. \tag{2.2}$$

$\pi(c)$ can be estimated by estimator $Z_m(c)$ as follows (see reference [35] for details).

$$\begin{aligned} Z_m(c) &= \frac{1}{m}\sum_{n=1}^{m} 1_{\{v(T_n)>c\}} \frac{a(T_n)}{\sum_{l=1}^{m} a(T_l)/m} \\ &= \sum_{n=1}^{m} 1_{\{v(T_n)>c\}} \frac{a(T_n)}{\sum_{l=1}^{m} a(T_l)} \end{aligned} \tag{2.3}$$

for sufficiently large m, where T_n $(n = 1, 2, \ldots, m)$ denotes the nth sampling time, and each time of sampling corresponds to a time of probe packet arrival. Active and one-point passive measurement are used to observe $v(T_n)$ and $a(T_n)$, respectively. Note that measuring the volume of traffic by one-point passive measurement is achieved much more easily than measuring the one-way delay by two-point passive measurement.

If we extract quantity $\sum_{n=1}^{m} 1_{\{v(T_n)>c\}}/m$ from (2.3), we can use it as a simple active estimator that counts the packets whose delay exceeds c. However, (2.3) is weighted by $a(T_n)/(\sum_{l=1}^{m} a(T_l)/m)$, which is decided by the traffic in the target flow when probe packets arrive. This means that the one-way delay distribution (measured by active measurement without bias) is corrected to the empirical one-way delay distribution by the bias of the target flow (observed by passive measurement). $a(T_n)/(\sum_{l=1}^{m} a(T_l)/m)$ in (2.3) corresponds to $\mathrm{d}F_k(Y(n))/\mathrm{d}G(Y(n))$ in (2.1).

Since the traffic is not really a fluid, we use the number of packets that are in the δ-neighborhood of T_n $[\max\{T_n - \delta/2, T_{n-1}\}, \min\{T_{n+1}, T_n + \delta/2\})$ instead of $a(T_n)$, where δ is a predefined small positive number [35].

2.3 Suboptimal Probe Intervals

2.3.1 NIMASTA

Since the PASTA property is good for non-biased measurement, Poisson arrivals (intervals follow an exponential distribution) have been widely used as the design policy of probe packet arrivals for active measurement. However, recent work [9] indicates that there may be many other distributions that can estimate the true value if a non-intrusive context (the effect of probe packets is ignored) can be assumed. This property was named Non-Intrusive Mixing Arrivals See Time Averages (NIMASTA) in [9].

NIMASTA contains three assumptions. First, the stochastic process that expresses the network state we are interested in (e.g. virtual delay) is stationary and ergodic. This process is called the ground truth process in [1]. Second, the point process of probe packets arrivals $\{T_n\}$ $(n = 1, 2, \ldots, m)$ is stationary and mixing. Mixing is the requirement to guarantee joint ergodicity between the probe and ground truth processes (see reference [9] for details). The last assumption is the non-intrusive context, i.e. we can ignore

the impact of probe packets. Namely, the ratio of the probe stream to all streams is very small.

Under the above assumptions, [9] proved that the following equation holds.

$$\lim_{m\to\infty}\frac{1}{m}\sum_{n=1}^{m} f(Y(T_n)) = \lim_{t\to\infty}\frac{1}{t}\int_0^t f(Y(t))\mathrm{d}t$$
$$= \mathrm{E}[f(Y(0))] \qquad \text{a.s.,} \tag{2.4}$$

where f and $Y(t)$ denote an arbitrary positive function and the ground truth process, respectively. (2.4) means that we can estimate the ensemble mean of the ground truth process $\mathrm{E}[f(Y(0))]$ by using any probe packet policy if the point process of probe packet arrival $\{T_n\}$ is mixing. An example of the mixing point process has processes whose intervals follow the Gamma distribution and the uniform distribution. Note that periodic-probing with fixed intervals is not a mixing process, and does not satisfy (2.4).

2.3.2 Setting Probe Intervals to Decrease Variance

A recent study [1] reported that NIMASTA-based probing offers improved measurement precision. We can select a suboptimal (in terms of precision) probing process under a specific assumption by using the inter-probe time given by the parameterized Gamma distribution.

If we estimate the mean of $Y(0)$ by using active measurement, estimator $\hat{p}$ is

$$\hat{p} = \frac{1}{m}\sum_{n=1}^{m} Y(T_n). \tag{2.5}$$

Thus the variance of $\hat{p}$ is

$$\mathrm{Var}[\hat{p}] = \frac{1}{m^2}\mathrm{Var}\left[\sum_{n=1}^{m} Y(T_n)\right]$$
$$= \frac{1}{m^2}\sum_{n=1}^{m}\mathrm{Var}[Y(T_n)] + \frac{2}{m^2}\sum_{n\neq l}\mathrm{Cov}\left(Y(T_n), Y(T_l)\right) \tag{2.6}$$
$$= \frac{1}{m}\mathrm{Var}[Y(0)] + \frac{2}{m^2}\sum_{n\neq l}\int R(\tau) f_{|n-l|}(\tau)\mathrm{d}\tau \tag{2.7}$$

where f_k is probability density function (pdf) of T_k, $R(\tau) = \mathrm{Cov}\left(Y(t), Y(t-\tau)\right)$ is the AutoCovariance Function (ACF) of the ground truth process $Y(t)$ (we can express $R(\tau, t)$

by τ alone, because $Y(t)$ is stationary) and the last equality follows from the stationary property of $Y(t)$ and the probe packet process.

If $R(\tau)$ is convex, the following can be proven by using Jensen's inequality. No other probing process with an average interval of μ has a variance that is lower than that of periodic-probing (see reference [1]). Estimator variance is connected with precision, lower is better, so periodic-probing is the best policy if we focus only on variance.

On the other hand, periodic-probing does not satisfy the assumptions of NIMASTA due to non-mixing, so periodic-probing is not necessarily the best. This is because a phase-lock phenomenon may occur and the estimator may converge on a false value when the cycle of the ground truth process corresponds to the cycle of the probing process. Namely, periodic-probing has a bias.

To tune the tradeoff between traditional policies obeying Poisson arrivals and periodic-probing (which has a bias but has the advantage in terms of variance), [1] proposes a suboptimal policy that gives an inter-probe time that obeys the parameterized Gamma distribution. The pdf that is used as the interval between probe packets is given by

$$g(x) = \frac{x^{\beta-1}}{\Gamma(\beta)} \left(\frac{\beta}{\mu}\right)^{\beta} \mathrm{e}^{-x\beta/\mu} \qquad (x > 0), \tag{2.8}$$

where $g(x)$ is the Gamma distribution whose shape and scale parameters are β and μ/β, respectively. μ (> 0) denotes the mean, and β (> 0) is the parameter. When $\beta = 1$, $g(x)$ reduces to the exponential distribution with mean μ. When $\beta \to \infty$, the policy reduces to periodic-probing because $g(x)$ converges on $\delta(x - \mu)$.

If ACF is convex, it has been proven that the variance of estimator $\hat{p}$ sampled by intervals that follow (2.8) monotonically decreases as β increases. This decrease is caused by the decrease of the covariance part which is the second term on the right-hand side of (2.7). We can achieve small variance (it approaches the variance of periodic-probing) by setting β to a large value since (2.8) converges on periodic-probing towards limit $\beta \to \infty$.

The problem of bias due to the phase-lock phenomenon can be avoided if we tune β to a limited value (the probing process that has intervals set by (2.8) is mixing). Resolving the tradeoff between a traditional policy that assumes Poisson arrivals and periodic-probing yields a suboptimal probing process if we give β an appropriate value.

2.4 The Application to CoMPACT Monitor

This section discusses the application of Gamma-probing to CoMPACT monitor. First, we must determine the ground truth process observed by CoMPACT monitor. Comparing (2.5) with (2.3), we can consider that stochastic process $Y(t)$ observed by CoMPACT monitor is

$$Y(t) = 1_{\{V(t)>c\}} \frac{A(t)}{\mathrm{E}[A(t)]} \ , \tag{2.9}$$

where $V(t)$ and $A(t)$ are stochastic processes corresponding to sample path $v(t)$ and $a(t)$, respectively. If it is confirmed that the ACF $R(\tau)$ of stochastic process $Y(t)$ is convex, we can guarantee an improvement in precision due to Gamma-probing by applying the theory in section 2.3.

The convexity of ACF has been verified for cases of simple virtual delay process and loss process using data of large-scale passive measurements and simulations [1]. However, $Y(t)$ observed by CoMPACT monitor is weighted by traffic $A(t)$ of a specific flow, so the property of $Y(t)$ clearly differs from the delay/loss processes that are influenced by all flows on the network. Therefore, we must confirm the convexity of $R(\tau)$ in the CoMPACT monitor case. In section 2.5 and section 2.7, we will show that the assumption ($R(\tau)$ is convex) is appropriate to CoMPACT monitor.

As described in section 2.2, we consider $v(t)$ and $a(t)$ are sample paths of corresponding stochastic processes since CoMPACT monitor estimates the time average of sample path given by (2.2). However, as explained in section 2.3, the ground truth process $Y(t)$ is stationary stochastic process in [1], and the decrease of variance of $\hat{p}$ is guaranteed for the estimation of the ensemble mean of $Y(t)$. The variance of $\hat{p}$ depends on both stochastic variations of $Y(t)$ and T_n. On the other hand, CoMPACT monitor observe sample path $y(t)$ rather than stochastic process $Y(t)$, because CoMPACT monitor estimates one-way delay that is experienced by user flows.

Therefore, it is desired in CoMPACT monitor that variance of estimator $\hat{p}$ which depends only on sampling time T_n on certain sample path rather than $Y(t)$ decreases. In other words, variance we want to decrease is given by

$$\mathrm{Var}[\hat{p}] = \frac{1}{m^2} \sum_{n=1}^{m} \mathrm{Var}[y(T_n)] + \frac{1}{m^2} \sum_{n \neq l} \mathrm{Cov}(y(T_n), y(T_l)). \tag{2.10}$$

Note that (2.10) corresponds to (2.6). If the ACF of $Y(t)$ is convex, we can consider that the covariance part, which is the second term on the right-hand side of (2.10), tends to decrease as β increases. Thus the variance of inter-probe time given by (2.8) is μ^2/β; and it to decreases as β increases. Hence, we can also expect that the variance part, which is the first term on the right-hand side of (2.10), decreases as β increases since none of the observed values $y(T_n)$ vary. The convexity of ACF of $Y(t)$ is easily proven if $V(t)$ and $A(t)$ are independent and ACFs of them are convex. In section 2.5 and section 2.7, we will show that the variance of estimator which depends only on T_n decreases with increase of β by using Gamma-probing through the simulation.

2.5 The Effectiveness of Suboptimal Probe Intervals

2.5.1 Simulation Model

We used NS-2 [37] based simulations to investigate the effectiveness of Gamma-probing in the framework of CoMPACT monitor. The network model we used in the simulation is shown in Figure 2.6.

There are 20 pairs of source and destination end hosts. Each end host on the left in Figure 2.6 is a source and transfers packets by UDP to the corresponding destination end host on the right. User flows are given as ON/OFF processes and categorized into the four types listed in Table 2.1; there are five flows in each type.

Probe packet flows are categorized into the five types listed in Table 2.2. Note that *Exponential* and *Deterministic* in Table 2.2 are special cases of Gamma distribution, and parameters of *Exponential* and *Deterministic* are parameters of the Gamma distribution corresponding to each probe type. 300 flows of each type are streamed over the two routes shown in Figure 2.6, so the total number of probe packet flows in the network is 3000. To analyze the variance of the estimator, we streamed a large number of probe packet flows. Of course, we can estimate the empirical delay from just one probe packet in each flow.

User flow packets and probe packets are 1500 bytes and 64 bytes, respectively. Link capacities are identical at 64 Mbps. Delay occurs mainly in the link between the core routers, since it is a bottleneck, but no loss occurs, because there is sufficient buffering.

We observed the traffic by passive measurement at the queue of the edge router on the

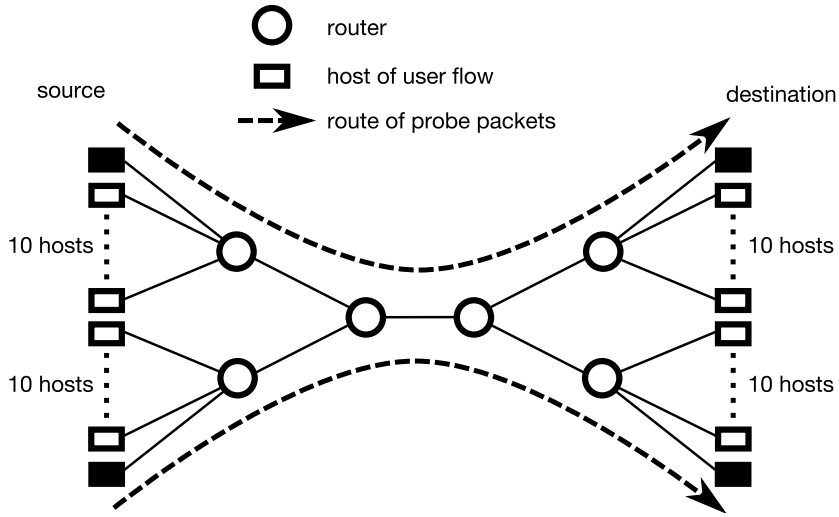

Figure 2.6: Network model

Table 2.1: Type of user flows

Flow type	Flow ID	Mean ON/OFF period	Distribution of ON/OFF length	Shape parameter	Rate at ON period
type 1	#1-5	10s/5s	Exponential	-	6 Mbps
type 2	#6-10	5s/10s	Exponential	-	6 Mbps
type 3	#11-15	5s/10s	Parete	1.5	9 Mbps
type 4	#16-20	1s/19s	Parete	1.5	9 Mbps

source side. Let δ denote 40 ms.

We ran the simulation for 500 s. The non-intrusive requirement (the effect of probe packets can be ignored) was satisfied, since the ratio of the probe stream to all streams is only 0.00197% or so.

2.5.2 The Convexity of ACF

In this subsection, we will discuss whether the ACF of the ground truth process $Y(t)$ is convex. Note that the ground truth process is treated as stochastic process $Y(t)$, not sample path $y(t)$.

The ground truth process observed by CoMPACT monitor is given by (2.9). We

Table 2.2: Type of probe

Distribution of probe intervals	Parameter β	Mean probe intervals
Exponential	$(\beta = 1)$	0.5 s
Gamma	$\beta = 5$	0.5 s
Gamma	$\beta = 25$	0.5 s
Gamma	$\beta = 125$	0.5 s
Deterministic (Periodic)	$(\beta \to \infty)$	0.5 s

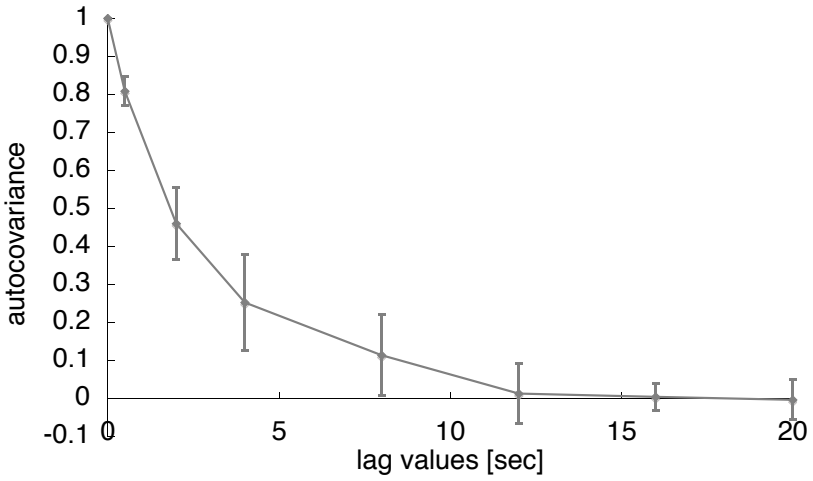

Figure 2.7: Autocovariance function (flow #1)

compute $V(t)$, which is the virtual one-way delay, by using the queue occupancy (byte) of the core router on the source side. In our simulation model, the greatest part of the delay occurs at the core router on source side, because the link between the core routers is a bottleneck. Thus we can ignore any delay at other routers.

The (standardized) ACF for $c = 0.1$ for flow #1 with 95% confidence intervals on 10 experiments is depicted in Figure 2.7. To plot Figure 2.7, we used data where the queue occupancy and the traffic were recorded every 0.01 seconds. Representing each flow type, we also plotted flows #6, #11 and #16. This permitted the conclusion that none of these results contradicted the assumption that ACF is convex.

2.5.3 One-way Delay Distribution

In this subsection, we will show that CoMPACT monitor can estimate the empirical one-way delay by using Gamma-probing. The estimation of the complementary Cumulative Distribution Function (CDF) of the one-way delay experienced by user flows (as given by (2.2)) will be shown below. Note that $v(t)$ and $a(t)$ are both sample paths in (2.2).

To estimate the complementary CDF of the one-way delay experienced by flow #1, we used probe packet flows with parameter $\beta = 1$, 25 and $\beta \to \infty$. Note that $\beta = 1$ corresponds to traditional PASTA-base probing. Each result, with 95% confidence intervals, is shown in Figure 2.8. Note that the horizontal axis, which is the one-way delay, corresponds to c in (2.2). To compare the empirical delay with the estimate from CoMPACT monitor, we include the estimate from active measurement in the plot.

In Figure 2.8, we can see that the CoMPACT monitor gives good estimates of the true value. We cannot judge the superiority or inferiority of any type of probe packet flows. Representing each flow type, we have plotted for flows #6, #11 and #16 and similar results are gained.

2.5.4 Precision Improvement of CoMPACT Monitor

In this subsection, we will verify the relationship between the parameter of Gamma distribution, used as the inter-probe time, and the variance of estimator. Note that we consider the variance of $\hat{p}$, which depends only on probe packet timing (namely, sampling time T_n).

We plot the standard deviation of each point of the complementary CDF (shown in subsection 2.5.3) in Figure 2.9. Note that the horizontal axis corresponds to the one-way delay, which is c in (2.2). Error bars indicate the 95% confidence intervals when the standard deviation calculated from 30 probe packet flows is considered to be a single data point.

The standard deviation clearly decreases as β increases from $\beta = 1$ to $\beta = 125$. Note that $\beta = 1$ corresponds to traditional PASTA-base probing. In periodic-probing, i.e. $\beta \to \infty$, the standard deviation is often larger than that with $\beta = 125$ or $\beta = 25$. Our belief is that this reversal is a sign of the phase-lock phenomenon, which occurs when the cycle of the ground truth process corresponds to the cycle of the probing process. In

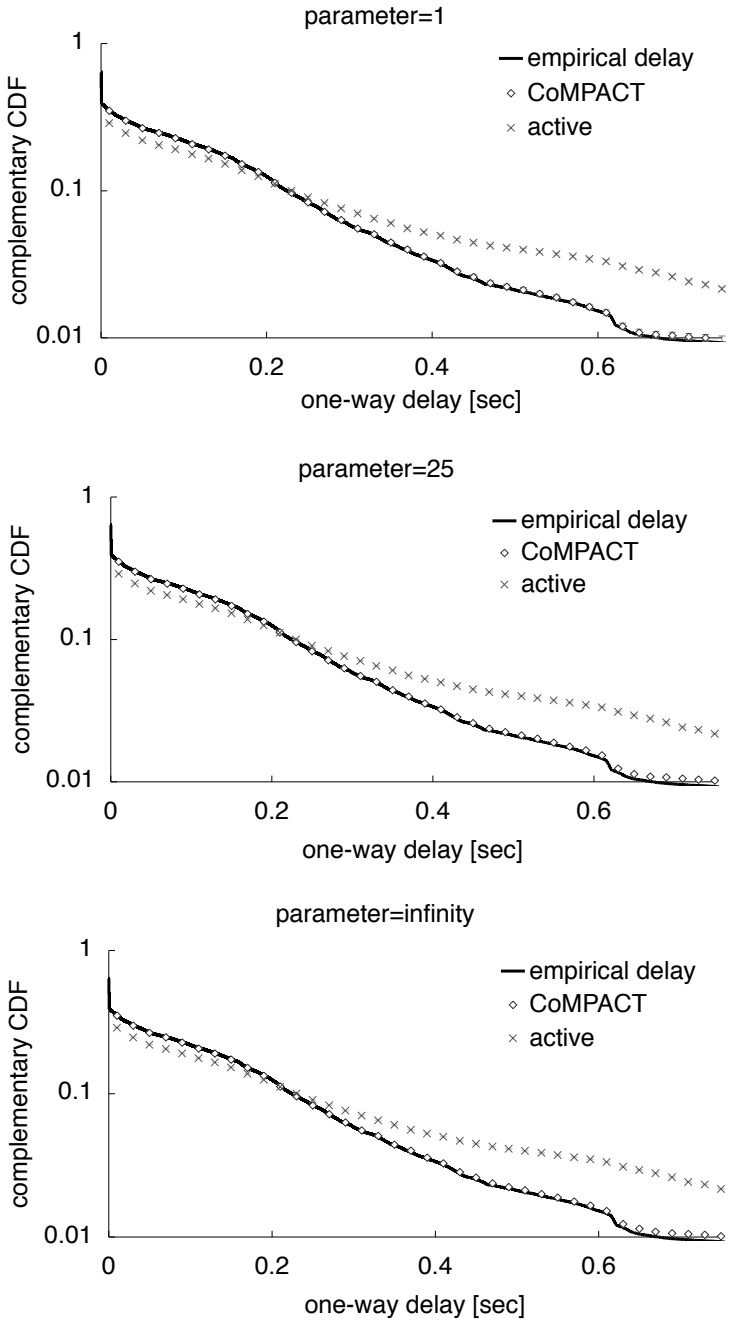

Figure 2.8: The estimation of complementary CDF (flow #1)

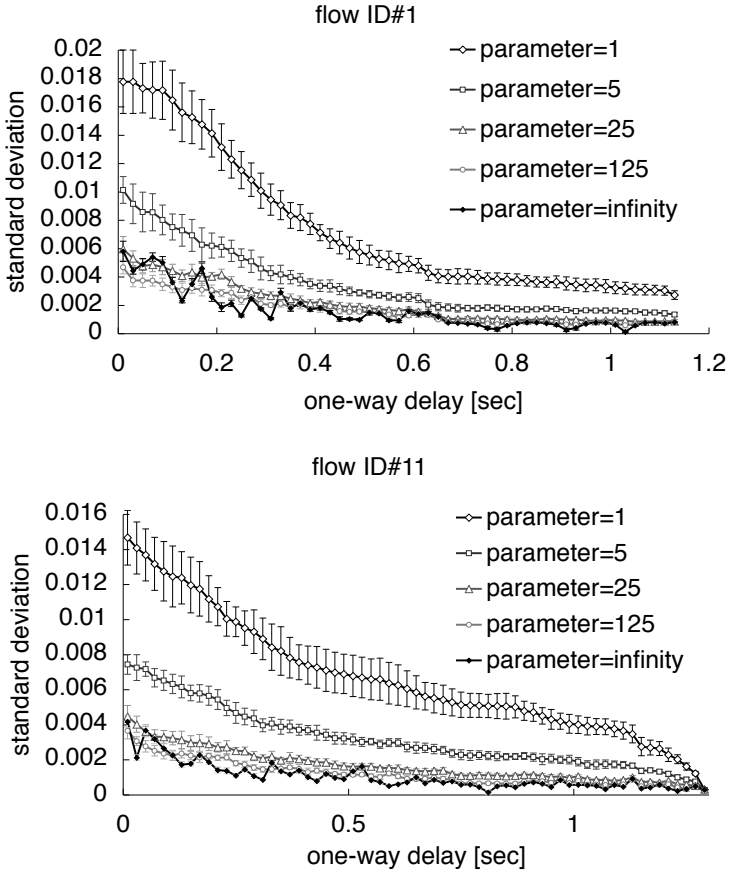

Figure 2.9: Standard deviation of estimator

section 2.6, we verify phase-lock phenomenon in detail. We got similar results for other flows though Figure 2.9 shows only the results of flow #1 and #11.

Consequently, it was confirmed that we can obtain adequate precision on variance, which depends only on sampling time T_n with a suboptimal probing process, if we tune the parameter of Gamma distribution, which is used as the inter-probe time.

2.5.5 The Upper Bounds of Variance

Supplementing the simulation results in previous subsection, we prove that periodic-probing is assuredly superior to the traditional PASTA-based probing.

Let us idealize the traffic process $a(t)$ as an ON/OFF process. We assume $a(t)$ is the

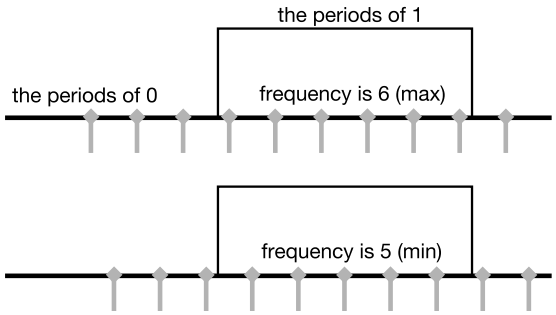

Figure 2.10: The observation frequency of periodic-probing

binary process which takes value α if the target flow streams, and 0 otherwise. Thus $\hat{p}$ is expressed by

$$\hat{p} = \sum_{n=1}^{m} 1_{\{v(T_n)>c\}} \frac{a(T_n)}{\sum_{l=1}^{m} a(T_l)} \tag{2.11}$$

$$= \sum_{n=1}^{m} 1_{\{v(T_n)>c\}} \frac{\alpha \cdot 1_{\{a(T_n)>0\}}}{\sum_{l=1}^{m} \alpha \cdot 1_{\{a(T_l)>0\}}}$$

$$= \frac{\sum_{n=1}^{m} 1_{\{v(T_n)>c \wedge a(T_n)>0\}}}{\sum_{l=1}^{m} 1_{\{a(T_l)>0\}}}. \tag{2.12}$$

Since UDP does not control the volume of traffic, this assumption is appropriate for UDP flows.

Now, we consider the range of (2.11). $1_{\{v(t)>c \wedge a(t)>0\}}$ and $1_{\{a(t)>0\}}$ are the binary processes, and we can divide them into the periods in which the processes take 0 and 1. If they are observed by periodic-probing, the difference between the maximum and minimum observation frequency is 1 at most in one period (see Figure 2.10).

The maximum range Δ of (2.11) is given by

$$\Delta = \frac{k_2}{mq - k_1}, \tag{2.13}$$

where k_1 and k_2 denote the number of periods of $1_{\{a(t)>0\}} = 1$ and $1_{\{v(t)>c \wedge a(t)>0\}} = 1$, respectively, and q denotes the time average of $1_{\{a(t)>0\}}$.

The distribution that has maximum variance with range Δ has the following pdf $h(x)$.

$$h(x) = \frac{1}{2}\delta(x-a) + \frac{1}{2}\delta(x-a-\Delta),$$

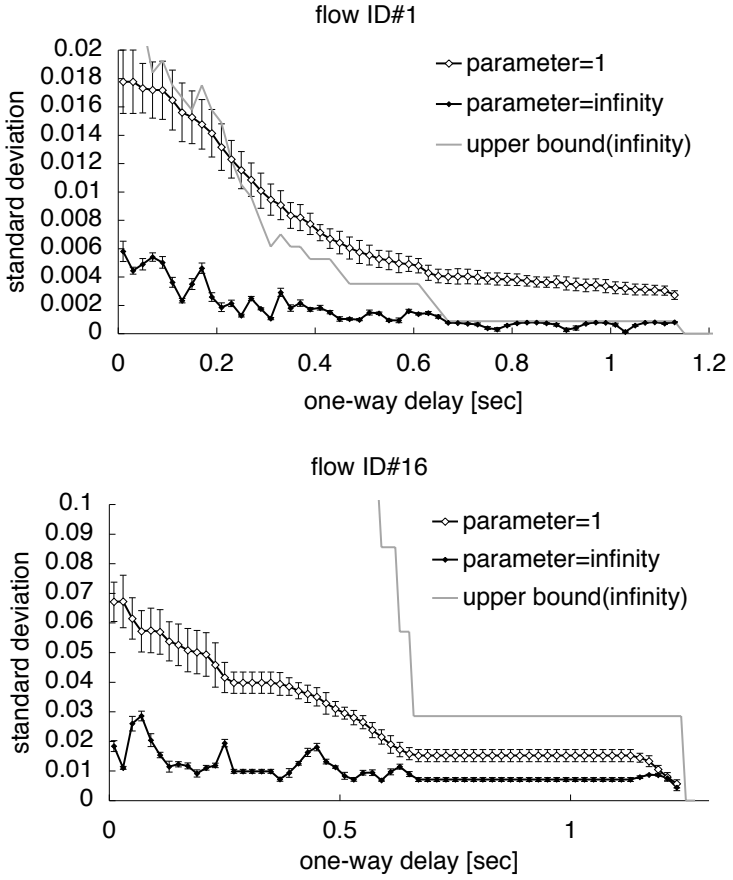

Figure 2.11: The upper bounds of periodic-probing

where $\delta(\cdot)$ denotes Dirac δ function and a is an arbitrary constant. Therefore, the upper bounds of estimator variance are as follows.

$$\begin{aligned} \mathrm{Var}[\hat{p}] &\leq \left(\frac{\Delta}{2}\right)^2 \\ &= \frac{{k_2}^2}{4(mq-k_1)^2}. \end{aligned} \tag{2.14}$$

Calculating k_1, k_2 and q in the above simulation, we plot the upper bounds of periodic-probing in Figure 2.11. Note that standard deviations of PASTA-based probing and periodic-probing (the same data as plotted in Figure 2.9) are displayed.

The results of flow #1 confirm that the upper bounds of periodic-probing are smaller than the standard deviation of PASTA-based probing in the domain of interest (the domain

with large delay). Therefore, it is guaranteed that periodic-probing is surely superior to PASTA-based probing. The results of flows #6, #11 (not displayed in Figure 2.9) are similar to the results of flow #1.

The results of flow #16 show that the upper bounds of periodic-probing are larger than the standard deviation of PASTA-based probing because the combination of flow type 4 (e.g. flow #16) and (2.14) is bad. The type 4 flows have short ON periods and long OFF periods as shown in Table 2.1. Thus the maximum range given by (2.13) becomes large because the denominator becomes small. Therefore, the appropriate upper bounds cannot be given by (2.14).

2.6 Phase-Lock Phenomenon

In this section, we will discuss the phase-lock phenomenon in sample path observation. We will show that the precision reversal between periodic-probing ($\beta \to \infty$) and Gamma-probing ($\beta = 125$) in Figure 2.9 occurs because periodic-probing locks the phase of the ground truth process.

Convex ACF means that the ground truth process does not have any specific periodicity. If the ACF is strictly convex, the variance of estimator with periodic-probing is minimum as described in section 2.3.

However, there is the possibility that sample path $y(t)$ has, over a finite interval, *accidental periodicity*, even if the ACF of the ground truth process $Y(t)$ is convex. This is because the sample path over a finite interval fails to well represent the characteristics of the corresponding stochastic process. Namely, it is possible that the sample path has, over a short time, some specific periodicity by chance, even if there is no specific periodicity over the long term. This accidental periodicity destroys the convexity of ACF with regard to the time average and thus causes the phase-lock phenomenon. If the interval in which we want to measure QoS is sufficiently long, the phase-lock phenomenon will not happen because the ACF of $y(t)$ over the long term converges on the ACF of $Y(t)$ in the meaning of ensemble mean (we must assume that $Y(t)$ is ergodic). Therefore, the phase-lock phenomenon is possible with finite observation intervals.

To verify the relation between accidental periodicity and precision, we altered the

simulation described in section 2.5. All conditions were unchanged except for the characteristics of probe packets which were altered as follows. The parameter of inter-probe time was set at $\beta \to \infty$ (periodic-probing) and $\beta = 125$. We examined probe packets with 61 different inter-probe times (namely 61 kinds of periodicity). Mean number of probe packets in the 500 s simulation (corresponding to m) ran from 970 to 1030 (e.g. if mean number of probe packets is 1000, the mean inter-probe time is 500 s / 1000 packet $= 0.5$ s).

We estimated one-way delay by probe packet flows which have 61 kinds of periodicity, and compared the variance of estimator with the power spectrum of the sample path over the simulation time $|\mathcal{F}[y(t)]|^2$ $(0 \leq t < 500)$ ($\mathcal{F}[\cdot]$ denotes Fourier transform and power spectrum refers to the energy of each frequency component). The result for flow #1 is shown in Figure 2.12. Note that we used 0.1s as the threshold of one-way delay c.

We can see that periodic-probing yields high estimator variance at the points with strong periodicity, which is indicated by power spectrum of finite time sample path. On the other hand, variance of estimator by Gamma-probing does not depend on the power spectrum. Therefore, the phase-lock phenomenon, which happens because probing locks due to accidental periodicity within a finite time sample path, was confirmed even if the ACF of the ground truth process is convex (namely the ground truth process does not have any specific periodicity).

2.7 Additional Simulation

We used UDP flows in the simulation of section 2.5, but we also simulated the network carrying TCP flows. We used the same conditions as used in section 2.5, expect for replacing UDP flows with TCP flows. 300 packets was specified as the maximum window size.

In the case of TCP, user traffic is strongly affected by TCP traffic control. Therefore, the observed traffic of a TCP flow can differ greatly depending on the timing of the sampling, unlike UDP. A key characteristic of this simulation is that user traffic is very unstable (see Figure 2.13). Comparing these results with those from the UDP simulation allows us to confirm whether Gamma-probing can be applied to flows with unstable

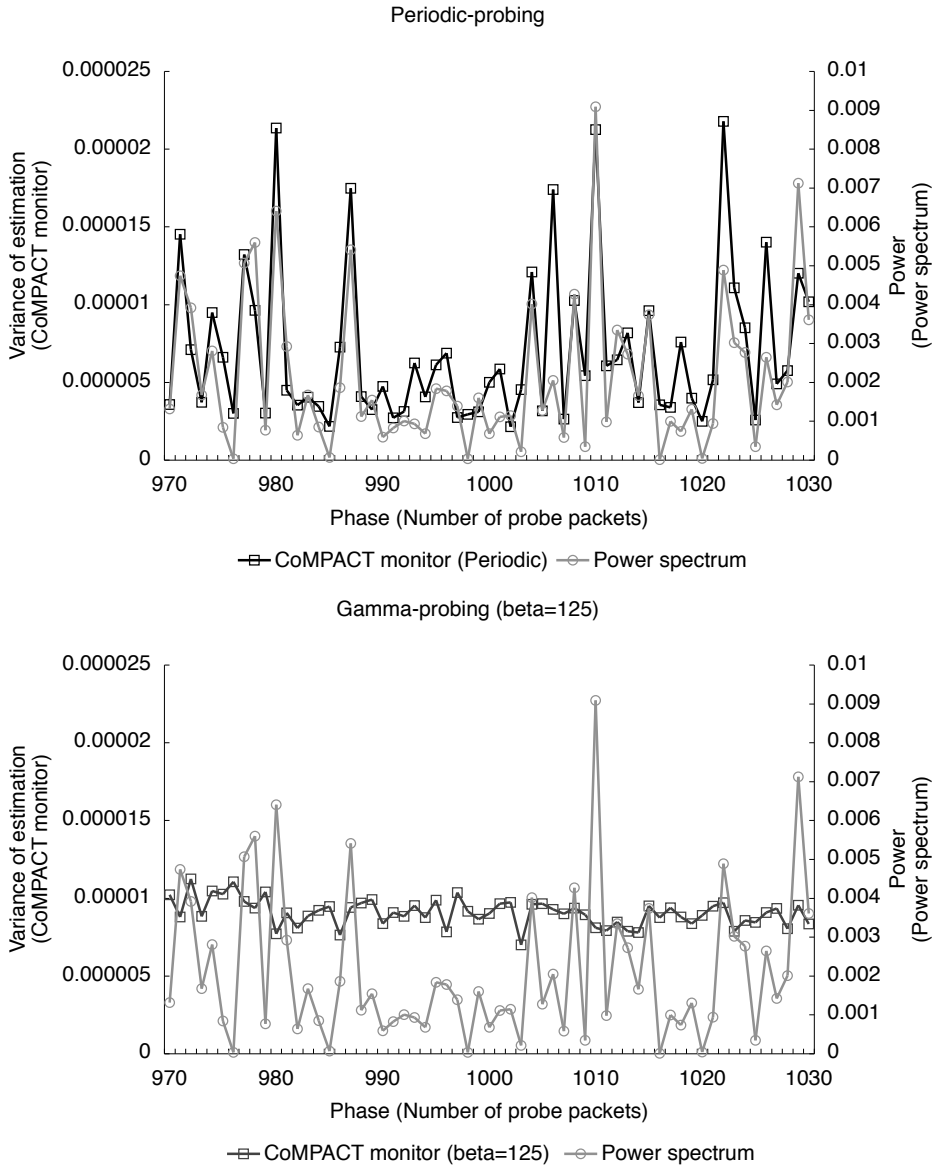

Figure 2.12: Power spectrum and variance of estimator

traffic, or not.

In fact, we were able to confirm that the ACF of the ground truth process was convex and that the estimator converged on the true value, as in the UDP simulation. The ACF for $c = 0.1$ for flow #11 with 95% confidence intervals taken over 15 experiments is depicted in Figure 2.14. The result of the estimation for flow #16 by using probe packets

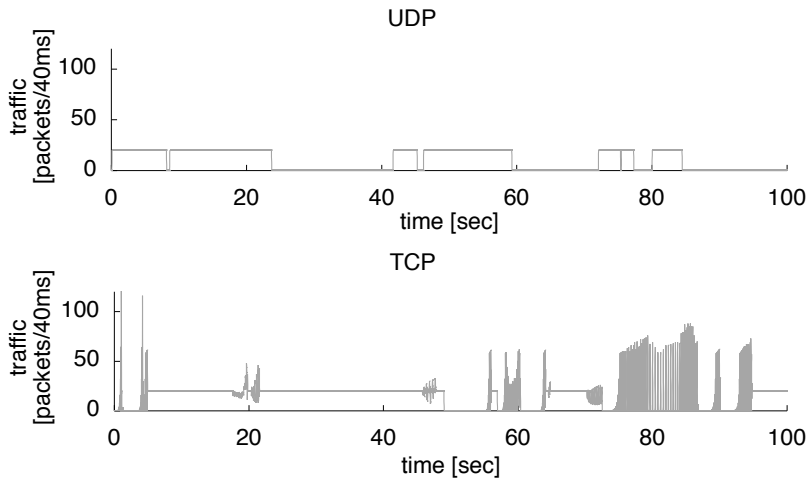

Figure 2.13: Traffic process

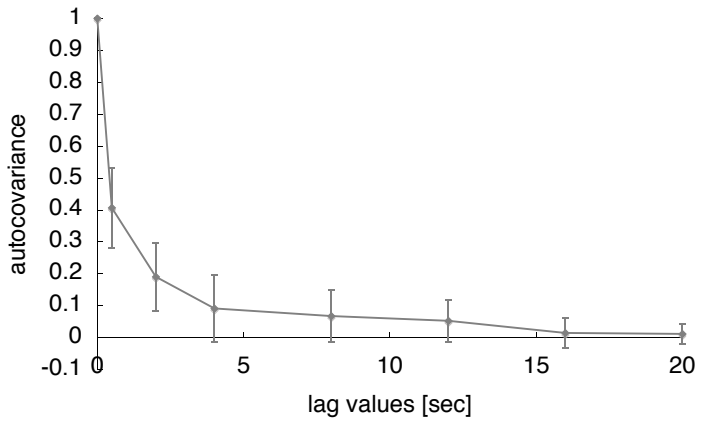

Figure 2.14: Autocovariance function in the case of TCP

with parameter $\beta = 25$ is shown in Figure 2.15. The traffic control of TCP has no negative effect on the convexity of ACF.

However, the standard deviation of the estimator was slightly different from that in the UDP simulation. Figure 2.16 shows a plot of the standard deviation of each point versus the corresponding CDF point. The error bars indicate 95% confidence intervals with the standard deviation calculated from 30 probe packet flows taken to be a single datum, as in the UDP simulation.

We can confirm that there is no significant difference. There is a tendency to decrease

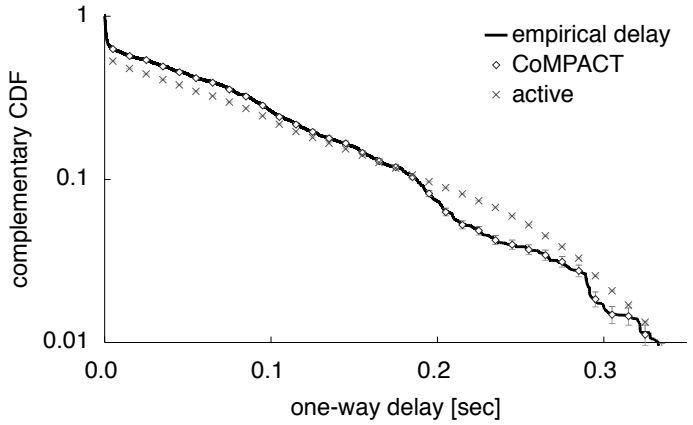

Figure 2.15: The estimation in case of TCP

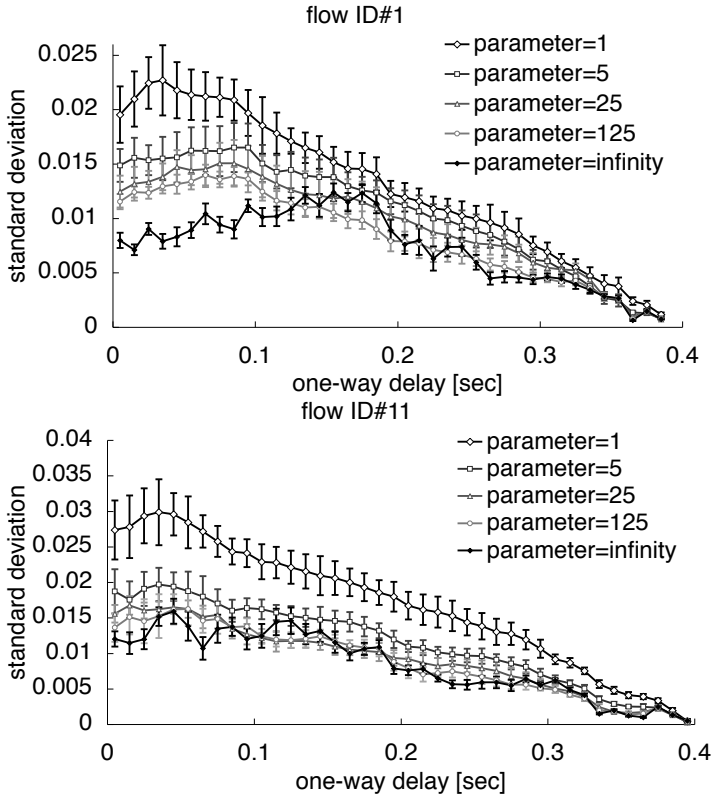

Figure 2.16: Standard deviation of estimator in the TCP case

from $\beta = 1$ to $\beta = 125$, but confidence intervals overlap each other. This overlap is caused by traffic instability. The variance of estimator is not steady when the target flow has strongly variable traffic. To stabilize the variance of estimator, we should set a longer observation period compared to the UDP case. However, we can well judge the tendency as regards the precision improvement from Figure 2.16.

Now let us focus on $\beta \to \infty$ (corresponding to periodic-probing) in Figure 2.16. The phase-lock phenomenon can be observed quite clearly by comparing these results with those of the UDP simulation. A clear reversal of the standard deviation is observed only with periodic-probing. This is the same as in the UDP simulation, though the reversal does not always happen. This result proves that periodic-probing is not optimal, even when the variance depends only on probe packet timing.

2.8 Summary

In a non-intrusive context where the effect of probe packets can be ignored, it was confirmed that the precision of estimating the complementary CDF of one-way delay can be improved by using Gamma-probing as part of determining CoMPACT monitor estimates. This means that the Gamma-probing proposed in [1] can be useful added to CoMPACT monitor for estimating the time average of sample paths.

The requirement that assures the achievement of precision improvement was clarified. [1] assumed that the ACF of a stochastic process taken to express the network state is convex. Using CoMACT monitor, we elucidated the stochastic process that expresses the network state and were able through simulations to confirm that its ACF is convex. The stochastic process observed by CoMPACT monitor depends on the traffic process of the observed flow. Compared to simple delay/loss processes, which are influenced by all traffic in the network, the traffic process of a specific flow sometimes exhibits periodicity. When we apply Gamma-probing to a real network, the convexity of ACF requires special attention because periodicity can destroy the convexity of ACF. The convexity contributes to the precision improvement possible when we estimate not only the ensemble mean of stochastic processes but also the time average of sample paths.

We have not addressed the issue of how to tune parameter β of Gamma-probing and

it remains as a key future task.

Chapter 3

On Optimal Magnitude of Fluctuations in Probe Packet Arrival Intervals

3.1 Introduction

Packet loss rate and delay are important factors that decide service performance since high values can trigger the dropping of audio and video frames, particularly in real time communication services like video conferencing. Consequently, a detailed analysis of the loss and delay generated in actual networks has obvious benefits for the design of loss and delay sensitive applications, and it is useful also from the viewpoint of traffic management. However, it is inherently difficult to gather information related to loss and delay, because the Internet is composed of multiple networks that are managed by different ISP or other organizations. Therefore, we need a way that offers end-to-end measurements of the QoS, which includes delay and loss.

Active measurement is an end-to-end measurement technique that can estimate the QoS of a network path. Active measurement derives the QoS from information obtained by injecting probe packets into the target network path [26, 27, 29, 30, 32]. From the delay/loss experienced by probe packets, active measurement can estimate one-way delay, RTT, and loss rate on the network path. It can also estimate link capacity [2, 3] and

available bandwidth [4, 5, 38] from changes in the delay or interval of the probe packets.

Active measurement is easy for the end user to perform but it is not trouble free due to the tradeoff between precision and the number of probe packets. The load of the probe packets affects the path's performance. We cannot estimate the true performance since that state occurs only without the probe stream. If we inject a lot of probe packets to increase the probing rate, the estimation precision would suffer since the extra traffic becomes appreciable. We do not deal here with the overheads imposed by the probe stream, but we state that a high probing rate does not necessarily provide precise measurement. A detailed discussion of overheads is given in reference [7]. Moreover, active measurements have great difficulty in determining the average loss rate because packet loss is a rare event and the rate is low in most current networks, especially in the Internet core. Long delay events are as rare as packet loss, and require many probe packets for detection.

Therefore, it is important to be able to achieve highly precise measurements with a limited number of probe packets. Then many prior works focus on the optimization of the operation to provide more precise estimation [1, 9, 39–43].

Work by Baccelli et al. [1, 9] gave an important suggestion on the precision of active measurement in assessing delay and loss. Two methods are now popular for determining probe timing in active measurement: PASTA-based probing and periodic-probing. PASTA-based probing is the probing policy that follows the well-known PASTA property [36], i.e. the packet injection is a Poisson process (arrival intervals follow an exponential distribution), and periodic-probing is based on fixed probe packet intervals. A comparison of PASTA-based probing and periodic-probing was discussed in RFC [44] and prior work [45]. The works showed that periodic-probing might achieve more precise measurement compared with PASTA-based probing though it can become synchronized with the target. The above discussions consider, however, only two alternatives. In recent work [9], Baccelli et al. indicated that there might be many other probing policies that can estimate true performance values given the assumption of a non-intrusive context (the extra traffic of probe packets can be ignored). Moreover, according to the result in reference [1], the best policy in terms of precision is periodic-probing under the general condition. However, it may not be best overall because of the synchronization problem (the problem is referred to as the phase-lock phenomenon). To solve this problem, Bac-

celli et al. [1] proposed a probing policy that makes the probe packet intervals follow a parameterized Gamma distribution.

That is, Baccelli et al. provided multiple selections other than traditional PASTA-based probing and periodic-probing, and they suggested that the optimal probing policy might be one of the selections. The work has a serious problem with regard to practical measurements even though it represents a great advance in network measurement. Its weakness was that it failed to specify the optimal parameter of the Gamma distribution. Therefore, Gamma-probing has been unable to establish optimal probing policies.

In this paper, to provide guidance to researchers and practitioners regarding how they should inject probe packets, we analyze the fluctuation magnitude of optimal probing policy and clarify the relationships between the optimal fluctuation magnitude and the properties of the target process. The important point in avoiding synchronization is to shift probe packet periodicity by fluctuations. Baccelli et al. shift the periodicity by using a Gamma distribution to determine probe packet intervals. In our study, we introduce a probing policy that fluctuates the probe intervals by using a normal distribution and determine the optimal fluctuation magnitude for the target process. Our analysis is composed of the following three steps.

1. To define the optimal magnitude of fluctuations that are added to the timing of probe packets, we define an evaluation function that takes the phase-lock phenomenon into consideration.

2. We show our evaluation function is determined by the ACF of the target process and the probing policy. Moreover, we clarify the relationships between the optimal magnitude of fluctuations and ACF of target process.

3. We show some evaluation examples in which we change ACF, measurement period, and the number of probe packets variously. We provide some insights by clarifying the dependency of the optimal fluctuation magnitude on network/measurement parameters. These insights are useful for network researchers and practitioners in order to design experiments. Especially, for a situation where it is hard obtaining the knowledge of ACF on real measurement, we present the design criteria on the safe side in order to avoid the phase-lock phenomenon for various ACF.

We provide a detailed mathematical proof and simulation results on the validity of our method. We used some approximations to simplify the derivation of the optimal probing policy. Mathematical and simulation-based analyzes show that the approximations are valid.

The rest of the paper is organized as follows. Section 3.2 introduces some prior works regarding probing strategies. Next, in Section 3.3, we verify the cause of the phase-lock phenomenon and describe a method to assess it. Section 3.4 explains probing policy with fluctuated probe intervals. Section 3.5 analyzes the relationships between fluctuation magnitude and the precision of active measurement, and provides a method to specify the optimal fluctuation magnitude. We confirm the validity of our approximations that we use to derive the optimal probing, through M/M/1 simulation, and show evaluation examples in Section 3.6. In Section 3.7, we discuss the generality of our results. We summarizes the paper in Section 3.8.

3.2 Probing Policy and Precision of the Estimator

In this section, we overview the current state-of-the-art by introducing some prior works on probing strategies for active measurement.

PASTA-based probing and periodic-probing have been widely used as the probing policies for active measurement. These probing policies are described in RFCs [32, 44], respectively, and Roughan's work provided a comparison of the two policies [45] (periodic-probing is called uniform sampling in this). The key features of the PASTA-based probing and periodic-probing are as follows.

- **PASTA-based probing;** The probe packet intervals follow an exponential distribution, i.e. the probe packet arrivals process follows a Poisson arrival. It can provide bias-free measurement because of the PASTA property [36] but may be inferior in terms of estimation precision.

- **Periodic-probing;** This probing policy uses fixed probe packet intervals. It is easier to manipulate, and it may be superior to PASTA-based probing in terms of precision in many cases. However, it can suffer from the problem of synchronization with the target being measured.

It is unknown to this author how prevalent periodicities are in the modern Internet. However, some works reported theoretical grounds for their existence [46,47]. Hence, there is the tradeoff between the two policies, and we cannot judge which probing policy is better.

Baccelli et al. investigated alternatives to the above two probing policies, and suggested that there are better policies than these two probing policies. They indicate that there are many distributions other than PASTA-based probing that can provide bias-free measurements if a non-intrusive context (the load of probe packets is insignificant) can be assumed [9]. This property is named NIMASTA. NIMASTA contains the following three assumptions.

1. The stochastic process that expresses the network state we are interested in (e.g. virtual delay and loss/no-loss indication) is stationary and ergodic. This process is called the ground truth process.

2. The point process of probe packet arrivals $\{T_i\}$ $(i = 1, 2, \ldots, m)$ is stationary and *mixing*. Mixing is the requirement that guarantees joint ergodicity between the probe and ground truth processes (see reference [9] for details).

3. The last assumption is the non-intrusive context, i.e. we can ignore the impact of probe packet overhead. Namely, the ratio of the probe stream (extra traffic) to all streams is very small.

Under the above assumptions, it was proved that the following equation holds:

$$\lim_{m\to\infty} \frac{1}{m} \sum_{i=1}^{m} h(X(T_i)) = \mathrm{E}[h(X(0))] \qquad \text{a.s.}, \tag{3.1}$$

where $X(t)$ and h are the ground truth process and an arbitrary positive function, respectively. If we can obtain $X(T_i)$ (e.g. the delay of the probe packet or loss/no-loss of probe packet) from a probe packet injected at time T_i, (3.1) means that we can estimate $\mathrm{E}[h(X(0))]$ without bias by the injection of m probe packets. The only requirements placed on the point process of probe packet arrival $\{T_i\}$ $(i = 1, 2, \ldots)$ are that it be stationary and mixing. Therefore, there are many point processes that can achieve unbiased estimation of ensemble mean $\mathrm{E}[h(X(0))]$ besides PASTA-based probing, inter-probe time follows an exponential distribution. Such mixing point processes include

those whose intervals follow a Gamma distribution and a uniform distribution. Note that periodic-probing with fixed interval is not a mixing process, and does not satisfy (3.1).

Recent work [1] investigated how to select the optimal probing process. We can select the optimal (in terms of precision) probing process under a specific assumption by using the inter-probe time given by the parameterized Gamma distribution.

If we estimate the mean of $X(0)$ by using active measurement, the estimator $\hat{P}$ is

$$\hat{P} = \frac{1}{m}\sum_{i=1}^{m} X(T_i)\,.$$

Thus the variance of $\hat{P}$ is

$$\begin{aligned}
\mathrm{Var}[\hat{P}] &= \frac{1}{m^2}\mathrm{Var}\left[\sum_{i=1}^{m} X(T_i)\right] \\
&= \frac{1}{m^2}\sum_{i=1}^{m}\sum_{j=1}^{m}\mathrm{Cov}\left(X(T_i), X(T_j)\right) \\
&= \frac{1}{m^2}\sum_{i=1}^{m}\sum_{j=1}^{m}\int_{-\infty}^{\infty} r(\tau) f_{i-j}(\tau)\mathrm{d}\tau\,, \qquad (3.2)
\end{aligned}$$

where f_{i-j} is the pdf of $T_i - T_j$, $r(\tau) = \mathrm{Cov}\left(X(t), X(t+\tau)\right)$ is the ACF of the ground truth process $X(t)$ (we can express $r(\tau)$ by τ alone, because $X(t)$ is stationary) and the last equality follows from the stationary property of $X(t)$ and the probe packet process.

It was proved that no other probing process with an average interval d has a variance that is lower than that of periodic-probing [1]. Convexity of $r(\tau)$ in real network is evidenced by the network measurement [1] and if $r(\tau)$ is convex on the interval $[0, \infty)$ and the average of the inter-probe time is d, the following inequality can be proven by using Jensen's inequality [48].

$$\begin{aligned}
\int_{-\infty}^{\infty} r(\tau) f_k(\tau)\mathrm{d}\tau &\geq r\left(\int_{-\infty}^{\infty} t f_k(t)\mathrm{d}t\right) \\
&= r(kd) \\
&= \int_{-\infty}^{\infty} r(\tau)\delta(\tau - kd)\mathrm{d}\tau\,, \qquad (3.3)
\end{aligned}$$

where $\delta(\cdot)$ denote Dirac δ function, k is a integer, and the first equality follows from the average inter-probe time d of probing. Therefore, $f_{i-j}(\tau) = \delta(\tau - (i-j)d)$ minimizes

(3.2), and it corresponds to periodic-probing. Estimator variance is associated with precision, lower is better, so periodic-probing is the best probing process if we focus only on variance. On the other hand, periodic-probing does not satisfy the assumptions of (3.1) due to non-mixing, so periodic-probing is not necessarily the best. This is because the phase-lock phenomenon may occur and the estimator may converge on a false value when the cycle of the ground truth process is synchronized with that of the probing process. For instance, if we inject the probe packets at time $\{0, d, 2d, \dots\}$ by periodic-probing with inter-probe time d to measure a process $X(t) = \sin(2\pi(t - S)/d)$ where S denotes random variable that follows a uniform distribution $U(0, d)$, the observed values take the same value $X(0) = X(d) = X(2d) = \dots$, and the estimator $\hat{P}$ does not converge on $\mathrm{E}[X(0)] = 0$. Namely, periodic-probing can become biased. Therefore, we cannot conclude that periodic-probing is always the optimal probing process.

To tune the tradeoff between PASTA-based probing and periodic-probing (which has bias but superior variance), Baccelli et al. proposed a probing process whose inter-probe time follows a parameterized Gamma distribution [1]. The pdf that is used as the interval between probe packets is given by

$$g(x) = \frac{x^{\beta-1}}{\Gamma(\beta)} \left(\frac{\beta}{d}\right)^{\beta} \mathrm{e}^{-x\beta/d} \qquad (x > 0)\,, \tag{3.4}$$

where $g(x)$ is the Gamma distribution whose shape and scale parameters are β and d/β, respectively. d (> 0) denotes the mean, and β (> 0) is the parameter. When $\beta = 1$, $g(x)$ reduces to the exponential distribution with mean d. When $\beta \to \infty$, the probing process reduces to periodic-probing because $g(x)$ converges on $\delta(x - d)$. If ACF of $X(t)$ is convex, it has been proven that the variance of estimator $\hat{P}$ sampled by intervals that follow (3.4) monotonically decreases as β increases. We can achieve small variance (it approaches the variance of periodic-probing) by setting β to a large value since (3.4) converges on periodic-probing towards the limit $\beta \to \infty$. The problem of bias due to the phase-lock phenomenon can be avoided if we tune β to a limited value (the probing process that has intervals set by (3.4) is mixing). We can resolve the tradeoff between PASTA-based probing and periodic-probing if we give β an appropriate value. This Gamma-probing provides multiple selections lying between traditional PASTA-based probing and periodic-probing through parameter β, and it is a great advance in network measurement techniques.

However, since reference [1] did not indicate how to decide upon the optimal β, it has remained a problem with no solution. To solve this problem, we introduce in this paper a method that can specify the optimal probing policy.

3.3 Evaluation of Phase-Lock Phenomenon

This study examines the phase-lock phenomenon in detail because our goal, specifying the optimal probing process, demands avoidance of this phenomenon. Reference [1] did not mention this cause of the phase-lock phenomenon in detail because it was not main topic. Accordingly, this section investigates the cause and effect of the phase-lock phenomenon and introduces an evaluation function that can assess this phenomenon appropriately.

The convex ACF $r(\tau)$ of the ground truth process $X(t)$ means $X(t)$ has no special periodicity (see Figure 3.1). The phase-lock phenomenon occurs when the cycle of the ground truth process synchronizes to that of the probing process. Hence, the phase-lock phenomenon will not occur if the ACF is strictly convex. (3.3) showed that variance is minimized with periodic probing, and it means that it will not realize large variance (imprecision) due to phase-lock phenomenon, under the strictly convex ACF. However, the experiments in reference [1] demonstrated that there are multiple instances in which the precision of the estimator of periodic-probing was worse than that of other probing processes (periodic-probing is not always imprecise).

We consider that the phase-lock phenomenon is caused by *accidental periodicity* that is realized by using finite measurement periods. Even if the ground truth process has no special periodicity (in terms of long-time average), accidental periodicity is possible. Thus, there is a possibility that a specific frequency component will be present by chance if the measurement period is limited. Even if ACF in terms of ensemble mean (namely long-time average)

$$r(\tau) = \mathrm{E}[X(t)X(t+\tau)] - \{\mathrm{E}[X(t)]\}^2$$

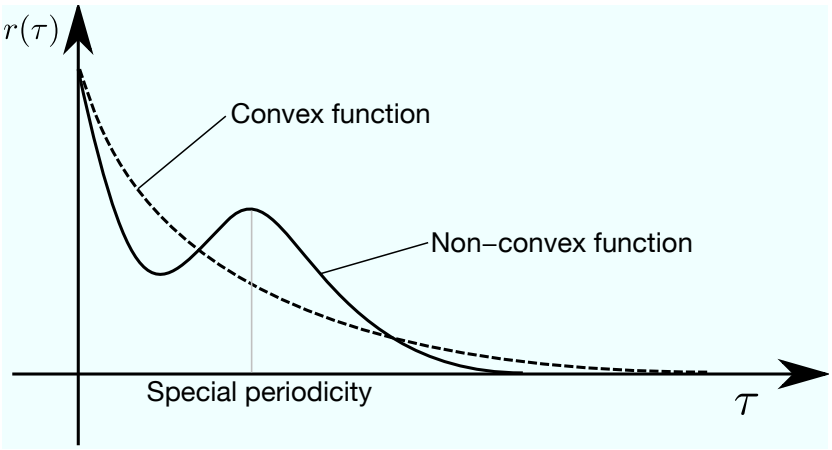

Figure 3.1: Convexity of ACF and special periodicity of the ground truth process

is strictly convex, ACF in terms of a time average on finite period $(0, l]$

$$R(\tau) = \frac{1}{l-\tau}\int_0^{l-\tau} X(t)X(t+\tau)\mathrm{d}t - \frac{1}{(l-\tau)^2}\int_0^{l-\tau} X(t)\mathrm{d}t \int_0^{l-\tau} X(t+\tau)\mathrm{d}t \tag{3.5}$$

is not necessarily convex. Note that $R(\tau)$ is a stochastic process that depends on X(t). If we measure the $X(t)$ on limited measurement period $(0, l]$, we should consider (3.5) that is generated by $X(t)$ on $(0, l]$. In Figure 3.2, we display the ACF of M/M/1 queue length. The arrival rate and the service rate are 0.75 and 1.0, respectively. The line of time average in Figure 3.2 represents the time average on a finite period $(0, 10000]$ for a single sample path generated by simulation. According to the figure, we can confirm that the ACF in terms of a time average is not a convex function though the ACF exhibits, in terms of ensemble mean, convexity. In a sample path we show in the figure, we can find accidental periodicity at $\tau \simeq 250$, and the estimator is imprecise due to the phase-lock phenomenon if we set a probe interval to 250.

Unpredictability is what distinguishes accidental periodicity from special periodicity in terms of long-time average. Special periodicity continues into the future constantly since it reflects the structure of the target, and hence we can predict the cycle using knowledge of the past ground truth process. On the other hand, we cannot predict accidental periodicity, no matter what knowledge of past ground truth process we may use. Because

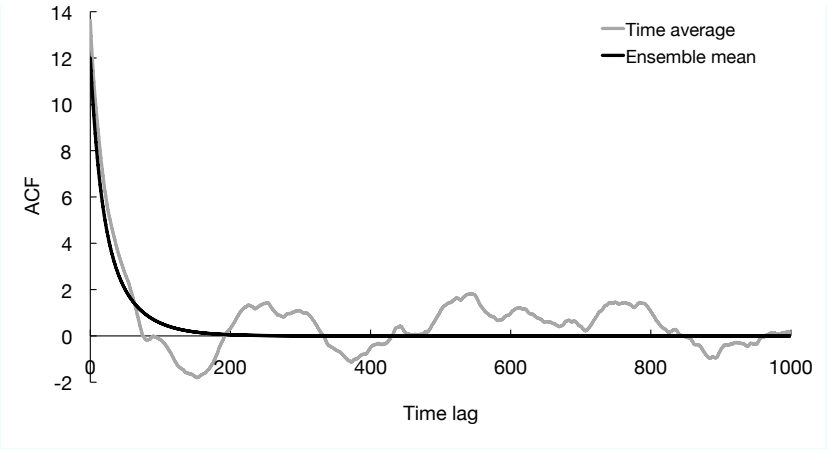

Figure 3.2: ACF in terms of time average and ensemble mean

the unexpected behavior that is the difference between the behavior of the real sample path and the expected behavior (that is expressed by ACF) yields accidental periodicity. If we can obtain knowledge of past ground truth process before a measurement, we can avoid synchronization with special periodicity by changing the cycle of the probing process. However, accidental periodicity cannot be predicted and can be generated on any cycle, and hence we cannot avoid synchronization with accidental periodicity by changing the cycle of the probing process.

Therefore, precision will fall if a sample path of the ground truth process contains a lot of frequency components to which the probing process can become synchronized. Conversely, if it contains few such frequency component, the precision will be remarkably high. The precision of periodic-probing may become extremely bad for the specific sample path though it is reasonable on average.

Accordingly, to assess the phase-lock phenomenon appropriately we must consider the precision that corresponding to the target sample path. We assume the metric that we want to measure is the time average $\overline{X}_l = \int_0^l X(t)/l \, \mathrm{d}t$ on the measurement period $(0, l]$ and $\mathrm{E}[\hat{P}|X(t)] = \overline{X}_l$ holds (namely we can achieve bias-free measurement and the assumption suits our probing method which we will mention in Section 3.4). Note that our target $\overline{X}_l$ is not ensemble mean $\mathrm{E}[X(0)]$ but empirical average, and it is random variables. By using a conditional variance, we can express the precision for the target

sample path as

$$\mathrm{Var}[\hat{P}|X(t)]\,. \tag{3.6}$$

Note that the conditional variance (3.6) is random variable that depends on stochastic process $X(t)$. We discriminate between precision regarding a time average and precision regarding an ensemble mean. The former is expressed by (3.6), and the latter is expressed by normal variance $\mathrm{Var}[\hat{P}]$. Reference [1] proved that periodic-probing gives $\mathrm{Var}[\hat{P}]$ the minimal value (we introduced this in Section 3.2), and we can understand that $\mathrm{Var}[\hat{P}]$ corresponds to the expectation of the (3.6) according to the following equation:

$$\mathrm{E}[\mathrm{Var}[\hat{P}|X(t)]] = \mathrm{Var}[\hat{P}] - \mathrm{Var}[\overline{X}_l]\,. \tag{3.7}$$

Note that the second term on the right-hand side of (3.7) does not depend on the probing policy. Therefore, by using (3.7), we can assess the average precision (in which periodic-probing is superior). On the other hand, the effect of the phase-lock phenomenon is that (3.6) is varied with the intensity of the frequency component (which is synchronized with the probing process). The effect of the phase-lock phenomenon can be assessed by the following:

$$\mathrm{Var}[\mathrm{Var}[\hat{P}|X(t)]]\,. \tag{3.8}$$

This paper looks for a probing process that can avoid the extreme drops in precision created by the phase-lock phenomenon. In addition, the probing process should also achieve a small (3.7) (In other words, it should also be precise in terms of average precision).

To find a probing policy that satisfies the above two requirements (which are assessed by (3.7) and (3.8), respectively), we introduce the following evaluation function:

$$\Big\{\mathrm{E}[\mathrm{Var}[\hat{P}|X(t)]]\Big\}^2 + \mathrm{Var}[\mathrm{Var}[\hat{P}|X(t)]] = \mathrm{E}\left[\Big\{\mathrm{Var}[\hat{P}|X(t)]\Big\}^2\right]\,. \tag{3.9}$$

Our evaluation function is defined by the square of l_2-norm of (3.8), and it is equivalent to Mean Square Error (MSE) with estimated parameter $\theta = 0$. We define the probing process that minimizes evaluation function (3.9) as the optimal probing process, and we investigate the optimal probing process as determined by the property of the target network.

3.4 Probing Method with Fluctuations

In this section, to analyze the optimal probing policy, we will introduce the probing process with fluctuated intervals that avoids the phase-lock phenomenon. As we mentioned in Section 3.3, the cause of the phase-lock phenomenon is accidental periodicity. We cannot avoid the phase-lock phenomenon by changing the cycle of the probing process (i.e. the average probe interval), since accidental periodicity can be generated on any cycle. Therefore, to avoid the phase-lock phenomenon, we use a random variable to fluctuate the probe intervals. In other words, we force the probing process to exhibit multiple cycles (i.e. variable intervals). Actually, the Gamma-probing proposed by Baccelli et al. in reference [1] is one approach to adding fluctuations. The method we introduce in this section takes three parameters into consideration: measurement period, number of probe packets, and fluctuation magnitude. It is expected that measurement period has a critical affect on the intensity of accidental periodicity. In terms of avoiding the phase-lock phenomenon, there is no essential difference between our approach and Gamma-probing, but our approach simplifies the analysis of the relationship between the evaluation function and the parameters of the probing policy. We use the method that we introduce in this section since our aim here is principally to clarify the relationship between fluctuation magnitude and the value of evaluation function.

We add fluctuations that obey a normal distribution to the timing of probe packet arrivals, while specifying the measurement period. We assume that the interval $(0, l]$ is the measurement period and m is the number of probe packets sent in the measurement period. Our probing method gives the point process of probe packet arrivals $\{T_i\}$ $(i = 1, 2, \ldots, m)$ as follows.

$$T_i = S + G_i - l \left\lfloor \frac{S + G_i}{l} \right\rfloor , \tag{3.10}$$

where S and G_i denote the random variables that follow a uniform distribution $U(0, l/m)$ and a normal distribution $N((i-1)l/m, \sigma^2)$, respectively, $\lfloor \cdot \rfloor$ denotes a floor function and σ denotes the magnitude parameter of the fluctuations. To prevent $\{T_i\}$ from taking a value outside the measurement period $(0, l]$, we add the third term. The second term contributes to the fluctuation of probe packet interval. The first term determines a phase, and does not affect the probe packet interval (note that the first term does not depend on

i). Note that the order of packet injection could be changed when the point process of probe packet arrivals is given by (3.10). The packets are injected in random order if the fluctuation magnitude is sufficiently large. It is easy to prove that the probability that at least one packet of m probe packets injects in $[t, t+\Delta t)$ is $(m\Delta t)/l$ for any t $(0 \leq t < l)$ since all of the phases are mixed uniformly by the random variable S if we inject the probe packets at $\{T_i\}$ $(i = 1, 2, \ldots, m)$ given by (3.10) (see Appendix A). Therefore, estimator $\hat{P} = \sum_{i=1}^{m} X(T_i)/m$ is an unbiased estimator for our target $\overline{X}_l$.

Our probing process provides multiple selections lying between traditional PASTA-based probing and periodic-probing as well as Gamma-probing. If $\sigma = 0$ (namely there is no fluctuation), $\{T_i\}$ corresponds to periodic-probing. On the other hand, if $\sigma \rightarrow \infty$, T_i follows a uniform distribution $U(0, l)$. Therefore, intervals between T_i follow an exponential distribution for sufficiently large l. In Gamma-probing, the inter-probe time distributions are Gamma distribution and the distributions can be approximated as normal distribution with variance $1/\beta$ for sufficiently large β. The inter-probe time distributions of our method follow a normal distribution with variance $2\sigma^2$. Therefore, the inter-probe time distributions of Gamma-probing correspond to that of our method when $\sqrt{2}\sigma\beta = 1$ and β is sufficiently large.

3.5 Fluctuation Magnitude and Precision

In this section, we will clarify the relationship between fluctuation magnitude imposed on probe timing and the evaluation function (3.9), and we will detail a method that specifies the optimal fluctuation magnitude, theoretically. As we mentioned in Section 3.3, periodic-probing is the optimal probing process if we consider only average precision. It is important to specify the minimal fluctuation magnitude that can avoid the phase-lock phenomenon, because large fluctuations cause the probing process to deviate too far from periodic-probing.

Our evaluation function (3.9) is composed of the average and variance of (3.6). Therefore, we first address the stochastic behavior of (3.6). We define $\tilde{X}_l(t) = X(t - l\lfloor t/l \rfloor)$ which depends on stochastic process $X(t)$ in measurement period $(0, l]$. In addition, we define $\tilde{T}_i = S + G_i$, which is composed of a simple uniform and normal random variable.

Since $X(t)$ observed at the timing of $\{T_i\}$ is equal to $\tilde{X}_l(t)$ observed at the timing of $\{\tilde{T}_i\}$, the following equation holds:

$$\begin{aligned}\hat{P} &= \frac{1}{m}\sum_{i=1}^{m} X(T_i) \\ &= \frac{1}{m}\sum_{i=1}^{m} \tilde{X}_l(\tilde{T}_i)\,.\end{aligned}$$

Therefore, by using ACF $\tilde{R}_l(\tau) = \int_0^l \tilde{X}_l(t)\tilde{X}_l(t+\tau)/l\,\mathrm{d}t - \{\int_0^l \tilde{X}_l(t)/l\,\mathrm{d}t\}^2$ in terms of time average, (3.6) can be expressed as follows (as well as (3.2)).

$$\begin{aligned}\mathrm{Var}[\hat{P}|X(t)] &= \frac{1}{m^2}\mathrm{Var}\left[\sum_{i=1}^{m}\tilde{X}_l(\tilde{T}_i)\,\middle|\,X(t)\right] \\ &= \frac{1}{m^2}\sum_{i=1}^{m}\sum_{j=1}^{m}\int_{-\infty}^{\infty}\tilde{R}_l(\tau)f_{i-j}(\tau)\mathrm{d}\tau\,,\end{aligned}$$

where f_{i-j} is the pdf of $T_i - T_j$, and it obeys the normal distribution $N((i-j)l/m, 2\sigma^2)$ when $i \neq j$. Note that $\tilde{R}_l(\tau)$ is a stochastic process that depends on $X(t)$.

Furthermore, when we expand $\tilde{R}_l(\tau)$ in Fourier series, we find that

$$\begin{aligned}\mathrm{Var}[\hat{P}|X(t)] &= \frac{1}{m^2}\sum_{n=1}^{\infty}K_n\left\{\sum_{i=1}^{m}\sum_{j=1}^{m}\int_{-\infty}^{\infty}\cos\left(\frac{2\pi n}{l}\tau\right)f_{i-j}(\tau)\mathrm{d}\tau\right\}, \qquad (3.11)\\ K_n &= \frac{2}{l}\int_0^l \cos\left(\frac{2\pi n}{l}\tau\right)\tilde{R}_l(\tau)\mathrm{d}\tau,\end{aligned}$$

where the second equality follows from the periodic and even function $\tilde{R}_l(\tau)$. Note that $\{K_n\}$ $(n = 1, 2, \dots)$ are random variables that depend on $X(t)$; they represent the intensity of each frequency component of $X(t)$. Since $\tilde{T}_i - \tilde{T}_j = G_i - G_j$ $(i \neq j)$ follows a normal distribution, $N((i-j)l/m, 2\sigma^2)$, the following equation holds:

$$\int_{-\infty}^{\infty}\cos\left(\frac{2\pi n}{l}\tau\right)f_k(\tau)\mathrm{d}\tau = \int_{-\infty}^{\infty}\cos\left(\frac{2\pi n}{l}\tau\right)f_{m-k}(\tau)\mathrm{d}\tau\,.$$

Therefore, we obtain

$$
\begin{aligned}
&\sum_{i=1}^{m}\sum_{j=1}^{m}\int_{-\infty}^{\infty}\cos\left(\frac{2\pi n}{l}\tau\right)f_{i-j}(\tau)\mathrm{d}\tau \\
&\quad= m\sum_{i=0}^{m-1}\int_{-\infty}^{\infty}\cos\left(\frac{2\pi n}{l}\tau\right)f_{i}(\tau)\mathrm{d}\tau \\
&\quad= m+m\int_{-\infty}^{\infty}\cos\left(\frac{2\pi n}{l}\tau\right)\sum_{i=1}^{m-1}\frac{1}{2\sigma\sqrt{\pi}}\mathrm{e}^{-\frac{(\tau-il/m)^2}{4\sigma^2}}\mathrm{d}\tau \\
&\quad= m-m\int_{-\infty}^{\infty}\cos\left(\frac{2\pi n}{l}\tau\right)\frac{1}{2\sigma\sqrt{\pi}}\mathrm{e}^{-\frac{\tau^2}{4\sigma^2}}\mathrm{d}\tau \\
&\qquad\quad+m\int_{-\infty}^{\infty}\cos\left(\frac{2\pi n}{l}\tau\right)\sum_{i=0}^{m-1}\frac{1}{2\sigma\sqrt{\pi}}\mathrm{e}^{-\frac{(\tau-il/m)^2}{4\sigma^2}}\mathrm{d}\tau \\
&\quad= \begin{cases} m+(m^2-m)\int_0^{\infty}\cos\left(\frac{2\pi n}{l}\tau\right)\frac{1}{\sigma\sqrt{\pi}}\mathrm{e}^{-\frac{\tau^2}{4\sigma^2}}\mathrm{d}\tau, & n=mj \\ & (j=1,2,\dots) \\ m-m\int_0^{\infty}\cos\left(\frac{2\pi n}{l}\tau\right)\frac{1}{\sigma\sqrt{\pi}}\mathrm{e}^{-\frac{\tau^2}{4\sigma^2}}\mathrm{d}\tau, & \text{otherwise} \end{cases} \\
&\quad= \begin{cases} m+(m^2-m)\mathrm{e}^{-\left(\frac{2\pi n}{l}\right)^2\sigma^2}, & n=mj\ \ (j=1,2,\dots) \\ m-m\,\mathrm{e}^{-\left(\frac{2\pi n}{l}\right)^2\sigma^2}, & \text{otherwise} \end{cases},
\end{aligned}
\tag{3.12}
$$

where the last equality follows from the following integral (see reference [49]).

$$
\int_0^{\infty}\mathrm{e}^{-ax^2}\cos bx\,\mathrm{d}x=\frac{1}{2}\sqrt{\frac{\pi}{a}}\,\mathrm{e}^{-\frac{b^2}{4a}},
$$

where a and b denote an arbitrary positive real number and an arbitrary real number, respectively.

Substituting (3.12) for (3.11), the precision achieved for target sample path $\mathrm{Var}[\hat{P}|X(t)]$ is expressed as follows using the intensity of each frequency component $\{K_n\}\,(n=1,2,\dots)$.

$$
\mathrm{Var}[\hat{P}|X(t)]=\sum_{i=1}^{\infty}w_iK_i\,, \tag{3.13}
$$

$$
w_i=\begin{cases} \frac{1+(m-1)\mathrm{e}^{-\left(\frac{2\pi i}{l}\right)^2\sigma^2}}{m}, & i=mj\ \ (j=1,2,\dots) \\ \frac{1-\mathrm{e}^{-\left(\frac{2\pi i}{l}\right)^2\sigma^2}}{m}, & \text{otherwise} \end{cases}.
$$

Note that $K_0=0$ because $\int_0^l\tilde{R}_l(\tau)\mathrm{d}\tau=0$.

To clarify the average and standard deviation of $\mathrm{Var}[\hat{P}|X(t)]$, we must investigate the stochastic behavior of $\{K_n\}$ $(n = 1, 2, \dots)$. Since Fourier transformation of autocorrelation function $\tilde{R}_l(t) + \overline{X}_l^2$ of the stochastic process yields a power spectrum (Wiener-Khintchin theorem [50]), the following equation holds for any sample path $x(t)$ of $X(t)$,

$$\mathcal{F}\left[\tilde{r}_l(t) + \overline{x}_l^2\right] = \left|\mathcal{F}\left[\tilde{x}_l(t)\right]\right|^2 ,$$

where $\tilde{r}_l(t) + \overline{x}_l^2$ and $\tilde{x}_l(t)$ represent the sample paths of $\tilde{R}_l(t) + \overline{X}_l^2$ and $\tilde{X}_l(t)$ that correspond to the sample path $x(t)$. Consequently, K_n relates to the Fourier coefficients of $X(t)$ as follows.

$$K_n = \frac{{C_n}^2 + {S_n}^2}{2} , \tag{3.14}$$

where

$$C_n = \frac{2}{l}\int_0^l \cos\left(\frac{2\pi n t}{l}\right) X(t)\mathrm{d}t ,$$
$$S_n = \frac{2}{l}\int_0^l \sin\left(\frac{2\pi n t}{l}\right) X(t)\mathrm{d}t .$$

Note that Fourier coefficients C_n and S_n are random variables because they depend on $X(t)$.

Hence, by using (3.13) and (3.14), we can express the evaluation function (3.9) by the covariance of C_i or S_i. (3.7) which composes our evaluation function is given as follows.

$$\begin{aligned}\mathrm{E}\left[\mathrm{Var}[\hat{P}|X(t)]\right] &= \sum_{i=1}^{\infty} w_i \mathrm{E}\left[\frac{{C_i}^2 + {S_i}^2}{2}\right] \\ &= \frac{1}{2}\sum_{i=1}^{\infty} w_i \left\{\mathrm{Cov}(C_i, C_i) + \mathrm{Cov}(S_i, S_i)\right\} .\end{aligned} \tag{3.15}$$

Similarly, the other component (3.8) forming the evaluation function is as follows.

$$\begin{aligned}\mathrm{Var}\left[\mathrm{Var}[\hat{P}|X(t)]\right] &= \sum_{i=1}^{\infty}\sum_{j=1}^{\infty} w_i w_j \mathrm{Cov}\left(\frac{{C_i}^2 + {S_i}^2}{2}, \frac{{C_j}^2 + {S_j}^2}{2}\right) \\ &= \frac{1}{4}\sum_{i=1}^{\infty}\sum_{j=1}^{\infty} w_i w_j \Big\{\mathrm{Cov}\left({C_i}^2, {C_j}^2\right) \\ &\qquad + 2\,\mathrm{Cov}\left({C_i}^2, {S_j}^2\right) + \mathrm{Cov}\left({S_i}^2, {S_j}^2\right)\Big\} .\end{aligned}$$

We assume that C_i and S_i follow normal distributions since it is difficult to treat covariance between the squares of random variables. We can provide the rationale of the approximation that C_i and S_i follow normal distributions. By separating the integrals, we get the following equations:

$$C_i = \frac{2}{l}\sum_{k=0}^{i-1}\int_{lk/i}^{l(k+1)/i}\cos\left(\frac{2\pi it}{l}\right)X(t)\mathrm{d}t\,, \tag{3.16}$$

$$S_i = \frac{2}{l}\sum_{k=0}^{i-1}\int_{lk/i}^{l(k+1)/i}\sin\left(\frac{2\pi it}{l}\right)X(t)\mathrm{d}t\,. \tag{3.17}$$

(3.16) and (3.17) are the summation of the i random variables that obey the same distribution. Note that they are not independent of each other. Suppose that random variables $X_k\,(k = 0, 1, \ldots, n)$ are stationary and α-mixing with $O(k^{-5})$, and these expectation and the 12th moments are 0 and finite, respectively. The central limit theorem for dependent cases guarantees that the distribution of the summation $X^n_{\mathrm{sum}} = \sum_{k=1}^{n} X_k$ can approximate normal distribution for sufficiently large n [51]. The condition that is required for X_k is a sufficient condition, and the actual restriction is more relaxed (see reference [51] for details). The variance is given by

$$\mathrm{Var}[X^n_{\mathrm{sum}}] = n\left(\mathrm{E}[{X_1}^2] + 2\sum_{l=1}^{n-1}\mathrm{E}[X_1X_{1+l}]\right).$$

Therefore, if we assume

$$X_k = \int_{lk/i}^{l(k+1)/i}\cos\left(\frac{2\pi it}{l}\right)X(t)\mathrm{d}t,$$

we can guarantee that the (3.16) follows a normal distribution for sufficiently large i (we can also guarantee the (3.17) follows a normal distribution similarly). Sufficient conditions for target process $X(t)$ are as follows: (1) the target process $X(t)$ is stationary process; (2) Variance of $X(t)$ is finit; (3) the absolute value of ACF of $X(t)$ is $O(t^{-5})$. Though we can not apply the above approximation for small i, we can consider that the (3.16) and (3.17) are summations of non-identically distributed h random variables with

mean 0 by separating the integrals as follows.

$$C_i = \frac{2}{l}\sum_{k=0}^{h-1}\int_{lk/h}^{l(k+1)/h} \cos\left(\frac{2\pi i t}{l}\right) X(t)\mathrm{d}t\,,$$
$$S_i = \frac{2}{l}\sum_{k=0}^{h-1}\int_{lk/h}^{l(k+1)/h} \sin\left(\frac{2\pi i t}{l}\right) X(t)\mathrm{d}t\,.$$

The central limit theorem for non-identically distributed and independent random variables guarantees that the summation of random variables X_k follows a normal distribution when the following equation hold for some $\delta > 0$ [51].

$$\lim_{n\to\infty} \frac{\sum_{k=0}^{n} \mathrm{E}[|X_k - \mu_k|^{2+\delta}]}{\sqrt{\sum_{k=0}^{n} \nu_k}^{2+\delta}},$$

where μ_k and ν_k represent mean and variance of X_k. The above central limit theorems for dependent (but identically distributed) random variables and non-identically distributed (but independent) random variables motivate us to consider that (3.16) and (3.17) follow a normal distribution even though the explicit conditions to hold the central limit theorem for dependent and non-identically distributed random variables are not provided. Moreover, in Section 3.6, we will supplement the rationale of the assumption through the simulation result.

By using the approximation, we can derive $\mathrm{Var}[\mathrm{Var}[P|\hat{X}(t)]]$ as follows.

$$\begin{aligned}\mathrm{Var}\left[\mathrm{Var}[\hat{P}|X(t)]\right] &= \frac{1}{4}\sum_{i=1}^{\infty}\sum_{j=1}^{\infty} w_i w_j \Big\{ \mathrm{Cov}\left({C_i}^2, {C_j}^2\right) \\ &\qquad + 2\,\mathrm{Cov}\left({C_i}^2, {S_j}^2\right) + \mathrm{Cov}\left({S_i}^2, {S_j}^2\right) \Big\} \\ &= \frac{1}{4}\sum_{i=1}^{\infty}\sum_{j=1}^{\infty} w_i w_j \Big\{ 2\left\{\mathrm{Cov}\left(C_i, C_j\right)\right\}^2 \\ &\qquad + 4\left\{\mathrm{Cov}\left(C_i, S_j\right)\right\}^2 + 2\left\{\mathrm{Cov}\left(S_i, S_j\right)\right\}^2 \Big\}\,,\end{aligned}$$

where the second equality follows from the property of the moment of bivariate normal distributions.

Finally, if we can relate $\mathrm{Cov}(C_i, S_j)$, $\mathrm{Cov}(C_i, C_j)$ and $\mathrm{Cov}(S_i, S_j)$ to $r(\tau)$, our eval-

uation function can evaluate any probing method. Calculating $\mathrm{Cov}(C_i, S_j)$, we have

$$\begin{aligned}
\mathrm{Cov}(C_i, S_j) &= \frac{4}{l^2}\int_0^l\int_0^l \cos\left(\frac{2\pi i}{l}t\right)\sin\left(\frac{2\pi j}{l}s\right)\mathrm{E}\left[X(t)X(s)\right]\mathrm{d}s\mathrm{d}t - \mathrm{E}[C_i]\mathrm{E}[S_j] \\
&= \frac{4}{l^2}\int_0^l\int_0^l \cos\left(\frac{2\pi i}{l}t\right)\sin\left(\frac{2\pi j}{l}s\right) r(s-t)\mathrm{d}s\mathrm{d}t \\
&= \frac{4}{l^2}\int_0^l\int_{-t}^{l-t} \cos\left(\frac{2\pi i}{l}t\right)\sin\left(\frac{2\pi j}{l}(\tau-t)\right) r(\tau)\mathrm{d}\tau\mathrm{d}t \\
&= \frac{2}{l^2}\int_0^l\int_{-l}^{-\tau} \left\{\sin\left(\frac{2\pi(j+i)}{l}t + \frac{2\pi j}{l}\tau\right)\right. \\
&\qquad\qquad \left. + \sin\left(\frac{2\pi(j-i)}{l}t + \frac{2\pi j}{l}\tau\right)\right\}\mathrm{d}t\, r(\tau)\mathrm{d}\tau \\
&\qquad + \frac{2}{l^2}\int_{-l}^{0}\int_{-\tau}^{l} \left\{\sin\left(\frac{2\pi(j+i)}{l}t + \frac{2\pi j}{l}\tau\right)\right. \\
&\qquad\qquad \left. + \sin\left(\frac{2\pi(j-i)}{l}t + \frac{2\pi j}{l}\tau\right)\right\}\mathrm{d}t\, r(\tau)\mathrm{d}\tau\,.
\end{aligned}$$

Moreover, by creating two cases $i = j$ and $i \neq j$ and integrating the result, we get $\mathrm{Cov}(C_i, S_j) = 0$. Similarly, we can calculate $\mathrm{Cov}(C_i, C_j)$ and $\mathrm{Cov}(S_i, S_j)$ as follows.

$$\mathrm{Cov}(C_i, C_j) = \begin{cases} -\frac{2}{il\pi}r_{S,i} + \frac{4}{l}r_{C,i}, & (i=j) \\ \frac{4}{l\pi(j^2-i^2)}\left(ir_{S,i} - jr_{S,j}\right), & (i\neq j) \end{cases},$$

$$\mathrm{Cov}(S_i, S_j) = \begin{cases} \frac{2}{il\pi}r_{S,i} + \frac{4}{l}r_{C,i}, & (i=j) \\ \frac{4}{l\pi(j^2-i^2)}\left(jr_{S,i} - ir_{S,j}\right), & (i\neq j) \end{cases},$$

$$r_{S,i} = \int_0^l \sin\left(\frac{2\pi i}{l}\tau\right) r(\tau)\mathrm{d}\tau\,,$$

$$r_{C,i} = \int_0^l \left(1-\frac{\tau}{l}\right)\cos\left(\frac{2\pi i}{l}\tau\right) r(\tau)\mathrm{d}\tau\,.$$

Substituting them into (3.15), we have

$$\begin{aligned}
\mathrm{E}\left[\mathrm{Var}[\hat{P}|X(t)]\right] &= \sum_{i=1}^{\infty}\frac{4}{l}w_i r_{C,i}\,, \\
\mathrm{Var}\left[\mathrm{Var}[\hat{P}|X(t)]\right] &= \sum_{i=1}^{\infty}\left\{\frac{4}{l}w_i r_{C,i}\right\}^2 + \sum_{i=1}^{\infty}\left\{\frac{2}{li\pi}w_i r_{S,i}\right\}^2 \\
&\qquad + \sum_{i\neq j} 16 w_i w_j \frac{(i^2+j^2)\left\{{r_{S,i}}^2 + {r_{S,j}}^2\right\} - 4ij r_{S,i} r_{S,j}}{l^2\pi^2(i^2-j^2)^2}\,.
\end{aligned} \tag{3.18}$$

However, the second and the third terms on the right-hand side of (3.18) are trivial compared with the first term if we give actual parameters to $r(\tau)$, l and m. Hence, (3.18) is approximated as

$$\mathrm{Var}\left[\mathrm{Var}[\hat{P}|X(t)]\right] \simeq \sum_{i=1}^{\infty}\left\{\frac{4}{l}w_i r_{C,i}\right\}^2 .$$

In Section 3.6, we will confirm the validity of the approximation.

Thus, the evaluation function $e(\sigma)$ that corresponds to (3.9) is given by the following:

$$e(\sigma) = \left\{\sum_{i=1}^{\infty}\frac{4}{l}w_i r_{C,i}\right\}^2 + \sum_{i=1}^{\infty}\left\{\frac{4}{l}w_i r_{C,i}\right\}^2 . \tag{3.19}$$

We can plot evaluation function $e(\sigma)$ if we specify the following: measurement period l, number of probe packets m, the ACF $r(\tau)$ of $X(t)$, and fluctuation magnitude σ (which is added to the timing of probe packets). This means that we can obtain the optimal fluctuation magnitude to suit the properties of the target network.

3.6 Approximation Validity and an Evaluation Examples

In this section, we confirm the validity of our approximations through simulation, and we will show an evaluation example. We should check the approximations that were used to derive (3.19). Moreover, at the end of this section, we show some examples of our evaluation function for the case of M/M/1 queue measurement.

We use the queue length (i.e. the number in the system) of M/M/1 as $X(t)$. The behavior of the M/M/1 queue is very well studied. The mean and variance of the queue length of an M/M/1 system are

$$\begin{aligned}\mathrm{E}[X(t)] &= \frac{\rho}{1-\rho},\\ \mathrm{Var}[X(t)] &= \frac{\rho}{(1-\rho)^2} .\end{aligned} \tag{3.20}$$

The ACF of the queue length of an M/M/1 system is as follows [52].

$$r(\tau) = \frac{(\mu-\lambda)^3}{\pi}\int_0^{2\pi}\sin^2\theta\frac{\mathrm{e}^{-w|\tau|}}{w^3}\mathrm{d}\theta ,$$

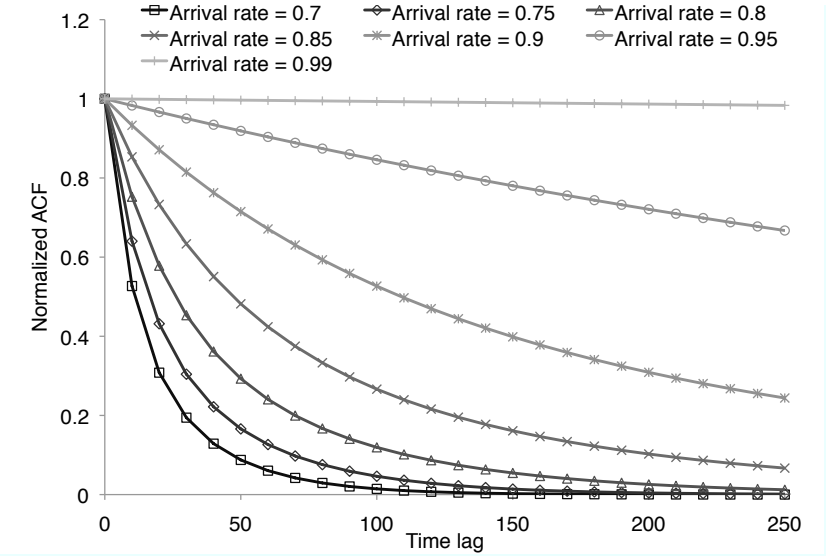

Figure 3.3: Normalized ACFs of M/M/1 queue process for various arrival rates

where

$$w = \lambda + \mu - 2\sqrt{\lambda\mu}\cos\theta\,.$$

Furthermore, if $\mu = 1$, we can approximate the normalized ACF by the following simple form (see (3.7) in reference [53]).

$$r'(\tau) \simeq \frac{1}{2}\left\{\mathrm{e}^{-A|\tau|} + \mathrm{e}^{-B|\tau|}\right\}\,,$$

where

$$A = \frac{(1-\lambda)^2}{1+\lambda+\sqrt{\lambda}}\,, \qquad B = \frac{(1-\lambda)^2}{1+\lambda-\sqrt{\lambda}}\,.$$

Therefore, by using (3.20), we can get the ACF of the M/M/1 queue as follows.

$$r(\tau) \simeq \frac{\rho}{(1-\rho)^2} r'(\tau)\,. \tag{3.21}$$

We show the normalized ACF for various arrival rates λ in Figure 3.3. Generally, the most important parameter that characterizes each ACF is the rate that $r(t)$ approaches to 0.

On active measurement of delay, the probe packets obtain information of the waiting time, not the number in the system. Compared to the queue length case, the correlation

structure of the waiting time on the M/M/1 system is extremely complicated, and does not provide any additional insight for our study. Thus we choose the queue length process as the target in our verification, though it does not correspond to actual measurements completely.

We discuss the validity of our approximations by using the ACFs that are obtained from a M/M/1 queue length. To derive (3.19), we used two approximations. One is a Fourier coefficient, which obeys a normal distribution, and the other is negligible terms on the right-hand side of (3.18).

First, we confirm that Fourier coefficients C_n and S_n obey normal distributions. We already showed the analytical rationale by using the extended central limit theorem in Section 3.5. We executed an M/M/1 simulation 3000 times and calculated the CDF of the C_1 through the simulation. The CDF calculated through the simulation and the CDF of a normal distribution are displayed in Figure 3.4. The parameters we used in the simulations are as follows. The arrival rate λ is 0.75, the service rate μ is 1.0, and the simulation time is 50000. According to the figure, we confirm that these distributions are corresponding to each other. We gained similar results for $C_n\,(n = 1, 2, \dots)$. In Section 3.5, we used the property of moment of bivariate normal distributions with the approximation, i.e. we considered $\mathrm{Cov}({C_i}^2, {C_j}^2) = 2\{\mathrm{Cov}(C_i, C_j)\}^2$ and the other version of the combination of C_i and S_i. To verify the approximation precision, we executed an M/M/1 simulation 3000 times, and computed $\mathrm{Var}[{C_n}^2]$ and $2\{\mathrm{Var}[C_n]\}^2$ directly. Note that $\mathrm{Var}[{C_n}^2]$ and $2\{\mathrm{Var}[C_n]\}^2$ are special cases of $\mathrm{Cov}({C_i}^2, {C_j}^2)$ and $2\{\mathrm{Cov}(C_i, C_j)\}^2$, respectively. Figure 3.5 displays $\mathrm{Var}[{C_n}^2]$ and $2\{\mathrm{Var}[C_n]\}^2$ through the simulations. From Figure 3.5, we can confirm that $\mathrm{Var}\left[{C_n}^2\right]$ is close to $2\{\mathrm{Var}[C_n]\}^2$, for every n. We plotted $\mathrm{Var}[{S_n}^2]$ and $2\{\mathrm{Var}[S_n]\}^2$, and gained similar results.

Furthermore, we show that the second and the third terms on the right-hand side of (3.18) are negligible. By using (3.21), we computed the first term and other terms on the right-hand side of (3.18) separately. Figure 3.6 represents the first term and other terms. The parameters we used are as follows. The arrival rate λ is 0.75, the service rate μ is 1.0, the measurement period l is 50000, and the probing rate m/l is 0.01. Note that the horizontal axis represents the fluctuation magnitude σ. According to the figure, it is clear that the effects of the second and the third term are much less that those of the first term.

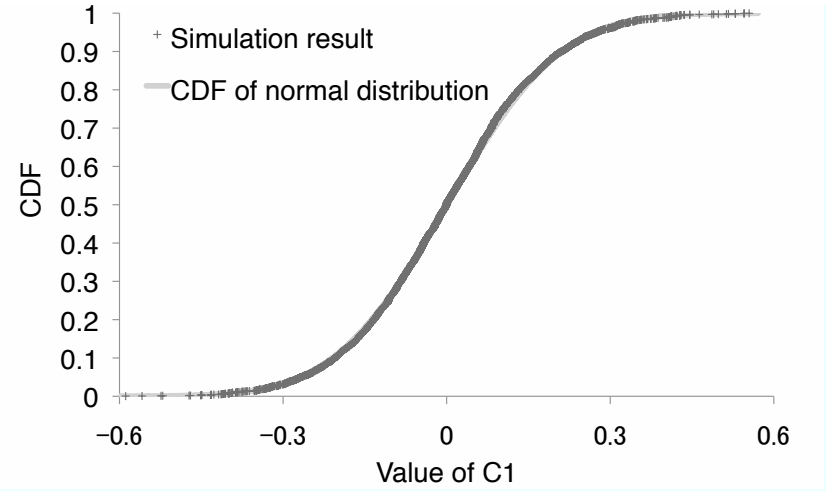

Figure 3.4: CDF of the C_1 calculated through the simulation

Next, we show the complementary CDF of the precision that is expressed by (3.6) in the case of the M/M/1 queue measurement in Figure 3.7. The parameters we used are as follows. The arrival rate λ is 0.75, the service rate μ is 1.0, the measurement period l is 1000, and the probing rate m/l is 0.01. We plotted for three different probing policies: periodic-probing, our probing method with $\sigma = 20$ and PASTA-based probing. According to the figure, we can find that the variance $\mathrm{Var}[\hat{P}|X(t)]$ in the case of PASTA-besed probing is so large (i.e. imprecise), and larger variance in the case of periodic-probing occurs more frequently compared with that in the case of $\sigma = 20$ (but the mean of the variance in the case of periodic-probing is smaller than that of $\sigma = 20$). The result is consistent with our discussion in Section 3.3.

Finally, we show some examples of our evaluation function by using the ACFs that are obtained from a M/M/1 queue length. Please note that, in the rest of this section, we will not execute any simulation. We use the ACF that is derived from a M/M/1 queue process, but our result does not depend on any properties of M/M/1 except the ACF. Therefore, the result can be generalized to the processes that have similar ACF structure. These examples can provide us some insights for tuning the optimal fluctuation magnitude in actual measurements.

In Figure 3.8, we display the evaluation function (3.19) with parameters of $\lambda = 0.75$,

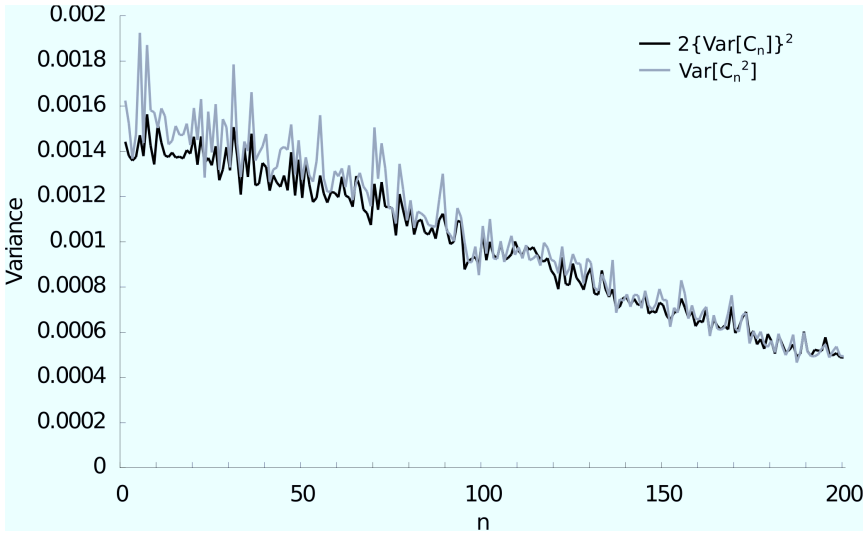

Figure 3.5: Comparison of $\mathrm{Var}[{C_n}^2]$ and $2\{\mathrm{Var}[C_n]\}^2$

$\mu = 1.0$, $l = 50000$, and $m = 500$. We also plotted the first term of (3.19) (shown in the figure as crosses) in Figure 3.8. Note that the horizontal axis represents the fluctuation magnitude σ. The first term of (3.19) expresses the square of the expectation of $\mathrm{Var}[P|X(t)]$ (it means the expectation of precision). According to Figure 3.8, the first term is the smallest when $\sigma = 0$ (i.e. the case of periodic-probing). On the other hand, our evaluation function is not the smallest because it assesses the phase-lock phenomenon by the second term. The evaluation function shows that the optimal value of σ is about 20 in this case.

In addition, we verified the dependence of the evaluation function on each measurement parameter. First, we confirmed the relationship between the evaluation function and the probing rate m/l. We plot the evaluation function of each probing rate while changing m in Figure 3.9. Parameters except m are as follows. $\lambda = 0.75$, $\mu = 1$, and $l = 50000$. We can confirm that the optimal fluctuation magnitude decreases as the probing rate increases. Since the average probe packet intervals decrease with increase of the probing rate, the timing of probe packet injection is randomized with slight fluctuations when a probing rate is high. Adding fluctuations with magnitude σ to the probe packets with a rate m/l has a randomized effect equivalent to adding fluctuations with magnitude $\sigma/2$ to the probe packets with a rate $(2m)/l$. Therefore, we can avoid the phase-lock

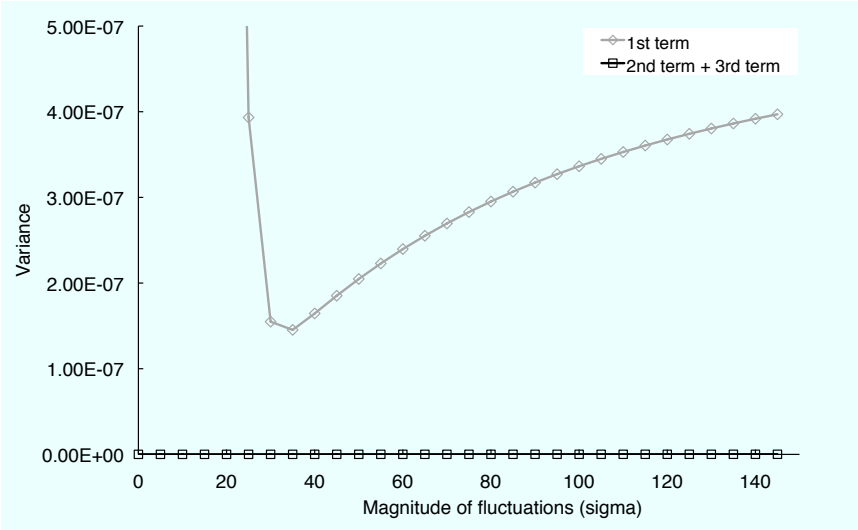

Figure 3.6: Comparison of first term and other terms on the right-hand side of (3.18)

phenomenon by adding slight fluctuations when a probing rate is high. Second, we confirmed the relation between the evaluation function and measurement period l with fixed probing rate. Figure 3.10 plots the evaluation function of each measurement period. Parameters except l are as follows. $\lambda = 0.75$, $\mu = 1$, and the probing rate is 0.01. We can confirm that the optimal fluctuation magnitude holds steady even as the measurement period changes (if probing rate is fixed).

We show the dependence of the optimal fluctuation magnitude on traffic intensity to help network researchers and practitioners in designing experiments. As we mentioned above, the measurement period has no critical effect on the optimal fluctuation magnitude. Therefore, we can cover all cases if we consider the arrival rate and the probing rate. In Figure 3.11, we display the ratio of the optimal fluctuation magnitude to the average probe intervals l/m for each arrival rate. Namely, we plot $m\sigma^*/l$ where σ^* is the optimal fluctuation magnitude. Note that the probing rate means the ratio of probe packet traffic to the regular traffic, since the service rate is fixed at 1 in our example. We plotted a wide variety of values of arrival rate in terms of the speed that ACF $r(\tau)$ approaches to 0 (in Figure 3.3, we showed the ACFs that correspond to the values of arrival rate we displayed). According to the Figure 3.11, we can find that all of points are less than 20% though ACFs $r(\tau)$ are extremely various. Practically, it is difficult to gain the

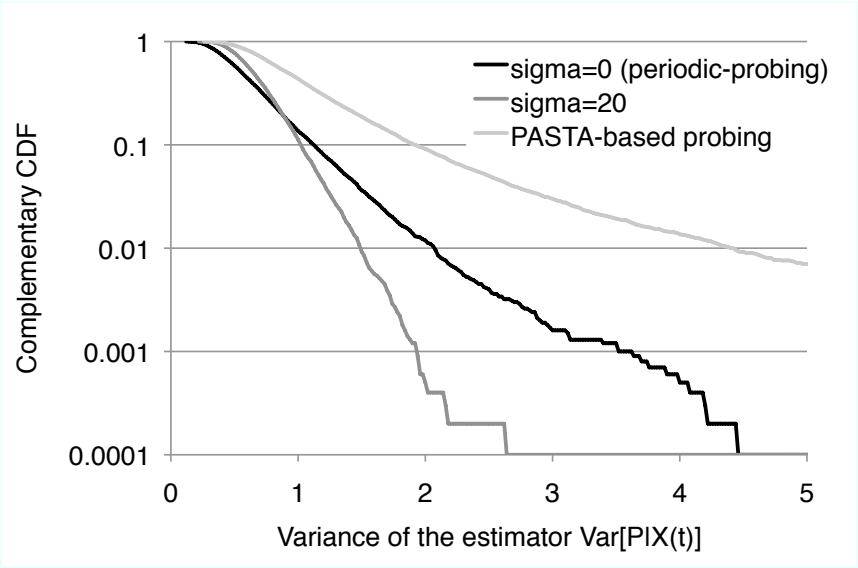

Figure 3.7: Distribution of (3.6) in the case of the M/M/1 queue measurement.

exact knowledge of the ACF without a measurement. However, our result suggests that fluctuation magnitude corresponding to 20% is enough to avoid phase-lock phenomenon for a wide variety of ACFs.

We should take into account intrusiveness when we choose the probing rate m/l. High probing rate leads an precise estimation normally though excessive injections of probe packets lead a deterioration of precision. In this paper, we present a method to specify the optimal fluctuation magnitude of probe packet intervals under the non-intrusive context (the load of the probe packets is ignored in the non-intrusive context). In real measurement, we must design experiments in which impact of the probe packet load is insignificant. Reference [7] clarified the relationship between an asymptotic variance and ACF of target process, and discussed the optimal probing rate that keeps the precision deterioration insignificant. According to the results in reference [7], in M/M/1 model with the arrival rate λ and the service rate μ, an asymptotic variance $s^2(\lambda, \mu, p)$ is given by the following if we inject probe packet with probing rate $p\lambda$.

$$s^2(\lambda, \mu, p) \simeq \frac{\rho^2}{(1-\rho)^2} + p\frac{4\rho^3}{(1-\rho)^4}, \tag{3.22}$$

where $\rho = (1+p)\lambda/\mu$. The optimal probing rate is $p\lambda$ that minimizes (3.22). p means the ratio of the probe stream to all streams, and the p that gives optimal probing rate provides

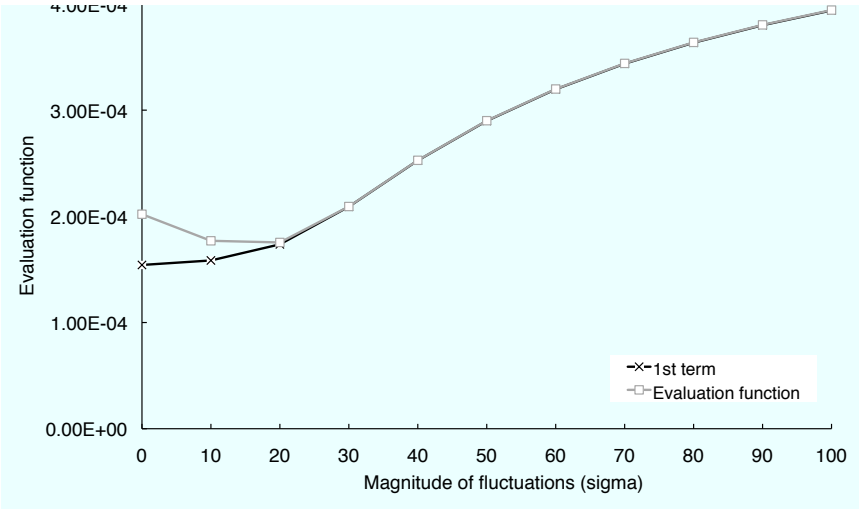

Figure 3.8: Comparison of first term and other terms on the right-hand side of (3.19)

insight to choose probing rate m/l.

3.7 Generality of the Result

We discuss generality of the result of M/M/1 model presented in Section 3.6. In Section 3.6, we presented the evaluation examples based on the ACF of M/M/1 queue length process, and obtained some insights regarding the relationship among ACF, measurement period, the number of probe packets, and the optimal fluctuation magnitude. It is not the contention of this paper that the M/M/1 model is a good model for the modern networks. Of course, M/M/1 model is fundamental but unreal model and the modern networks are not well-modeled as it. However, the optimal fluctuation magnitude that specified by our method does not depend on any properties of M/M/1 except the ACF. Therefore, we obtain same results if the shape of ACF of process that we want to measure is similar to that of M/M/1 queue length process even if M/M/1 does not exactly model the inside of the target network (e.g. behavior of packet, network topology, and queueing, etc.).

The ACFs of processes that we are targeting are monotonically decreasing and convex functions on the interval $[0, \infty)$ though our method that presented in Section 3.5 can apply to a process with any ACF. Monotonically decreasing and convex ACFs of delay/loss

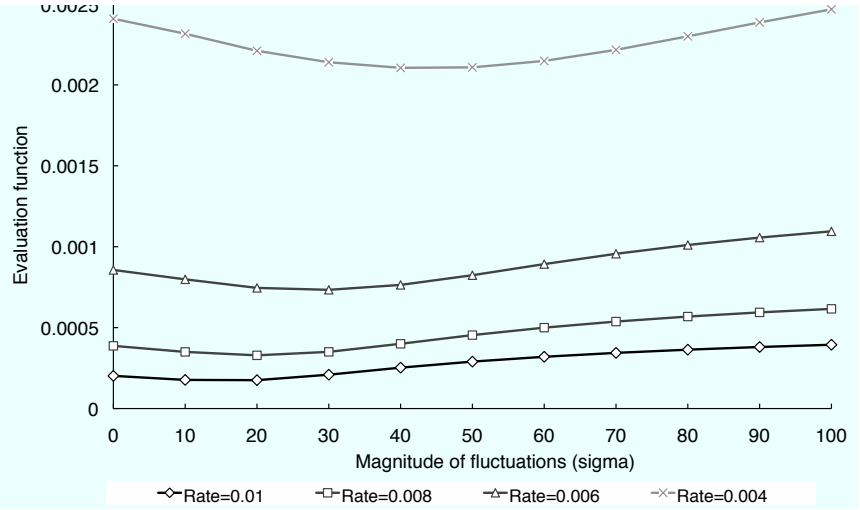

Figure 3.9: Relationship between the optimal fluctuation magnitude and probing rate

processes are well-motivated by analysis of real Internet traffic [1]. The most important parameter to characterize these ACFs is decreasing rate for $\tau \to \infty$.

ACF (3.21) of M/M/1 queue length process is simple function that satisfies above two conditions, and it can have various decay rate by changing parameter ρ as shown in Figure 3.3. We can consider that the family of ACFs (3.21) that are based on M/M/1 queue length process represents various ACFs that we are targeting since target ACFs are characterized by decay rate.

We can expect that the insights that we obtained in Section 3.6 can be utilized when we design experiments for measurements of delay/loss processes whose ACF is monotonically decreasing and convex. In Section 3.6, we gained two main insights: (1) the optimal fluctuation magnitude has robustness to a change of measurement period l; (2) the fluctuation magnitude of 20% of the average probe interval is enough to avoid phase-lock phenomenon for various probing rate and ACFs that have a wide variety of decay rate. As we mentioned above, it is difficult to gain the exact knowledge of the ACF. However, these insights can apply to various target processes that have similar ACF structure even if we cannot gain the knowledge of the ACF. Therefore, we can design a measurement on the safe side by setting the fluctuation magnitude to 20% of probe intervals (needless to say, we can design experiments optimally if we can gain the knowledge of the ACF). In

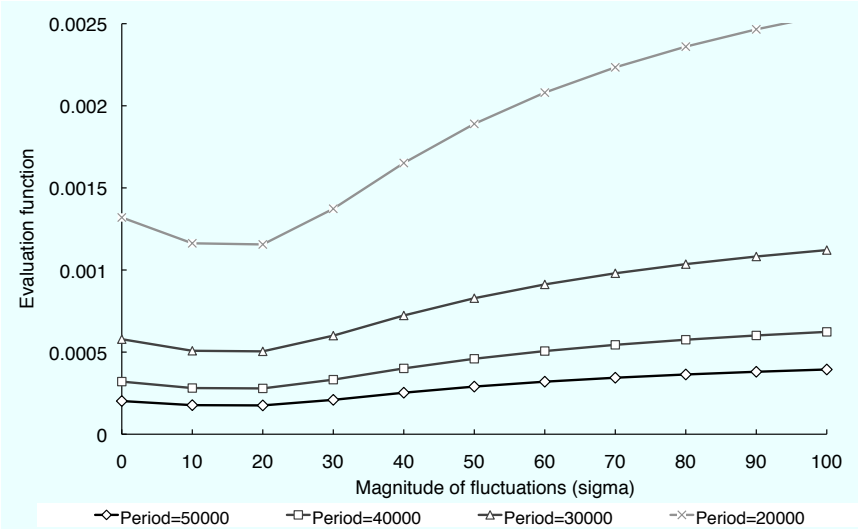

Figure 3.10: Relationship between the optimal fluctuation magnitude and measurement period

addition to above insights, we understand that the results of validation of approximation that the second and the third terms on the right-hand side of (3.18) are negligible can also apply to various target processes that have similar ACF structure.

Finally, we add analysis of phase-lock phenomenon due to accidental periodicity in actual delay of the Internet. Sending probe packets with very short interval (1.00 msec) by the ping tool, we obtained an actual RTT process from the host (192.168.10.48) in Osaka university to google.com (74.125.235.232). We sent probe packets for 5 min per test and performed the test 12 times. Figure 3.12 shows the two RTT processes (data 1 and data 2) with large average RTT among RTT processes we obtained. The loss rates of the probe packets of data 1 and data 2 are 0.21% and 0.44%, respectively, and we interpolated lack of RTT values due to packet loss by a linear interpolation. To confirm the periodicity of RTT processes, we show the power spectrum of the RTT processes in Figure 3.13 and Figure 3.14. Note that the values of power spectrum correspond to K_i in (3.14), and the high value of power with a frequency leads low precision of estimation by periodic-probing with the corresponded frequency. It was confirmed in Chapter 2 that values of power spectrum are strongly correlated to precision (i.e. variance of estimator) of estimation with periodic-probing. According to Figure 3.13, we can confirm the

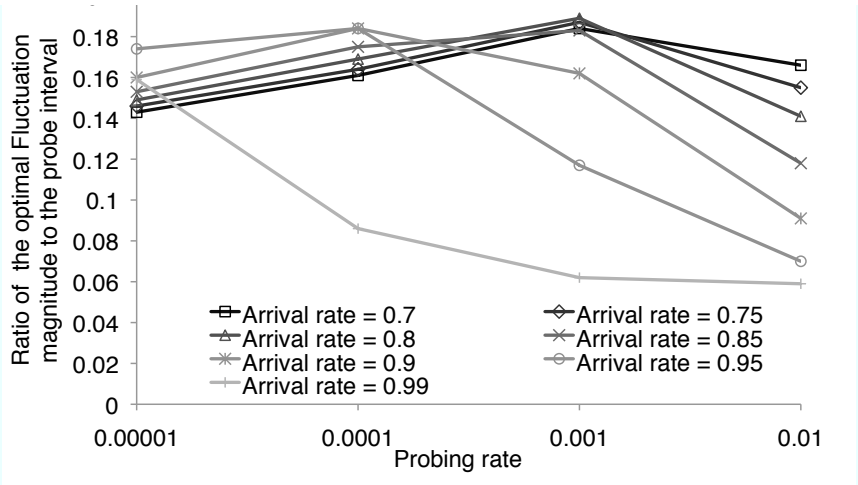

Figure 3.11: Ratio of the optimal fluctuation magnitude to the average probe intervals is less than 20%

periodicity with the frequency 100.00 Hz and expects that the estimation by periodic-probing with interval 10.00 msec is imprecise due to the phase-lock phenomenon. By comparing the Figure 3.13 and Figure 3.14, we can understand that the periodicity is not path-specific periodicity but accidental periodicity since the form of the power spectrum of data 1 differs from that of data 2. Moreover, when a measurement period is short, an accidental periodicity appears remarkably. Figure 3.15 shows the power spectrum of RTT process on 30 sec period (the process is a part of the process of data 1), and the variance of the values of the power is larger than that of RTT process on 5 min period. We can confirm that the value of power with frequency 100.00 Hz ($=$ 3000 times $/$ 30.00 sec) is about 21 times that of power with 99.97 Hz ($=$ 2999 times $/$ 30.00 sec), and the result suggests that a slight difference of intervals of probe packets leads significant diference of precise in periodic-probing.

The above results suggest that imprecise measurements with periodic-probing frequently occur, and it was shown in Chapter 2 that they can be avoided by probing with fluctuations though we do not verify an estimator of probing with fluctuations in an actual measurement. According to the M/M/1 based verification, the variance of estimator by the probing with optimal fluctuations is about half of the variance of estimator by

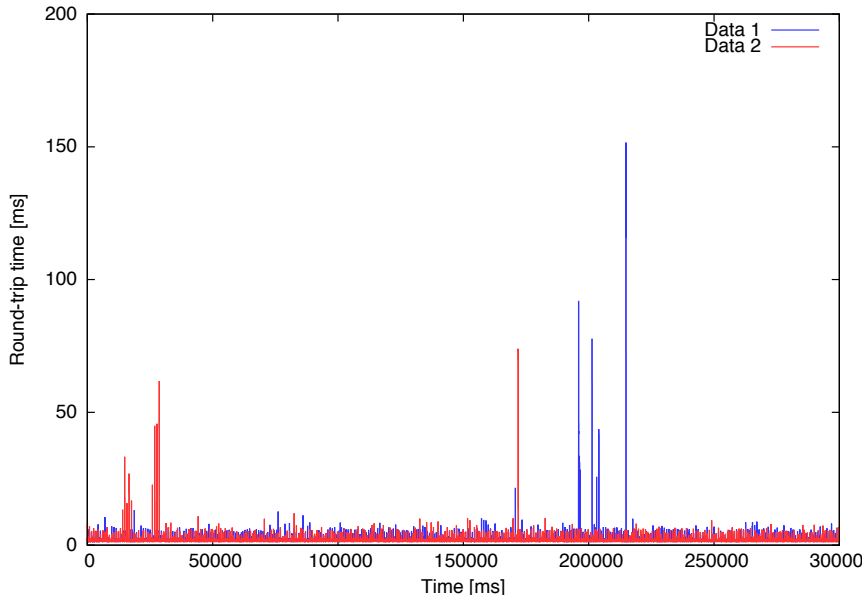

Figure 3.12: RTT processes measured by probe packets with short intervals

PASTA-based probing, and the results mean that probe packet traffic can be decreased in half. Note that our method does not require little introduction cost. It is essential to achieve precise measurement of path performance in short period with light probe packet traffic. The loss rate of probe packets are between 0.2-0.5% in above tests. If we want to measure the loss rate in 30 sec period in which user communicate by VoIP application to evaluate its communication quality, we should inject 300 probe packets per second at least. Moreover, the occurrence rate of long delay (e.g. delay that exceeds 100 msec) is lower than loss rate and therefore it is more difficult to measure. The number of paths is of order n^2 (n denotes the number of nodes), and the load of probe packet traffic is not negligible since the probe packet traffic of these paths is aggregated in core network.

3.8 Summary

In this paper, we analyzed the optimal fluctuation magnitude that should be added to the timing of probe packets. For the analysis, we introduced a probing policy that randomly perturbs the timing of probe packets by using a normal distribution. Moreover, we defined an evaluation function that can well assess the phase-lock phenomenon, and we provided

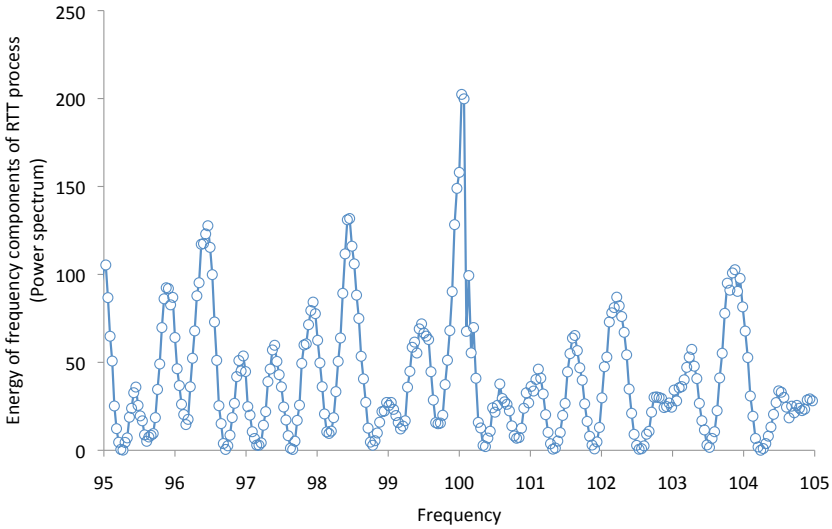

Figure 3.13: Power spectrum of RTT processes (data 1)

a method that can specify the optimal fluctuation magnitude by using the ACF of the target process that we want to measure.

We confirmed the validity of our method by applying it to M/M/1 queue measurement. Furthermore, we showed that the probing rate greatly affects the optimal fluctuation magnitude. The measurement period is not a critical parameter. Through our evaluation examples, we were able to find that a fluctuation magnitude of 20% of the average probe interval is enough to avoid the phase-lock phenomenon for a wide variety of ACFs. The contributions of this chapter are as follows: (1) we showed accidental periodicity as a cause of the phase-lock phenomenon; (2) we clarified that the optimal fluctuation magnitude to avoid the phase-lock phenomenon is characterized by the ACF of the target process; (3) we showed that a fluctuation magnitude of 20% of the average probe interval is enough to avoid phase-lock phenomenon for a wide variety of ACFs; (4) we showed that accidental periodicity can appear in actual network remarkably.

In the future, we will validate the method in detail including verification on an actual network. We are not able to show that how much improvement of precision can be achieved by the optimization of fluctuation magnitude of probe packet timing in an actual measurement though our analysis including RTT processes of the Internet is strongly indicating precision improvement of measurements. To implement our probing policy as

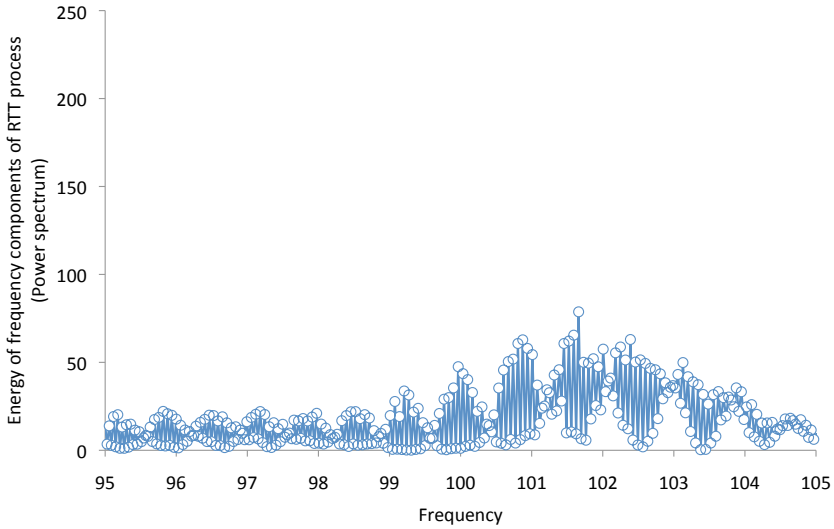

Figure 3.14: Power spectrum of RTT processes (data 2)

an actual measurement method, we need to know the ACF of the target process (delay or loss process etc.) because it is needed to specify the optimal probing policy. Thus we will determine how to estimate the properties of the target network from past measurement data.

Appendix

We prove that the probability that at least one packet of m probe packets injects in $[t, t + \Delta t)$ is $(m\Delta t)/l$ for any t $(0 \leq t < l)$ when we inject the probe packets at $\{T_i\}$ given by (3.10).

Proof. The probability that ith packet is injected in infinitesimal difference $[t, t+\Delta t)$ $(0 \leq t < l)$ under the condition $S = s$ is

$$\Delta t \cdot \sum_{k=-\infty}^{\infty} p_{\mathrm{norm}}\left(t + kl - \frac{l(i-1)}{m} - s\right),$$

where $p_{\mathrm{norm}}(t)$ denotes a pdf of normal distribution with average 0 and standard deviation σ. Then, the probability that one of packet of m probe packets is injected in $[t, t + \Delta t)$

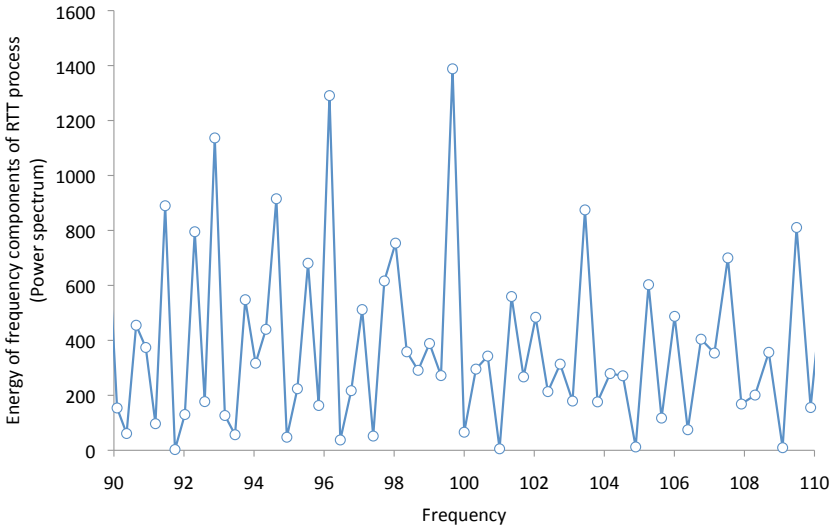

Figure 3.15: Power spectrum of RTT processes on 30 sec period (that is a part of data 1)

under the condition $S = s$ is

$$\Delta t \cdot \sum_{i=1}^{m} \sum_{k=-\infty}^{\infty} p_{\text{norm}}\left(t + kl - \frac{l(i-1)}{m} - s\right).$$

Therefore, since S follows a uniform distribution $U(0, l/m)$, the probability that one of packet is injected in $[t, t + \Delta t)$ is as follow.

$$\begin{aligned}
&\Delta t \cdot \frac{m}{l} \int_0^{\frac{l}{m}} \sum_{i=1}^{m} \sum_{k=-\infty}^{\infty} p_{\text{norm}}\left(t + kl - \frac{l(i-1)}{m} - s\right) \mathrm{d}s \\
&= \Delta t \cdot \frac{m}{l} \int_0^{l} \sum_{k=-\infty}^{\infty} p_{\text{norm}}\left(t + kl - \frac{l(i-1)}{m} - s\right) \mathrm{d}s \\
&= \Delta t \cdot \frac{m}{l}.
\end{aligned}$$

□

Chapter 4

Modeling Fluctuations in the Quasi-static Approach Describing the Temporal Evolution of Retry Traffic

4.1 Introduction

One significant problem with the Internet is node failure due to congestion or overloading. A key factor behind overloading is retry traffic, where users repeatedly attempt to access links and in doing so generate duplicate service requests. To optimize resource allocation and construct stable systems, an evaluation method that precisely models retry traffic is therefore essential.

Retry traffic can be classified into the following two types:

- **Retry traffic due to request discard:** Caused by a shortage of system resources. Requests that exceed service capacity are discarded, regardless of whether the shortfall is temporary or chronic. Rejected users then reattempt service access.

- **Retry traffic due to impatience:** Human nature drives most users who have been kept waiting to issue duplicate service requests; the original request is not

cancelled.

The M/G/s/s retrial queue model is a well-known attempt at using a queuing model to replicate retry traffic [54]. In that model, if all s servers are busy when a service request arrives at the system, the service request is discarded. Discarded requests reenter the system after a certain elapsed time that follows an exponential distribution. The conventional understanding is that the model describes communication services (including IP telephony) based on the Resource reSerVation Protocol (RSVP) [55]. In M/G/s/s, servers correspond to bandwidth, and a reattempt occurs if a service request arrives when all servers are busy, so there is no available bandwidth. Retry traffic in this model corresponds to the first of the two types mentioned above. That is, like most previous works [56–59], the M/G/s/s retrial queue model does not consider retry traffic due to user impatience.

Taking IP telephony as an example, [10] modeled the behavior of retry traffic by considering not only request discards but also impatience; the result is called the *quasi-static retry traffic model*. Traffic behavior is determined by interaction between users and a system because users' decisions are affected by the state of a system. The model of [10] allows the interaction to be very simply described if the system can respond infinitely faster than the users.

To evaluate the behavior of traffic on systems that offer real-world speeds, [10] proposed the *quasi-static approach*, in which the difference between the behavior of the infinitely high-speed system and that of the finite speed system is treated as stochastic fluctuation. Compared with the conventional Markov and Monte Carlo approaches, the quasi-static approach might be superior for estimating the probability of rare system outages on systems with finite but very high speed.

In this paper, we discuss how to model the fluctuation for exactly replicating the behavior of retry traffic caused by user impatience using the quasi-static approach. We demonstrate modeling of the fluctuation in M/M/1- and M/M/s-based systems with retry traffic, and confirm that the results of the quasi-static approach correspond to those of the slower conventional Monte Carlo simulation of queuing systems. Note that low-speed systems can be easily evaluated by conventional Monte Carlo simulation.

The rest of the paper is organized as follows. We summarize the quasi-static approach in Section 4.2. In Section 4.3, we compare the evaluation results of the quasi-static ap-

proach against those of Monte Carlo simulations of the input traffic under M/M/1- and M/M/s-based systems with retry traffic, and we introduce a fluctuation model for exactly replicating the behavior of retry traffic. The comparison demonstrates the validity of the quasi-static approach. We summarizes the paper in Section 4.4.

4.2 Quasi-static Approach for IP Telephony System

4.2.1 Quasi-static Retry Traffic Model

Reference [10] introduced the *quasi-static retry traffic model* model to describe an IP telephony system with retry traffic due to both request discard and impatience. The model describes the interaction between users and a system with different timescales, since retry traffic is generated by user reattempts, which occur much more slowly than the responses of the system. In this subsection, we briefly explain the quasi-static retry traffic model introduced in [10].

Figure 4.1 shows a model of the IP telephony system investigated in [10]. The model is composed of a control plane and a data plane connected in series. It describes the behavior as related to call setup and data transmission processing. The control plane and the data plane are modeled by M/M/1 and M/G/s/s, respectively. Service requests first arrive at the M/M/1 queue and receive service from the M/M/1 server. Next, service requests receive service from one of the s servers in M/G/s/s. Subsequent service requests are discarded if all s servers are busy when they arrive at M/G/s/s. Service requests discarded on the data plane are stored in a retrial queue, and re-enter the system after an elapsed time determined by an exponential distribution. The volume of duplicate service requests is proportional to the number of users in the system of the control plane. Retry traffic from the control plane is the result of user psychology: increased service access delays trigger more reattempts. This retry traffic caused by user impatience characterizes the model.

We assume that reattempts due to impatience have extremely long timescales, as compared to the timescales of the transitions of the number in the system caused by service request arrival. By assigning a discrete time transition to the former and a continuous time transition to the latter, [10] constructed a traffic model that can express the difference in

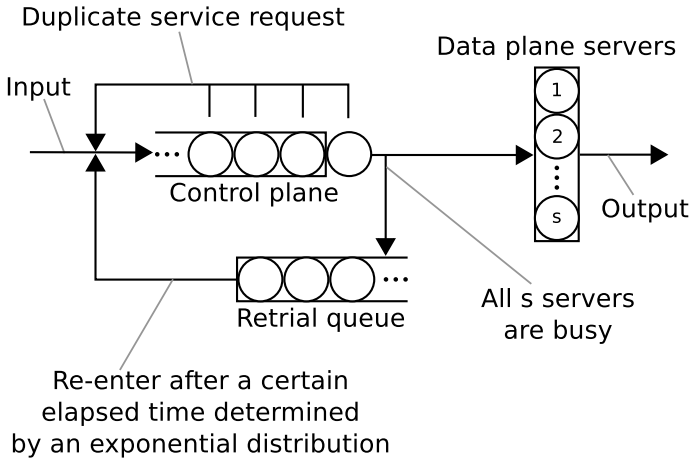

Figure 4.1: Model incorporating retry traffic from the control plane (M/M/1) and the data plane (M/G/s/s)

timescales.

For a certain constant $T\,(>0)$, where T denotes the timescale of user response, the traffic model is as follows:

- A change in the request arrival rate due to user reattempts occurs only when time $t = kT\,(k = 1, 2, \cdots)$.
- The arrival rate of retry traffic from the control plane in the time interval $(kT, (k+1)T]$ is proportional to the average number in the system in the time interval $((k-1)T, kT]$ (Figure 4.2).
- Compared to the speed of user response, the system works at infinitely high speed, and the average number in the system in finite time interval $(kT, (k+1)T]$ is equal to the mean calculated from the stationary state probability.

Reference [10] used 1 s for T, based on a study of user response times [60].

The system attains the stationary state in the finite time interval $((k-1)T, kT]$ because the arrival rate does not change in the interval, and we assume that the system can respond at infinitely high speed. Therefore, since the arrival rate λ_{k+1} of service requests in the time interval $(kT, (k+1)T]$ depends only on the arrival rate λ_k in the time interval

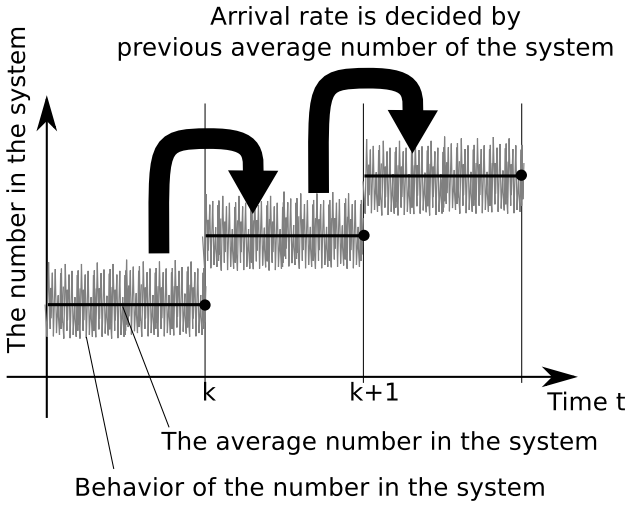

Figure 4.2: Relationship between a change in arrival rate and the number in the system

$((k-1)T, kT]$, we get λ_{k+1} by the recurrence equation

$$\lambda_{k+1} = \lambda_0 + \lambda_k B(\lambda_k/\mu, s) + \varepsilon \frac{\lambda_k/\eta}{1-\lambda_k/\eta}\,, \tag{4.1}$$

where λ_0 denotes the original arrival rate excluding retry traffic, η and μ denote service rates of the control and the data plane, respectively (i.e., the respective average service times are $1/\eta$ and $1/\mu$), and ε is a positive constant indicating the intensity of retry traffic generated from the control plane. $B(\rho, s)$ is the Erlang B formula and represents the discard rate on M/G/s/s, as follows:

$$B(\rho, s) = \frac{\rho^s/s!}{1+\rho+\rho^2/2!+\cdots+\rho^s/s!}\,.$$

The second and the third term on the right side of Eq. (4.1) represent retry traffic from the data and the control plane, respectively.

In this model, the rate of retry traffic from users in the control plane is proportional to the time average of the number in the system, and this means that the number of user reattempts is proportional to user time spent in the M/M/1 system on the control plane (the delay before service provision). According to the PASTA property [36], in M/M/1 the event-average of the number in the system just before service request arrival equals the time average of the process of the number in the system. If the system works at infinitely

high speed (namely, the limit for $\lambda_k \to \infty$, $\eta \to \infty$), the following equation holds:

$$\lim_{\lambda_k \to \infty} \frac{\lambda_k/\eta}{1-\lambda_k/\eta} = \lim_{\lambda_k \to \infty} \frac{1}{M(\lambda_k)} \sum_{i=1}^{M(\lambda_k)} Q_i^k \qquad \text{a.s.,} \tag{4.2}$$

where $M(\lambda_k)$ and Q_i^k $(i = 1, 2, \cdots, M(\lambda_k))$ denote the number of arrivals in the time interval $((k-1)T, kT]$ and the number in the system just before the ith arrival in the time interval $((k-1)T, kT]$, respectively. $M(\lambda_k)$ is a random variable that follows a Poisson distribution with parameter $\lambda_k T$. Note that the left side of Eq. (4.2) corresponds to the third term on the right side of Eq. (4.1). Moreover, using Little's formula [61], we find

$$\begin{aligned} \lim_{\lambda_k \to \infty} \frac{1}{M(\lambda_k)} \sum_{i=1}^{M(\lambda_k)} Q_i^k &= \lambda_k \lim_{\lambda_k \to \infty} \frac{1}{M(\lambda_k)} \sum_{i=1}^{M(\lambda_k)} W_i^k \\ &= \lim_{\lambda_k \to \infty} \sum_{i=1}^{M(\lambda_k)} W_i^k \qquad \text{a.s.,} \end{aligned}$$

where W_i^k $(i = 1, 2, \cdots, M(\lambda_k))$ denotes the time spent by the ith arrival in the system in the time interval $((k-1)T, kT]$, and the last equality follows from the following limit:

$$\lim_{\lambda_k \to \infty} \frac{M(\lambda_k)}{\lambda_k} = 1 \qquad \text{a.s.}$$

Therefore, if each user reattempts access in proportion to waiting time, the input traffic is determined by Eq. (4.1) on the limit $\lambda_k \to \infty$. Since we assume the system works at infinitely high speed, Eq. (4.2) holds, and we can get the transition of the arrival rate by determining λ_{k+1} in Eq. (4.1) from the original arrival rate λ_0. As a result, we can analyze the stability of the system [10, 62].

4.2.2 Quasi-static Approach

As mentioned above, Eq. (4.1) describes the behavior of a system with infinitely high response speed. Equation (4.1) may not describe real systems, since actual response speeds are finite. With real-world systems, since we cannot take the limit as in Eq. (4.2), we should add a fluctuation term $\phi(\lambda_k)$ as follows:

$$\frac{\lambda_k/\eta}{1-\lambda_k/\eta} + \phi(\lambda_k) = \frac{1}{M(\lambda_k)} \sum_{i=1}^{M(\lambda_k)} Q_i^k \,. \tag{4.3}$$

Note that $\phi(\lambda_k)$ is a random variable whose mean is 0.

If we analyze the behavior of the left side of Eq. (4.3) using the conventional Markov approach, we must consider a Markov model with $M(\lambda_k)$-dimensional state space consisting of the past $M(\lambda_k)$ states $\{Q_i^k\}$ $(i = 1, \cdots, M(\lambda_k))$. In the case of $M(\lambda_k) \gg 1$ (an extremely fast system, but not an infinitely fast one), the problem becomes intractable due to the excessive state space. When we use Monte Carlo simulation to analyze the behavior of a high-but-finite-speed system, the simulation must be quite long if we are interested in the probabilities of rare events (e.g. the probability of service failure is to be less than 10^{-6}). Therefore, it is difficult to analyze the behavior of high-speed systems by conventional approaches.

To solve the above problem, [10] proposed adding stochastic fluctuations to the behavior of a system with infinitely high response speed. This is called the quasi-static approach. The stochastic fluctuations mirror the difference between the behavior of finite speed systems and that of infinitely high-speed systems. Reference [10] defines $X(t)$ as the volume of input traffic, including retry traffic, at time t, and expresses the temporal evolution of $X(t)$ using the Langevin equation

$$\frac{\mathrm{d}}{\mathrm{d}t}X(t) = F(X(t)) + \sqrt{D(X(t))}\,\xi(t)\,, \tag{4.4}$$

where $\xi(t)$ denotes white Gaussian noise with the following property:

$$\mathrm{E}[\xi(t)] = 0, \qquad \mathrm{E}[\xi(t)\xi(t')] = \delta(t - t')\,.$$

Note that, for expedience, we replace discrete time kT with continuous time t in Eq. (4.4). $F(X)$ and $D(X)$ are given as

$$F(X) = \lambda_0 + B\left(\frac{X}{tT}, s\right) + \varepsilon\frac{X/(\eta T)}{1 - X/(\eta T)} - \frac{X}{T}\,, \tag{4.5}$$

$$D(X) = \frac{X}{T} + c(X)\,, \tag{4.6}$$

where $c(x)$ is a simple step function representing the fluctuations in retry traffic from the data plane (see [10] for details). In Section 4.3, we discuss the derivation and the validity of $F(X)$ and $D(X)$ in detail for M/M/1- and M/M/s-based systems with retry traffic.

Moreover, we can eliminate X-dependence from the second (fluctuation) term on the right side of Eq. (4.4) by transforming the random variable using $Y = 2\sqrt{D(X)}$. In other

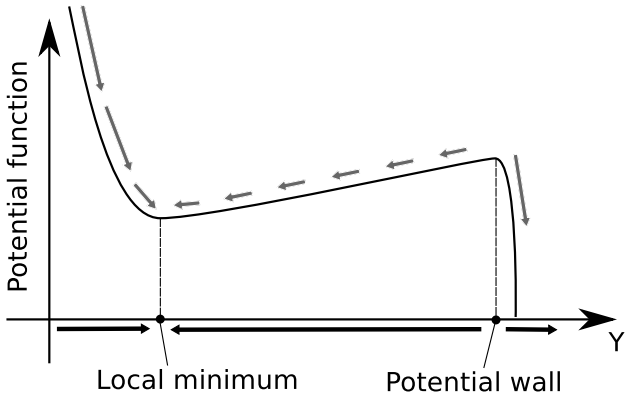

Figure 4.3: An example potential function

words, we can treat the magnitude of fluctuations as a constant for any X. The result of the transformation is as follows:

$$\frac{\mathrm{d}}{\mathrm{d}t}Y(t) = G(Y(t)) + \xi(t),$$

$$G(y) = \frac{F(x) - 1/4}{\sqrt{x/T + c(x)}}, \qquad y = 2\sqrt{x/T + c(x)}\,.$$

We can investigate the behavior of $Y(t)$ using the potential function given by $-\int G(y)\mathrm{d}y$.

The potential function indicates the tendency of the temporal evolution of Y, but Y fluctuates by the effect of $\xi(t)$ and often moves against the potential function. On average, Y moves in the direction that lowers the potential function. Figure 4.3 shows an example potential function. In that example, Y tends to be distributed near the local minimum point. If, however, Y reaches the potential wall due to fluctuations $\xi(t)$, Y diverges (namely, the arrival rate diverges and the system suffers overloading).

It is well known that the Langevin equation Eq. (4.4) is equivalent to the Fokker-Planck equation [63] as shown by

$$\frac{\partial}{\partial t}p(y,t) = -\frac{\partial}{\partial y}G(y)p(y,t) + \frac{1}{2}\frac{\partial^2}{\partial y^2}p(y,t)\,, \tag{4.7}$$

where $p(y,t)$ denotes the pdf of $Y(t)$. Using Eq. (4.7), we can simulate the transition of the pdf of the volume of traffic, and can assess the probability of its divergence and so forth.

4.3 Comparing the Quasi-static Approach with the Conventional Approach

4.3.1 Verification in a Simple M/M/1 Model

We verify that the quasi-static approach, which adds random fluctuations to the behavior of infinitely high-speed systems, can appropriately describe the behavior of finite-speed systems. We start our verification using one of the simplest models: an M/M/1 system without retry traffic. The quasi-static approach can describe a system that contains no retry traffic, though it was proposed to analyze the behavior of retry traffic. The arrival rate of a simple M/M/1 system is constant, and it is well known that the volume of traffic follows a Poisson distribution.

First, we consider the Langevin equation corresponding to the M/M/1 system. Since the second and third terms on the right side of Eq. (4.5) correspond to retry traffic from the data and control plane, respectively, we find that

$$F(X) = \lambda_0 - \frac{X}{T}\,. \tag{4.8}$$

Similarly, since the second term on the right side of Eq. (4.6) represents the fluctuation magnitude of retry traffic from the data plane, we obtain

$$D(X) = \frac{X}{T}\,. \tag{4.9}$$

We therefore get the Langevin equation corresponding to a simple M/M/1 system by substituting Eqs. (4.8) and (4.9) for Eq. (4.4).

Moreover, the Fokker-Planck equation equivalent to this Langevin equation is derived as follows:

$$\frac{\partial}{\partial t}p(x,t) = -\frac{\partial}{\partial x}F(x)p(x,t) + \frac{1}{2}\frac{\partial^2}{\partial x^2}D(x)p(x,t)\,. \tag{4.10}$$

Note that we do not transform the random variable, because our aim is not to consider system stability with respect to the potential function, but rather to compare the distribution of X against a Poisson distribution.

Using Eq. (4.10), we compute the input traffic of the simple M/M/1 system, and in Figure 4.4 the result of the stationary state is compared with the Poisson distribution that

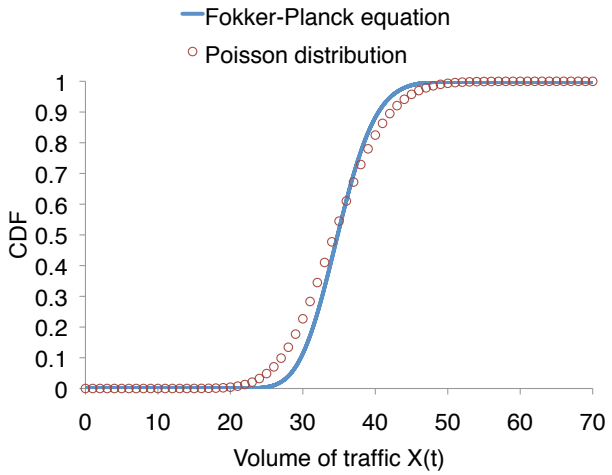

Figure 4.4: Poisson distribution and the distribution of $X(t)$ as computed by the Fokker-Planck equation with Eqs. (4.8) and (4.9)

is the theoretical result. The parameters of the M/M/1 system are the arrival rate $\lambda_0 = 35$, the service rate $\eta = 50$, and the timescale $T = 1$ s. The horizontal axis represents the volume of traffic $X(t)$ that is the number of arrivals in the interval $(t - T, t]$. Note that the figure displays the distributions as CDFs, not pdfs. According to the figure, the distribution does not correspond to a Poisson distribution, despite having already reached a stationary state. We must therefore reconsider Eqs. (4.8) and (4.9).

To solve this problem, we should exactly model the system as the Langevin equation. It is intuitive that $X(t)$ is defined as the actual number of arrivals in time interval $(t-T, t]$, since λ_k is the arrival rate in the time interval $((k-1)T, kT]$. If we define $\mathrm{d}X(t)$ as the change of $X(t)$ in a minute distance $\mathrm{d}t$, we find that

$$\begin{aligned} \mathrm{d}X(t) &= X(t + \mathrm{d}t) - X(t) \\ &= U(t, \mathrm{d}t) - U(t - T, \mathrm{d}t)\,, \end{aligned}$$

where $U(t, \mathrm{d}t)$ is the actual number of arrivals in the time interval $(t, t + \mathrm{d}t]$ (Figure 4.5). The expectation and variance of random variable $U(t, \mathrm{d}t)$ are both $\lambda_0 \mathrm{d}t$ because the future arrivals follow a Poisson arrival. Moreover, the conditional distribution of $U(t - T, \mathrm{d}t)$, given that $U(t - T, T) = X(t)$, obeys a binomial distribution $B(X(t), \mathrm{d}t/T)$ [64]. Therefore, the conditional expectation and variance of $U(t - T, \mathrm{d}t)$

is as follows:

$$\mathrm{E}[U(t-T,\mathrm{d}t)\,|\,U(t-T,T)=X(t)] = (X(t)/T)\mathrm{d}t,$$

$$\begin{aligned}\mathrm{Var}&[U(t-T,\mathrm{d}t)\,|\,U(t-T,T)=X(t)]\\ &= (X(t)/T)\mathrm{d}t - (X(t)/T^2)(\mathrm{d}t)^2\\ &\simeq (X(t)/T)\mathrm{d}t.\end{aligned}$$

As a result, we can write $\mathrm{d}X(t)$ as

$$\mathrm{d}X(t) \simeq \lambda_0 \mathrm{d}t - \frac{X(t)}{T}\mathrm{d}t + \sqrt{\lambda_0 + \frac{X(t)}{T}}\, N(t)\sqrt{\mathrm{d}t}\,,$$

where $N(t)$ is a random variable that obeys a standard normal distribution and time series $N(t)$ are independent for different t. Now, we define $W(t)$ as a Wiener process. Since $N(t)\sqrt{\mathrm{d}t}$ is $\mathrm{d}W(t)$, we get the Langevin equation as

$$\begin{aligned}\frac{\mathrm{d}}{\mathrm{d}t}X(t) &= \lambda_0 - \frac{X(t)}{T} + \sqrt{\lambda_0 + \frac{X(t)}{T}}\,\frac{\mathrm{d}W(t)}{\mathrm{d}t}\\ &= \lambda_0 - \frac{X(t)}{T} + \sqrt{\lambda_0 + \frac{X(t)}{T}}\,\xi(t)\,,\end{aligned}$$

and the appropriate fluctuation magnitude $D(X)$ is given by

$$D(X) = \lambda_0 + \frac{X(t)}{T}\,. \tag{4.11}$$

This is a necessary revision, because $X(t)$ is given as a function of time t, not as an amount that is defined in a time interval.

We recomputed the distribution of $X(t)$ using the above Fokker-Planck equation with exactly modeled fluctuation magnitude $D(X)$. Figure 4.6 shows the results; we can confirm that the behavior of input traffic for simple M/M/1 is described appropriately by the quasi-static approach. Figure 4.7 presents the potential function corresponding to the above experiment. Note that this potential function considers $X(t)$ (not $Y(t)$), and the fluctuations on each X are not constant. We can find the local minimum (stability point) at $X = 35.0$, and the volume of traffic X tends to be distributed around the stability point.

4.3.2 Verification in an M/M/1-based System with Retry Traffic

This subsection verifies the validity of the quasi-static approach for an M/M/1-based system with retry traffic. This model is significant because a control plane that generates

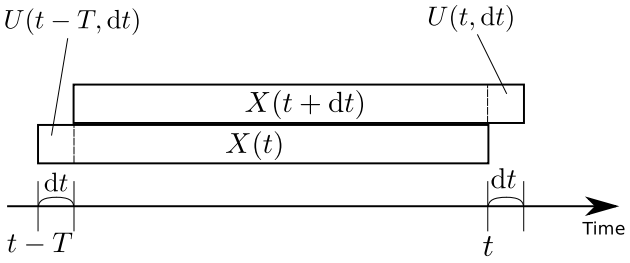

Figure 4.5: Transition of $X(t)$ that expresses actual input traffic in the past period T [s]

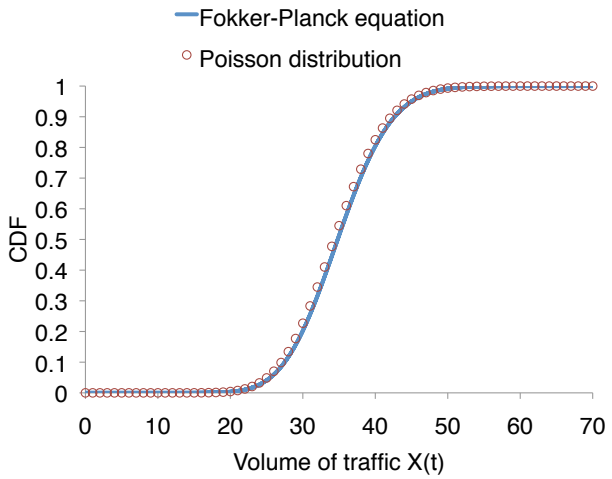

Figure 4.6: Poisson distribution and the distribution of $X(t)$, as computed by the Fokker-Planck equation with Eqs. (4.8) and (4.11)

retry traffic characterizes the model of an IP telephony system. In this subsection we treat M/M/1-FIFO-based systems, but the results can also apply to M/M/1-PS systems since a process of the number in the M/M/1-PS system is the same birth-death process as that of an M/M/1-FIFO system [65].

In the system of this section, the retry traffic rate at time t is proportional to the event-average of the number in the system at the time of request arrival in the time interval $(t-T, t]$, and it is added to the arrival rate at time t. Note that the traffic rate is changed not at discrete times as in the quasi-static retry traffic model, but rather using continuous time. Unfortunately, there is no analytical method to obtain the distribution of system traffic volume, unlike the case of the simple M/M/1 system. We therefore compute the

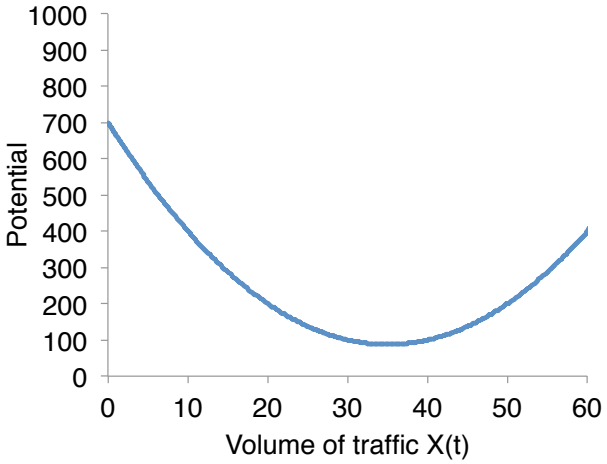

Figure 4.7: Potential function of the simple M/M/1

distribution of traffic volume (the number of arrivals including the retry traffic in an interval $(t-T,t]$) by Monte Carlo simulation, and compare with the results of the quasi-static approach.

As in the simple M/M/1 case, we investigate the Langevin equation corresponding to the M/M/1-based system with retry traffic. If we assume that the system works at infinitely high speed, the transition of the arrival rate in the quasi-static retry traffic model is given by

$$\lambda_{k+1} = \lambda_0 + \varepsilon \frac{\lambda_k/\eta}{1-\lambda_k/\eta}\,.$$

We rewrite this equation as difference $\Delta\lambda_k$,

$$\begin{aligned}\Delta\lambda_k &= \lambda_{k+1} - \lambda_k \\ &= \lambda_0 - \lambda_k + \varepsilon \frac{\lambda_k/\eta}{1-\lambda_k/\eta}\,.\end{aligned}$$

By a natural continuation to yield the Langevin equation, we have

$$\mathrm{d}\lambda(t) = \frac{1}{T}\left(\lambda_0 - \lambda(t) + \varepsilon \frac{\lambda(t)/\eta}{1-\lambda(t)/\eta}\right)\mathrm{d}t\,,$$

where $\lambda(t)$ denotes the arrival rate at time t. We substitute $X(t)/T$ (the actual number of arrivals per second) for $\lambda(t)$ to consider a finite speed system. As in the simple M/M/1 case, the change of $X(t)$, which is the number of arrivals in the past period T [s], is

composed of the increment $U(t, \mathrm{d}t)$ and the decrement $-U(t-T, \mathrm{d}t)$. Their conditional expectation and variance are given by

$$\mathrm{E}[U(t, \mathrm{d}t) \,|\, U(t-T, T) = X(t)] = \lambda_0 + \varepsilon \frac{X(t)/(\eta T)}{1 - X(t)/(\eta T)} \mathrm{d}t \,,$$

$$\mathrm{Var}[U(t, \mathrm{d}t) \,|\, U(t-T, T) = X(t)] = \lambda_0 + \varepsilon \frac{X(t)/(\eta T)}{1 - X(t)/(\eta T)} \mathrm{d}t \,,$$

$$\mathrm{E}[-U(t-T, \mathrm{d}t)] = -\frac{X(t)}{T} \mathrm{d}t \,,$$

$$\mathrm{Var}[-U(t-T, \mathrm{d}t)] = \frac{X(t)}{T} \mathrm{d}t \,.$$

As a result, $F(X)$ and $D(X)$ of the Langevin equation that describes the temporal evolution of $X(t)$ are given by

$$F(X) = \lambda_0 - \frac{X(t)}{T} + \varepsilon \frac{X(t)/(\eta T)}{1 - X(t)/(\eta T)} \,, \tag{4.12}$$

$$D(X) = \lambda_0 + \frac{X(t)}{T} + \varepsilon \frac{X(t)/(\eta T)}{1 - X(t)/(\eta T)} \,. \tag{4.13}$$

The third term on the right side of Eq. (4.13) corresponds to the fluctuations of retry traffic. However, Eq. (4.6) does not contain this term since it can be neglected under the conditions assumed in [10]. By substituting Eqs. (4.12) and (4.13) for Eq. (4.10), we find the Fokker-Planck equation that can compute the behavior of the M/M/1-based system with retry traffic.

We used two methods to compute the CDF of input traffic including retry traffic when $t = 1$, 10, 20, and 30 s: Monte Carlo simulation and the Fokker-Planck equation for the quasi-static approach. Figure 4.8 shows the results. The parameters used are as follows: The original arrival rate λ_0 excluding retry traffic is 35, the service rate η is 50, the intensity of retry traffic ε is 0.1, and user timescale T is 1 s. We set the initial distribution $p(x, 0)$ of the volume of traffic as a Poisson distribution with parameter $\lambda_0 T$. The figure confirms that the quasi-static approach yields results similar to those of the Monte Carlo simulation, though the model contains retry traffic. Figure 4.9 presents the potential function corresponding to the above experiment. Note that this potential function considers

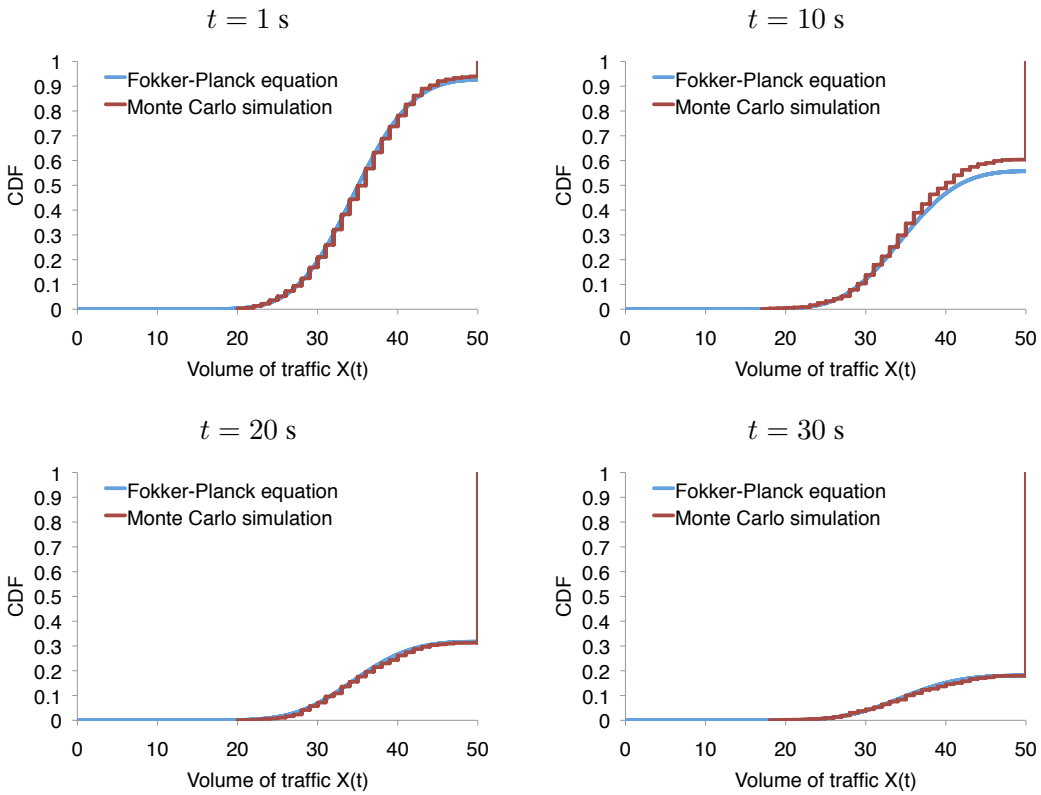

Figure 4.8: Distribution of input traffic at time t on the M/M/1-based system with retry traffic

$X(t)$ (not $Y(t)$), and the fluctuations on each X are not constant. We can find the local minimum (stability point) and the wall of the potential at $X = 35.25$ and $X = 50$, respectively. The volume of traffic X tends to be distributed around the stability point, but X diverges once it crosses the wall of potential because it exceeds the capacity ηT that the system can process in a period T and the number in the system diverge. It is of prime interest to evaluate traffic divergence, which corresponds to system overload. In Figure 4.8, the value of CDF at $X = 50$ falls with time, meaning that the diverge probability of traffic increases gradually. Note that we consider traffic to have diverged if $X(t)$ exceeds ηT once in the Monte Carlo simulation.

To verify the validity of the quasi-static approach, we check that its results correspond to those of Monte Carlo simulation with various parameters. First, we vary the original

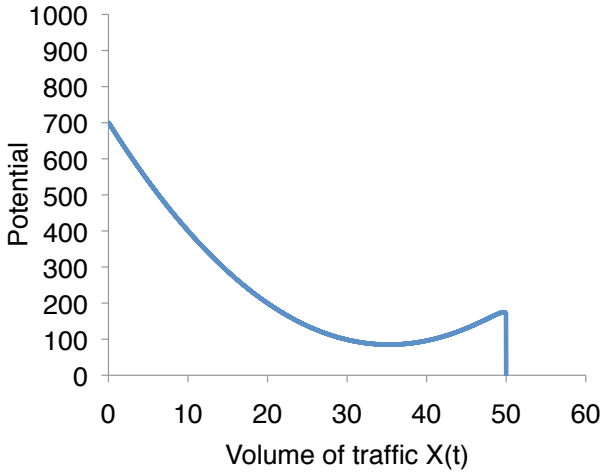

Figure 4.9: Potential function of the M/M/1-based system with retry traffic

input traffic rate λ_0 as 30, 35, and 40. The parameters of the experiment are the same as in the above experiment, except for λ_0. Figure 4.10 shows the results of the probability of traffic divergence. The horizontal and vertical axes represent time and the probability of traffic divergence, respectively. The figure therefore indicates the CDF of the time that the system will spend until the volume of traffic $X(t)$ in the interval $(t-T, t]$ first exceeds the capacity ηT that the system can process in a period T. The figure confirms that the divergence processes of the traffic calculated by the Fokker-Planck equation correspond to the results of Monte Carlo simulation for any λ_0. Similarly, we individually vary the user timescale T as 0.5, 1.0, and 1.5, and the intensity of retry traffic ε as 0.1 and 0.5. The other parameters of the experiment are the same as in the first experiment in this subsection. Figures 4.11 and 4.12 display the respective results and similar results are gained.

The above experiments confirm that the quasi-static approach can describe the behavior of retry traffic in an M/M/1-based system, like the conventional Monte Carlo simulation. We confirm that the probability of traffic divergence calculated by the quasi-static approach corresponds to the results of Monte Carlo simulation of the queuing system under slow system conditions. The target system that we want to evaluate using the quasi-static approach is a high-speed system that is difficult to evaluate using conventional Monte Carlo simulation. We expect that the quasi-static approach can appropriately eval-

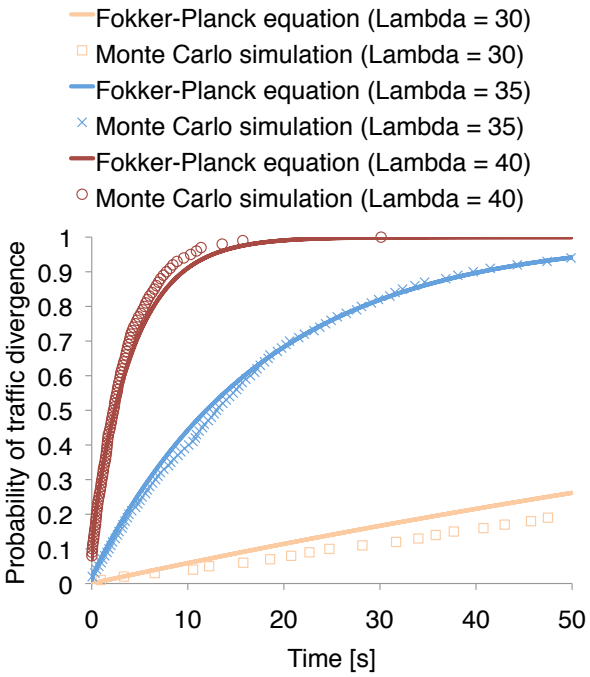

Figure 4.10: Probability of traffic divergence in an M/M/1-based system with retry traffic for various λ_0

uate the behavior of retry traffic for a high-speed system, since the quasi-static approach can evaluate a low-speed system despite the difficulty of evaluating a large magnitude of fluctuations.

4.3.3 Verification in an M/M/s-based System with Retry Traffic

Finally, we apply the quasi-static approach to an M/M/s-based system with retry traffic, and verify the validity of the quasi-static approach. We assume that retry traffic is generated at a rate proportional to the number in the system of M/M/s-based system, like the above-mentioned M/M/1-based system with retry traffic. The average number in the

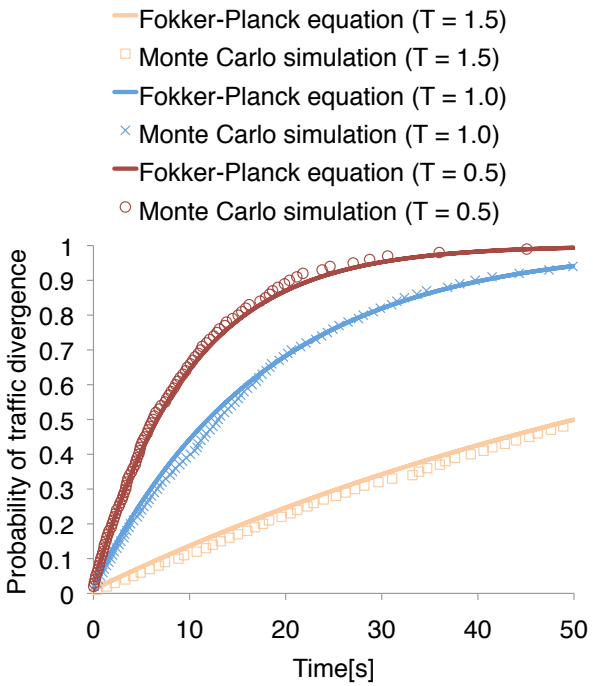

Figure 4.11: Probability of traffic divergence in an M/M/1-based system with retry traffic for various timescales T

system of the M/M/s system $q(\rho, c)$ is given by

$$q(\rho, c) = \frac{\rho(c\rho)^c}{c!(1-\rho)^2} P_0 + c\rho,$$

$$P_0 = \frac{1-\rho}{(1-\rho)\sum_{i=0}^{c} \frac{(c\rho)^i}{i!} + \frac{(c\rho)^c}{c!}\rho},$$

where λ, η, ρ, and c denote arrival rate, service rate, utilization factor λ/η, and the number of servers, respectively [66]. By replacing the third terms, which describe the behavior of retry traffic, we can easily extend Eqs. (4.12) and (4.13) of the M/M/1 model to the M/M/s model as follows:

$$F(X) = \lambda_0 - \frac{X(t)}{T} + \varepsilon q\left(\frac{X(t)}{\eta T}, c\right), \tag{4.14}$$

$$D(X) = \lambda_0 + \frac{X(t)}{T} + \varepsilon q\left(\frac{X(t)}{\eta T}, c\right). \tag{4.15}$$

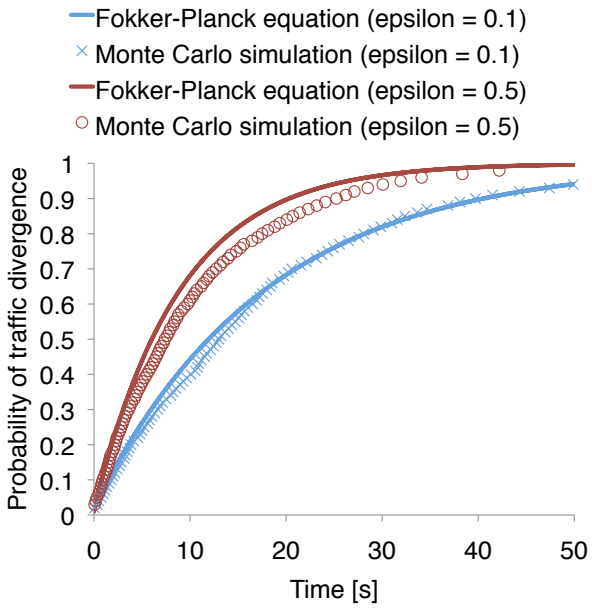

Figure 4.12: Probability of traffic divergence in an M/M/1-based system with retry traffic for various retry traffic intensities ε

We calculate the probability of traffic divergence in an M/M/s-based system with retry traffic using the Fokker-Planck equation with Eqs. (4.14) and (4.15). Figure 4.13 compares of the results of the Fokker-Planck equation and the Monte Carlo simulation for the number of servers $c = 1$, 25, and 50. The figure confirms that the results of the Fokker-Planck equation correspond to those of Monte Carlo simulation.

The quasi-static approach evaluates the behavior of retry traffic due to user impatience in various queuing systems, though this paper focused on M/M/1- (or M/M/1-PS-) and M/M/s-based systems with retry traffic. We can obtain $F(X)$ and $D(X)$ of another system version by replacing the function q in Eqs. (4.14) and (4.15) as the average number in the system if we assume that the request arrival process is a Poisson process.

4.4 Summary

This paper modeled the fluctuation for exactly replicating the behavior of retry traffic due to user impatience using the quasi-static approach, and showed the validity of an

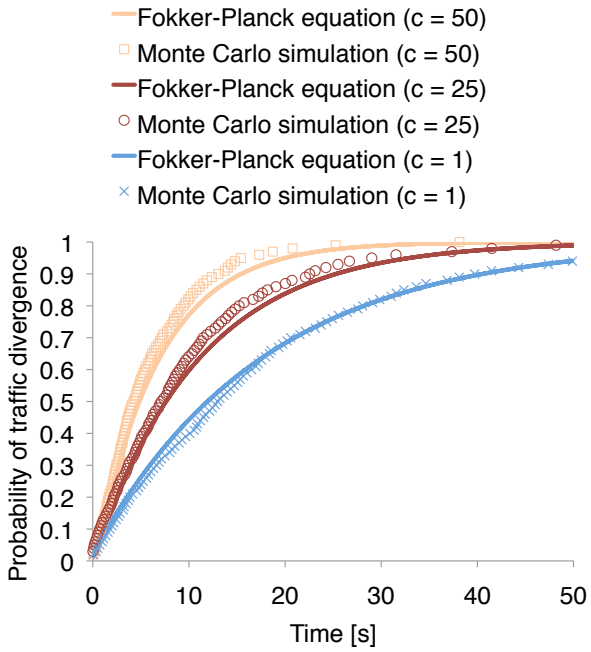

Figure 4.13: Probability of traffic divergence in an M/M/s-based system with retry traffic for various number of servers c

evaluation of the quasi-static approach. We compared the distribution of the volume of traffic and the probability of traffic divergence calculated by the quasi-static approach and conventional Monte Carlo simulation, in M/M/1- and M/M/s-based systems with retry traffic under the condition of a slow system. We confirmed that the evaluation results of the quasi-static approach and Monte Carlo simulation correspond, and so expect that the quasi-static approach can appropriately evaluate the behavior of retry traffic in a high-speed system, because the quasi-static approach can evaluate a low-speed system despite the large magnitude of its fluctuations that make evaluation more difficult.

Chapter 5

Conclusion

In this chapter, we summarize the research presented in this thesis, and present directions for future works.

Firstly, we have discussed how to control fluctuations due to measurement timing for deterministic process, through the investigation in which we have applied Gamma-probing to CoMPACT monitor. In Chapter 2, we have applied Gamma-probing to CoMPACT monitor that measures the time average of the sample path that is deterministic process. Performing simulations, it have been confirmed that the evaluation precision can be improved by using Gamma-probing as active measurement component of CoMPACT monitor. Investigating the characteristics of CoMPACT monitor and Gamma-probing carefully, we have clarified that the requirement to assures the achievement of precision improvement is the convexity of ACF of delay and traffic process in terms of long-time average. Moreover, we have understood that the phase-lock phenomenon happens because probing synchronizes with accidental periodicity on finite measurement period, analyzing the relationship between the power spectrum of the sample path and probe packet arrivals.

Secondly, we have discussed how to optimize fluctuations due to measurement timing for deterministic process, through the analysis of the optimal fluctuation magnitude that should be added to the timing of probe packets. In Chapter 3, we have introduced the probing in which a packet arrival process (i.e. measurement timing) is separated into a deterministic process and stochastic fluctuations, and have shown how to determine the optimal fluctuation from ACF of target process. In other word, we have achieved

to optimize fluctuations in measurement timing. The phase-lock phenomenon due to accidental periodicity is considered in the optimization. The fluctuations play the role of canceling the effect of a specific pattern (i.e. periodicity) of measurement time and thereby an evaluator avoids correspondence of patterns of measurement time (i.e. probe packet time) and target variable (i.e. delay or loss). Through our evaluation examples, we have been able to find that a fluctuation magnitude of 20% of the average probe interval is enough to avoid the phase-lock phenomenon for a wide variety of ACFs. We have confirmed that the result is consistent with the results of Chapter 2. The optimization method can be extend to control fluctuations due to measured variables for deterministic process.

Thirdly, we have discussed how to model fluctuations when we evaluate using a model, through the modeling of fluctuations for precisely evaluating the probability of rare system outages on highly reliable systems with retry traffic by the quasi-static approach. In Chapter 4, we have shown how to model the small fluctuations at each time precisely in the quasi-static approach in which behavior of the system is described as a deterministic process and an accumulation of small fluctuations. An evaluator can evaluate probability that a system enters an undesirable state (i.e. system outages) since the modeled fluctuations play the role of describing atypical transitions of the system state. We have demonstrated modeling of the fluctuation in M/M/1- and M/M/s-based systems with retry traffic, and have confirmed that our modeling achieve an precise evaluation.

Though we clarified that fluctuation magnitude of 20% of the average measurement period is appropriate for a common shape of ACF in Chapter 3, the result can not be applied to a target with a uncommon shape of ACF that reflects special structure of target system. To optimize fluctuation magnitude in measurement timing for a target with uncommon correlation structure, we should infer ACF from past measurement data or other available sources. In our future work, we will provide a optimization method of fluctuation magnitude in measurement timing for a target that has unknown correlation structure.

Moreover, analysis of decrease of probe packet traffic by optimizing the magnitude of fluctuations in probe packet timing in actual measurements is not enough though we showed that an accidental periodicity appears remarkably in RTT in actual network in

Chapter 3. Especially, we should verify the amount of probe packet traffic that is decreased by the optimization in network-wide measurements where probe packets pass over each path in a network since SAL monitoring is one of a typical application of active measurement.

One of our future directions is to provide a modeling methodology of fluctuations for wider classes of systems. In Chapter 4, we have demonstrated modeling of the fluctuation in the M/M/1- and M/M/s-based systems that are only a part of the scope of the quasi-static approach.

Finally, we believe that those above discussions of fluctuations in performance evaluations contribute to network researchers and practitioners.

Bibliography

[1] F. Baccelli, S. Machiraju, D. Veitch, and J. Bolot, "On Optimal Probing for Delay and Loss Measurement," in Proc. ACM Internet Measurement Conference (IMC 2007), pp.291–302, San Diego, CA, USA, October 2007.

[2] C. Dovrolis, P. Ramanathan, and D. Moore, "Packet-Dispersion Techniques and a Capacity-Estimation Methodology," IEEE/ACM Transactions on Networking, vol.12, no.6, pp.963–977, December 2004.

[3] R. Kapoor, L.J. Chen, A. Nandan, M. Gerla, and M.Y. Sanadidi, "CapProbe: A Simple and Accurate Capacity Estimation Technique for Wired and Wireless Environments," ACM SIGCOMM Computer Communication Review, vol.34, no.4, pp.67–78, 2004.

[4] M. Jain and C. Dovrolis, "End-to-End Available Bandwidth: Measurement Methodology, Dynamics, and Relation with TCP Throughput," IEEE/ACM Transactions on Networking, vol.11, no.4, pp.537–549, 2003.

[5] V.J. Ribeiro, R.H. Riedi, R.G. Baraniuk, J. Navratil, and L. Cottrell, "pathChirp: Efficient Available Bandwidth Estimation for Network Paths," in Proc. the 4th Passive and Active Measurement Conference (PAM 2003) Workshop, San Diego, CA, USA, April 2003.

[6] W. Heisenberg, "Critique of the Physical Concepts of the Corpuscular Theory of Matter," in The Physical Principles of the Quantum Theory, ch. 2, pp.13–46, Courier Dover Publications, 1949.

[7] M. Roughan, “Fundamental Bounds on the Accuracy of Network Performance Measurements,” ACM SIGMETRICS Performance Evaluation Review, vol.33, no.1, pp.253–264, 2005.

[8] C.E. Shannon, “Communication In The Presence Of Noise,” Proceedings of the IEEE, vol.86, no.2, pp.447–457, February 1998.

[9] F. Baccelli, S. Machiraju, D. Veitch, and J. Bolot, “The Role of PASTA in Network Measurement,” ACM SIGCOMM Computer Communication Review, vol.36, no.4, pp.231–242, 2006.

[10] M. Aida, C. Takano, M. Murata, and M. Imase, “A Proposal of Quasi-Static Approach for Analyzing the Stability of IP Telephony Systems,” in Proc. the 7th International Conference on Networking (ICN 2008), pp.363–370, Cancun, Mexico, April 2008.

[11] K. Watabe, Y. Honma, and M. Aida, “Probe Interval Designs that Improve Accuracy of CoMPACT Monitor,” Simulation Modelling Practice and Theory, vol.19, no.1, pp.56–68, January 2011.

[12] K. Watabe, Y. Honma, and M. Aida, “Accuracy Improvement of CoMPACT Monitor by Using New Probing Method,” in Proc. the 12th Asia-Pacific Network Operations and Management Symposium (APNOMS 2009), pp.31–40, Jeju, Korea, September 2009.

[13] K. Watabe, Y. Honma, and M. Aida, “Verification of Accuracy Improvement for CoMPACT Monitor Due to Suboptimal Inter-Probe Time,” in Proc. the 9th Annual International Symposium on Applications and the Internet (SAINT 2009), pp.133–136, Seattle, WA, USA, July 2009.

[14] K. Watabe, Y. Honma, and M. Aida, “Design of Probe Intervals to Improve Accuracy of CoMPACT Monitor,” in Proc. IEICE General Conference 2009, B-7-12, Ehime, Japan, March 2009 (in Japanese).

[15] K. Watabe, Y. Honma, and M. Aida, “Verification of Accuracy Improvement for CoMPACT Monitor Due to Suboptimal Inter-probe Time,” Technical Report of IEICE, IN2008-162, pp.179–184, March 2009 (in Japanese).

[16] K. Watabe, Y. Honma, and M. Aida, “A Study on the Probing Method and Accuracy for CoMPACT Monitor,” Technical Report of IEICE, IN2009-30, pp.31–36, July 2009 (in Japanese).

[17] K. Watabe and M. Aida, “On Optimal Magnitude of Fluctuations in Probe Packet Arrival Intervals,” IEICE Transactions on Communications, vol.E96-B, no.12, pp.3028–3040, December 2013.

[18] K. Watabe and M. Aida, “Analysis on the Fluctuation Magnitude in Probe Interval for Active Measurement,” in Proc. the 30th IEEE International Conference on Computer Communication (INFOCOM 2011) Mini-Conference, pp.161–165, Shanghai, China, April 2011.

[19] K. Watabe and M. Aida, “Optimization of the Magnitude of Fluctuations for Timing of Active Probe Packets,” Technical Report of IEICE, IN2010-50, pp.37–42, July 2010 (in Japanese).

[20] K. Watabe and M. Aida, “Analysis of the Magnitude of Fluctuations in Probe Timing for Active Measurement,” in Proc. IEICE Society Conference 2010, B-7-20, Osaka, Japan, September 2010 (in Japanese).

[21] K. Watabe and M. Aida, “Modeling Fluctuations in the Quasi-static Approach Describing the Temporal Evolution of Retry Traffic,” WSAES Transactions on Communications, vol.12, no.9, pp.488–498, September 2013.

[22] K. Watabe and M. Aida, “On Modeling of Fluctuations in Quasi-Static Approach Describing the Temporal Evolution of Retry Traffic,” in Proc. the 23rd International Teletraffic Congress (ITC 2011) Student Poster, pp.308–309, San Francisco, CA, USA, September 2011.

[23] K. Watabe, M. Tanabe, and M. Aida, "On Modeling of Fluctuations on Quasi-Static Approach Analyzing the Behavior of the Retry Traffic," Technical Report of IEICE, IN2010-178, pp.205–210, March 2011 (in Japanese).

[24] "CAIDA: The Cooperative Association for Internet Data Analysis." `http://www.caida.org/`.

[25] V. Paxson, J. Mahdavi, A. Adams, and M. Mathis, "An Architecture for Large Scale Internet Measurement," IEEE Communications Magazine, vol.36, no.8, pp.48–54, 1998.

[26] J. Bolot, "Characterizing End-to-End Packet Delay and Loss in the Internet," High Speed Networks, vol.2, no.3, pp.289–298, 1993.

[27] V. Paxson, "End-to-End Internet Packet Dynamics," ACM SIGCOMM Computer Communication Review, vol.27, no.4, pp.139–152, 1997.

[28] S. Savage, A. Collins, E. Hoffman, J. Snell, and T. Anderson, "The End-to-End Effects of Internet Path Selection," ACM SIGCOMM Computer Communication Review, vol.29, no.4, pp.289–299, 1999.

[29] G. Almes, S. Kalidindi, and M.J. Zekauskas, "A One-way Delay Metric for IPPM," RFC2679, 1999.

[30] G. Almes, S. Kalidindi, and M.J. Zekauskas, "A One-way Packet Loss Metric for IPPM," RFC2680, 1999.

[31] A. Pásztor and D. Veitch, "High Precision Active Probing for Internet Measurement," in Proc. the 11th Internet Society Conference (INET 2001), Stockholm, Sweden, June 2001.

[32] V. Paxson, G. Almes, J. Mahdavi, and M. Mathis, "Framework for IP Performance Metrics," RFC2330, 1998.

[33] M. Aida, N. Miyoshi, and K. Ishibashi, "A Scalable and Lightweight QoS Monitoring Technique Combining Passive and Active Approaches," in Proc. the 22nd

IEEE International Conference on Computer Communication (INFOCOM 2003), pp.125–133, San Francisco, CA, USA, March 2003.

[34] K. Ishibashi, M. Aida, and S. Kuribayashi, "Proposal and Evaluation of Method to Estimate Packet Loss-Rate Using Correlation of Packet Delay and Loss," IEICE Transactions on Information and Systems, vol.86, no.11, pp.2371–2379, 2003.

[35] M. Aida, N. Miyoshi, and K. Ishibashi, "A Change-of-Measure Approach to Per-Flow Delay Measurement Combining Passive and Active Methods: Mathematical Formulation for CoMPACT Monitor," IEEE Transaction Information Theory, vol.54, no.11, pp.4966–4979, 2008.

[36] R.W. Wolff, "Poisson Arrivals See Time Averages," Operations Research, vol.30, no.2, pp.223–231, March 1982.

[37] "The Network Simulator – ns-2." `http://www.isi.edu/nsnam/ns/`.

[38] J. Strauss, D. Katabi, and F. Kaashoek, "A Measurement Study of Available Bandwidth Estimation Tools," in Proc. the 3rd ACM SIGCOMM Conference on Internet Measurement (IMC 2003), pp.39–44, Miami, FL, USA, October 2003.

[39] F. Baccelli, S. Machiraju, D. Veitch, and J. Bolot, "Probing for Loss : the Case against Probe Trains," IEEE Communications Letters, vol.15, no.5, pp.590–592, 2011.

[40] J. Sommers, P. Barford, N. Duffield, and A. Ron, "Improving Accuracy in End-to-End Packet Loss Measurement," ACM SIGCOMM Computer Communication Review, vol.35, no.4, p.157, October 2005.

[41] M. Hasib, J. Schormans, and T. Timotijevic, "Accuracy of Packet Loss Monitoring over Networked CPE," IET Communications, vol.1, no.3, pp.507–513, 2007.

[42] J. Sommers, P. Barford, N. Duffield, and A. Ron, "A Geometric Approach to Improving Active Packet Loss Measurement," IEEE/ACM Transactions on Networking, vol.16, no.2, pp.307–320, April 2008.

[43] B.M. Parker, S.G. Gilmour, and J. Schormans, "Measurement of Packet Loss Probability by Optimal Design of Packet Probing Experiments," IET Communications, vol.3, no.6, pp.979–991, 2009.

[44] V. Raisanen, G. Grotefeld, and A. Morton, "Network Performance Measurement with Periodic Streams," RFC3432, 2002.

[45] M. Roughan, "A Comparison of Poisson and Uniform Sampling for Active Measurements," IEEE Journal on Selected Areas in Communications, vol.24, no.12, pp.2299–2312, 2006.

[46] S. Floyd and V. Jacobson, "Traffic Phase Effects in Packet-Switched Gateways," ACM SIGCOMM Computer Communication Review, vol.21, no.2, pp.26–42, 1991.

[47] S. Floyd and V. Jacobson, "The Synchronization of Periodic Routing Messages," IEEE/ACM Transactions on Networking, vol.2, no.2, pp.122–136, 2002.

[48] I.S. Gradshteyn, I.M. Ryzhik, A. Jeffrey, and D. Zwillinger, "Table of Integrals, Series, and Products," ch. 12, p.1066, Academic press, New York, USA, seventh ed., 1980.

[49] I.S. Gradshteyn, I.M. Ryzhik, A. Jeffrey, and D. Zwillinger, "Table of Integrals, Series, and Products," ch. 3, p.488, Academic press, New York, USA, seventh ed., 1980.

[50] H. Stark and F.B. Tuteur, "Modern Electrical Communications: Theory and Systems," pp.421–422, Prentice Hall, 1979.

[51] P. Billingsley, "Probability and Measure," ch. 5, pp.366–382, John Wiley & Sons, 1986.

[52] P.M. Morse, "Stochastic Properties of Waiting Lines," Operations Research Society of America, vol.3, no.3, pp.255–261, 1955.

[53] J. Abate and W. Whitt, "The Correlation Functions of RBM and M/M/1," Stochastic Models, vol.4, no.2, pp.315–359, 1988.

[54] G.I. Falin and J.G.C. Templeton, Retrial queues, Chapman and Hall, 1997.

[55] B. Braden, L. Zhang, S. Berson, S. Herzog, and S. Jamin, "Resource ReSerVation Protocol (RSVP) – Version 1 Functional Specification," RFC2205, 1997.

[56] A. Gómez-Corral, "Stochastic Analysis of a Single Server Retrial Queue with General Retrial Times," Naval Research Logistics, vol.46, no.5, pp.561–581, August 1999.

[57] J. Wang and J. Cao, "Reliability Analysis of the Retrial Queue with Server Breakdowns and Repairs," Queueing Systems, vol.38, no.4, pp.363–380, August 2001.

[58] J. Wang and P. Zhang, "A Discrete-Time Retrial Queue with Negative Customers and Unreliable Server," Computers & Industrial Engineering, vol.56, no.4, pp.1216–1222, May 2009.

[59] B. Krishna Kumar, G. Vijayalakshmi, A. Krishnamoorthy, and S. Sadiq Basha, "A Single Server Feedback Retrial Queue with Collisions," Computers & Operations Research, vol.37, no.7, pp.1247–1255, July 2010.

[60] J. Nielsen, "Usability Heuristics," in Usability Engineering, ch. 5, p.135, Academic Press, 1993.

[61] J.D.C. Little, "A Proof of the Queuing Formula: $L = \lambda W$," Operations Research, vol.9, no.3, pp.383–387, March 1961.

[62] M. Aida, C. Takano, M. Murata, and M. Imase, "A Study of Control Plane Stability with Retry Traffic : Comparison of Hard- and Soft-State Protocols," IEICE Transactions on Communications, vol.91, no.2, pp.437–445, February 2008.

[63] N.G. van Kampen, Stochastic Processes in Physics and Chemistry, Elsevier, 1992.

[64] N.L. Johnson, A.W. Kemp, and S. Kotz, "Poisson Distribution," in Univariate Discrete Distributions, ch. 4, p.166, John Wiley & Sons, third ed., 2005.

[65] E.G. Coffman, R.R. Muntz, and H. Trotter, "Waiting Time Distributions for Processor-Sharing Systems," Journal of the ACM, vol.17, no.1, pp.123–130, January 1970.

[66] M. Barbeau and E. Kranakis, “Medium Access Control,” in Principles of Ad Hoc Networking, ch. 2, p.42, John Wiley & Sons, 2007.